Exploring ν Physics with LArTPC

Jay Hyun Jo
Yale University

BNL Particle Physics Seminar
April 12, 2022

standard model of particle physics

- standard model that describes the elementary particles has been very successful so far
- however, there are still unsolved questions in SM, especially in neutrino sector
  – neutrino oscillation observation implies neutrino has non-zero mass
  – but we still do not know neutrino masses, mass ordering, precise value of δ_{CP}, …

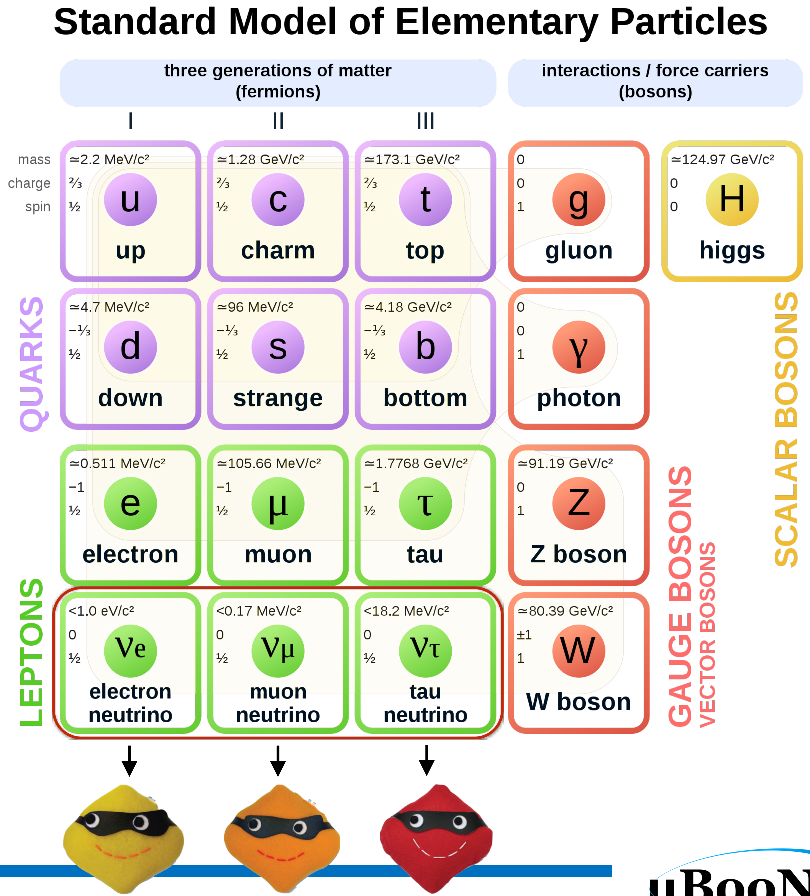

neutrino oscillation

https://en.wikipedia.org/wiki/Neutrino_oscillation

$$|\nu_\alpha\rangle = \sum_i U^*_{\alpha i}|\nu_i\rangle$$

Mixing matrix

Flavor eigenstates participating in weak interactions

Mass eigenstates ν_1, ν_2, ν_3

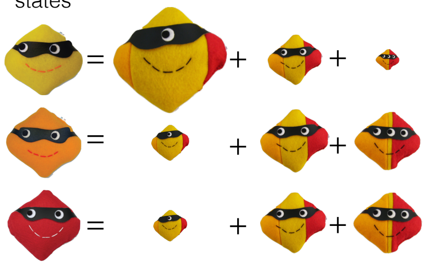

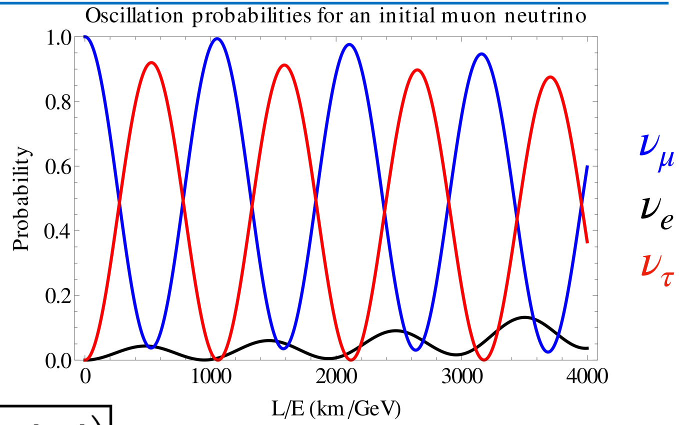

two-neutrino model

$$P(\nu_\alpha \to \nu_\alpha) = 1 - \sin^2 2\theta \sin^2\left(1.27\frac{\Delta m^2\ [\mathrm{eV}]^2 \cdot L\ [\mathrm{km}]}{E_\nu\ [\mathrm{GeV}]}\right)$$

- neutrino flavor eigenstates are not the same as the mass eigenstates
- neutrinos generally are produced in a *flavor* eigenstate, which is a superposition of three *mass* eigenstates
- this critical phenomenon is now very well known for 3-neutrino oscillation, and physics parameters precisely measured with experiments in last two decades

short-baseline neutrino experiment anomalies

- Series of anomalous results seen at short-baselines using a variety of neutrino sources
  - LSND ν_e excess
  - MiniBooNE $\nu_e/\bar{\nu}_e$ excess
  - GALLEX/SAGE/BEST ν_e deficit
  - Reactor $\bar{\nu}_e$ deficit
    - recent experiments/joint analyses addressed this fairly well: issues in predicting reactor neutrino flux

- Interpretations initially focused on oscillations driven by “vanilla” eV-scale sterile neutrinos

- Disfavored by non-observation of ν_μ disappearance, so explanation of these requires a more rich phenomenology

Phys. Rev. D 64 112007, 2001

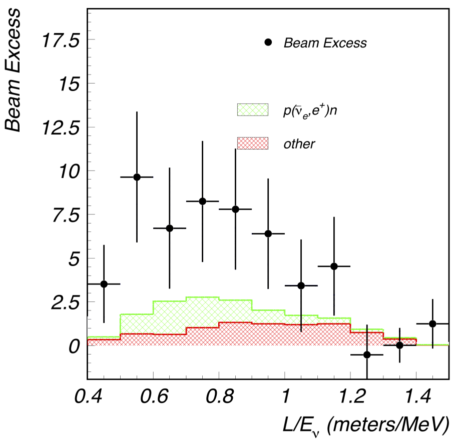

Phys. Rev. D 103, 052002 (2021)

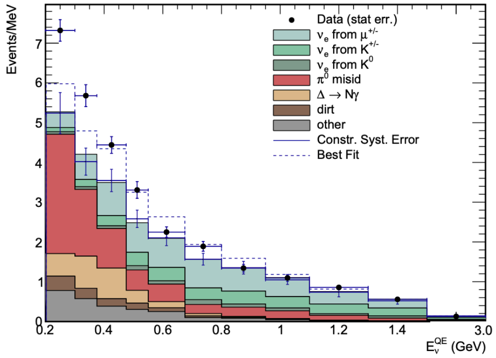

Phys. Rev. C 73, 045805 (2006)

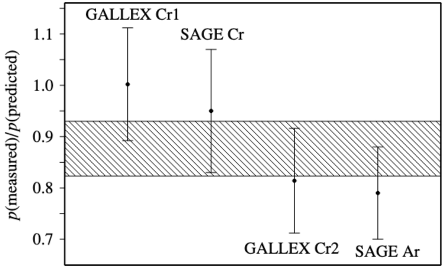

arXiv:1204.5379

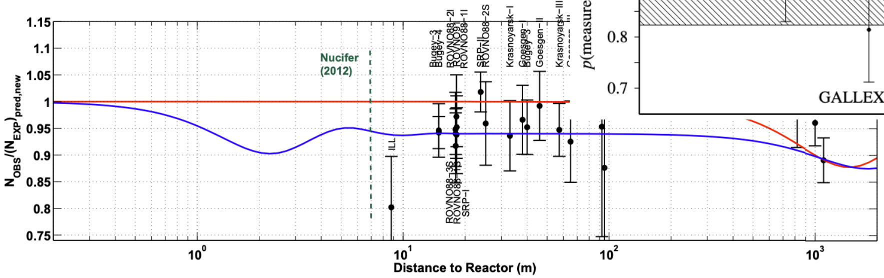

MiniBooNE low energy excess

- nature of the excess could be "electron-like" (eLEE) or "photon-like" (γLEE)
  - MiniBooNE could not distinguish between electrons and photons, also did not have hadron information
- *can we separate electrons and photons?*
- *can we understand the excess with enough event topology information such as hadronic activities?*

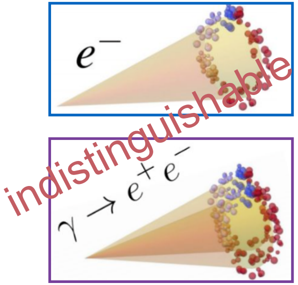

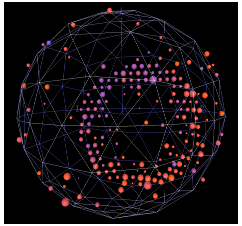

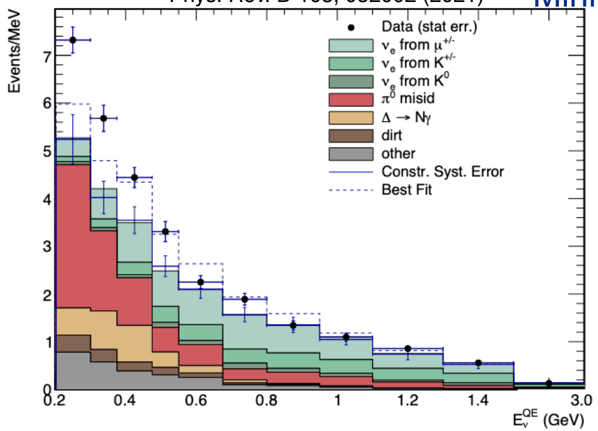

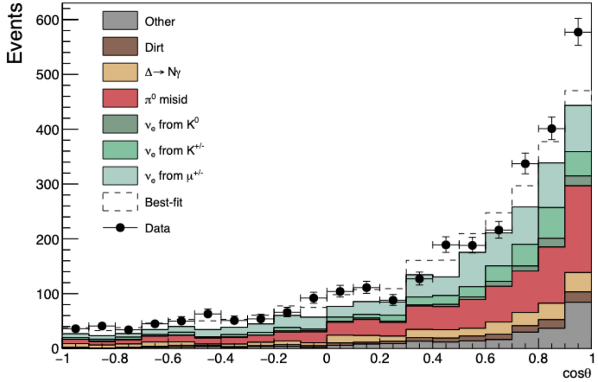

µBooNE

LArTPC: Liquid Argon Time Projection Chamber

- **LAr** as total absorption calorimeter
  - denser than water, leads to more interactions
  - abundant and cheap
  - easy ionization and high scintillation light
- **TPC** as 4π charged particle detector
  - 3D reconstruction with fully active volume
- **LAr+TPC** to obtain fine-grained 3D tracking with local dE/dx information and fully active target medium

NUCLEAR INSTRUMENTS AND METHODS 120 (1974) 221–236; © NORTH-HOLLAND PUBLISHING CO.

LIQUID-ARGON IONIZATION CHAMBERS AS TOTAL-ABSORPTION DETECTORS*

W. J. WILLIS†
Department of Physics, Yale University, New Haven, Connecticut 06520, U.S.A.
and
V. RADEKA
Instrumentation Division, Brookhaven National Laboratory, Upton, New York 11973, U.S.A.

Received 14 May 1974

1974

The Time-Projection Chamber
- A new 4π detector for charged particles

David R. Nygren
Lawrence Berkeley Laboratory
Berkeley, California 97420

1976

THE LIQUID-ARGON TIME PROJECTION CHAMBER:
A NEW CONCEPT FOR NEUTRINO DETECTORS

C. Rubbia

1977

μBooNE

LArTPC: Liquid Argon Time Projection Chamber

charged particle enters detector

⬇

scintillation light emitted by excited Ar, detected by PMTs

⬇

ionization electrons drift to anode plane, detected by sense wires

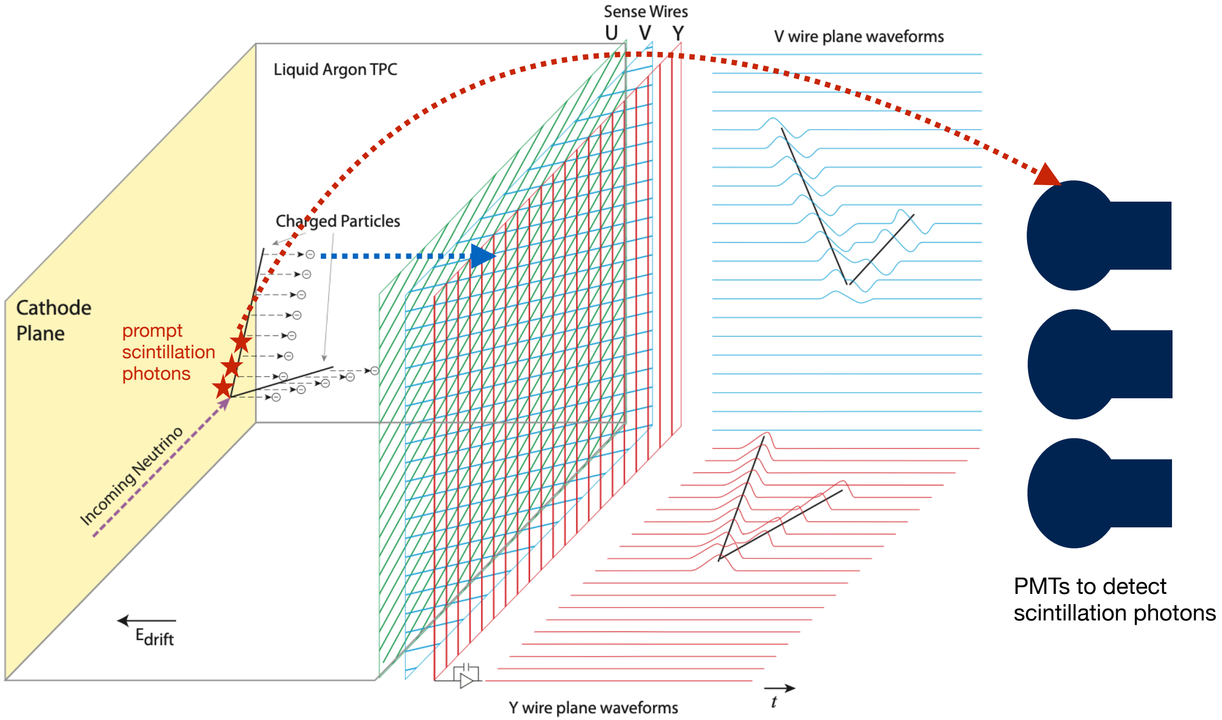

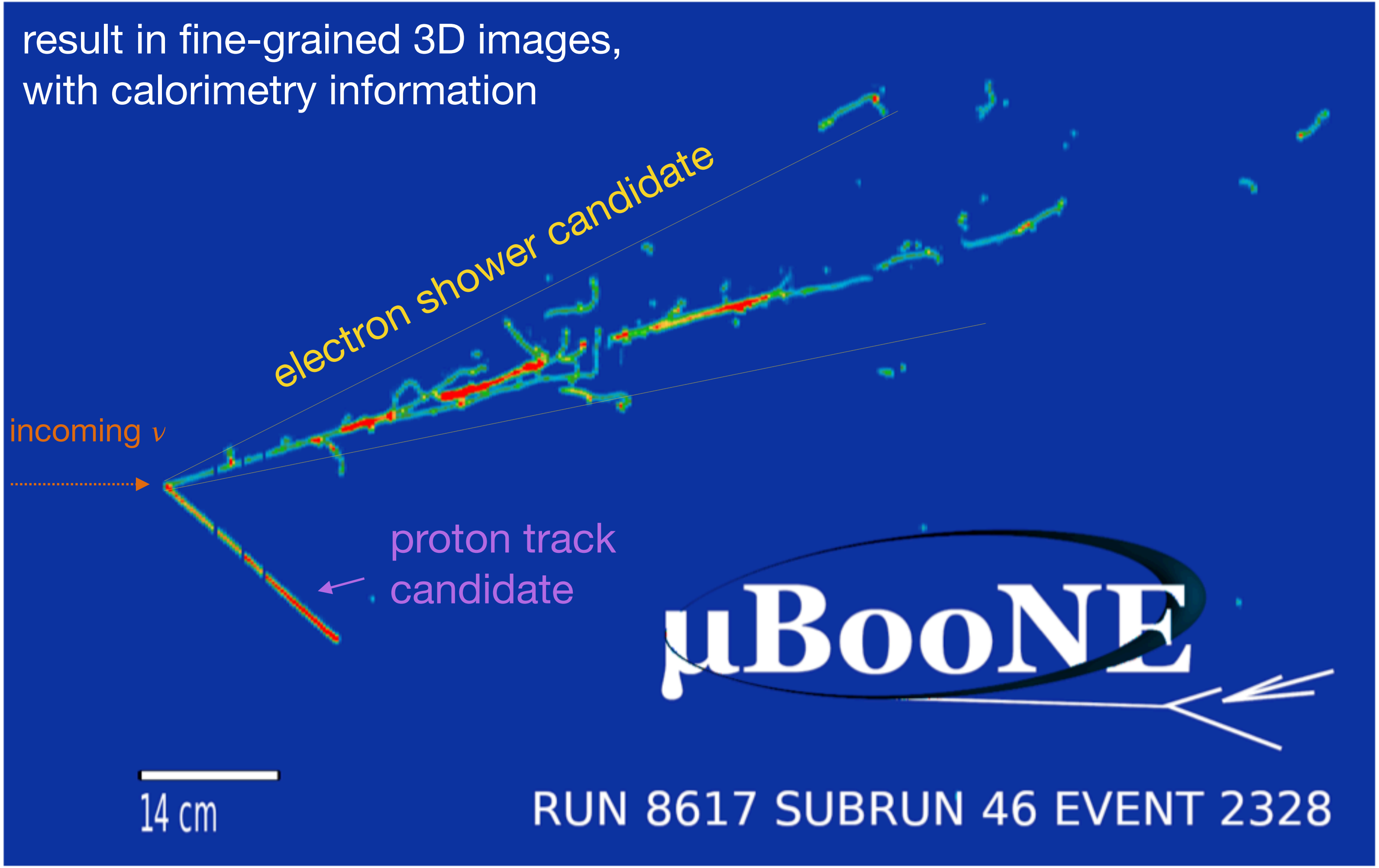
result in fine-grained 3D images,
with calorimetry information
electron shower candidate
incoming ν
proton track
candidate
μBooNE
14 cm
RUN 8617 SUBRUN 46 EVENT 2328

testing eLEE vs. γLEE hypotheses with MicroBooNE

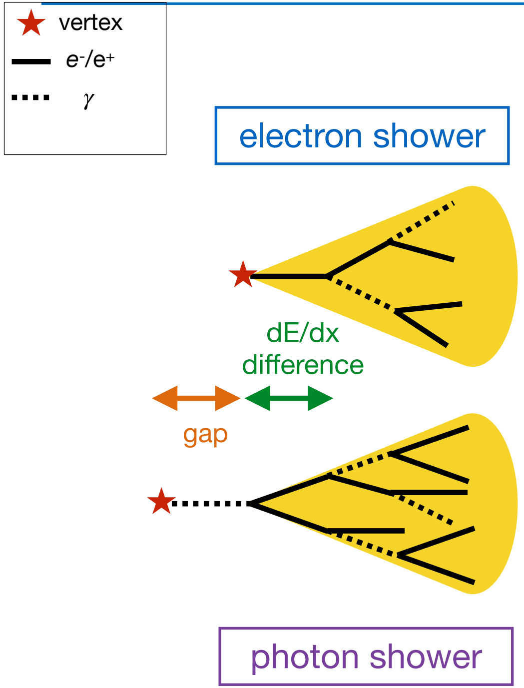

topology information

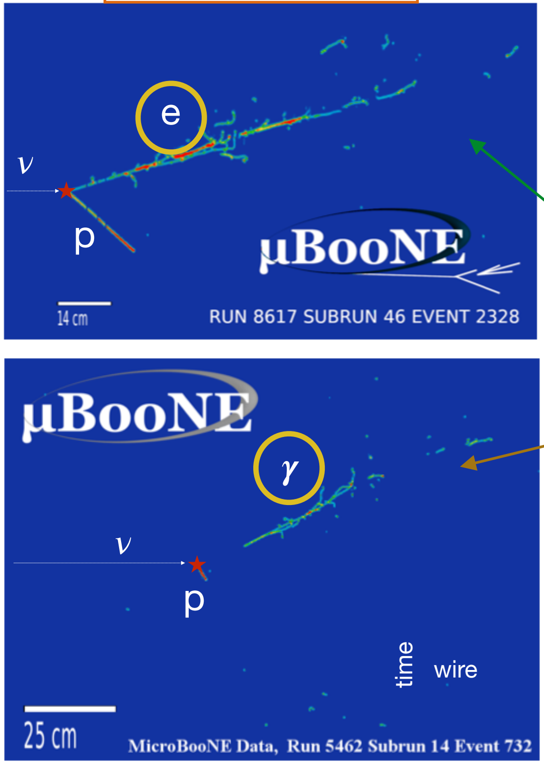

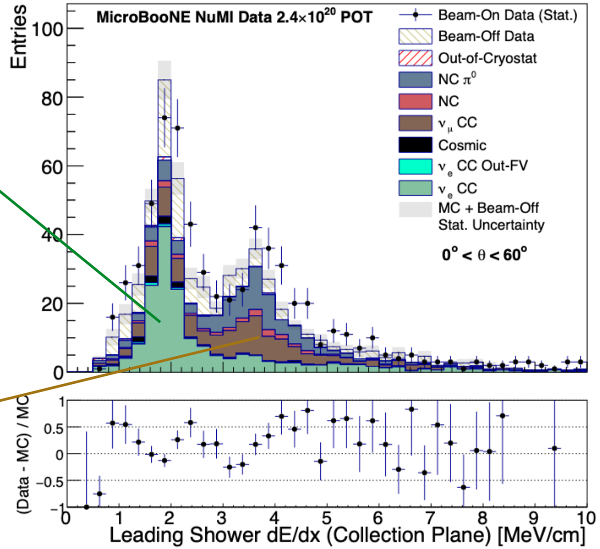

ionization dE/dx

MicroBooNE uses the excellent properties and resolution of its LArTPC to select both eLEE and γLEE signals with high purity

testing eLEE vs. γLEE hypotheses with MicroBooNE

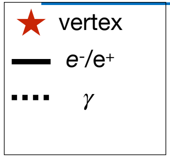

electron shower

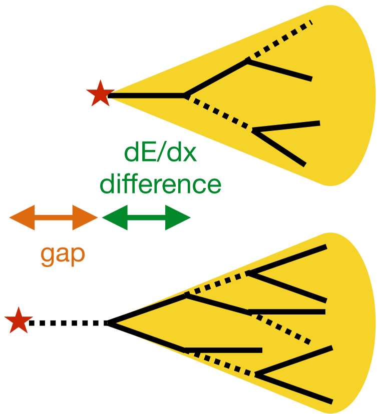

photon shower

topology information

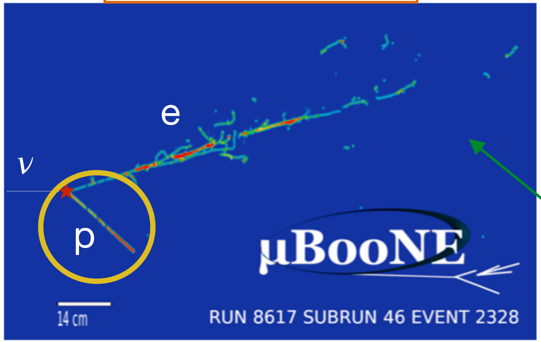

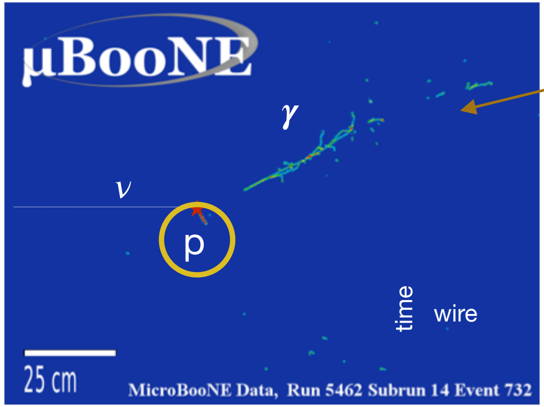

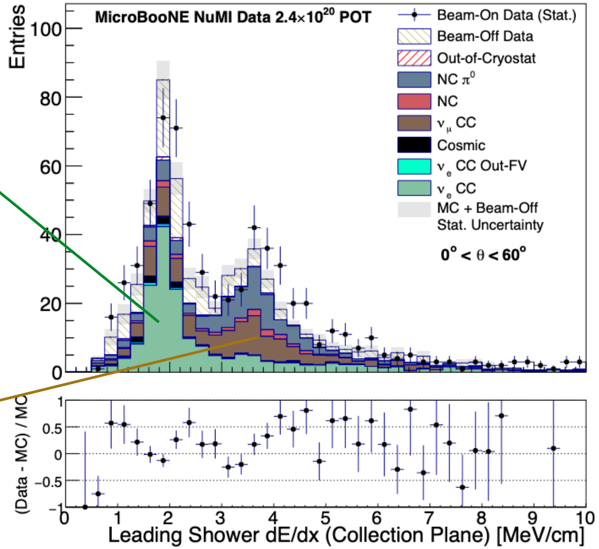

ionization dE/dx

…also to identify hadronic final states to provide more information of different interactions

MicroBooNE experiment

- **LArTPC Detector**
  - 85 tons of LAr active volume
  - TPC: 8192 anode sense wires in 3 planes
    PMT: 32 8-inch PMTs
  - CRT (cosmic ray tagger) is installed around TPC
  - located at BNB beamline in Fermilab, started taking data since Oct. 2015
- **physics goal**
  - strong understanding of the detector and highly developed event reconstruction, paving the way to future LAr detectors (SBN & DUNE)
  - neutrino interaction measurements
  - towards low-energy excess: definitively address the MiniBooNE anomaly

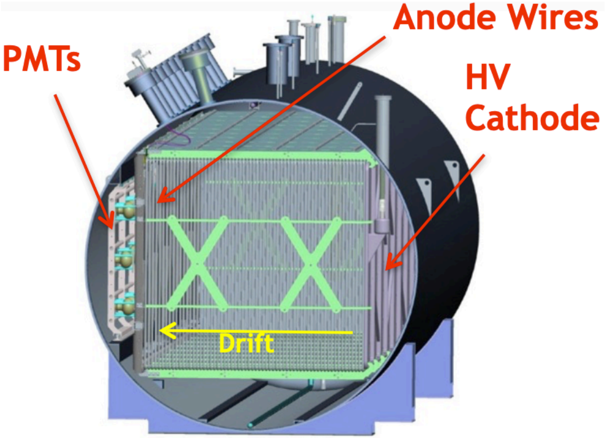

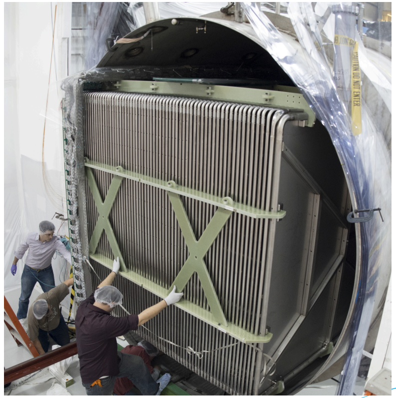

MicroBooNE experiment

2017 | 2018 | 2019 | 2020 | 2021 | 2022

- strong track record of publications
  - >40 papers
    - ~1/2 JINST, ~1/2 Phys Rev, EPJC
  - >60 public notes
    - sharing with the community as we go

Observation of radon mitigation in MicroBooNE by a liquid argon filtration system
Cosmic ray muon clustering for the MicroBooNE liquid argon time projection chamber using sMask-RCNN
Novel approach for evaluating detector-related uncertainties in a LArTPC using MicroBooNE data
First measurement of energy-dependent inclusive muon neutrino charged-current cross sections on argon with the MicroBooNE detector
Search for an anomalous excess of inclusive charged-current ν_e interactions without pions in the final state with the MicroBooNE experiment
Search for an anomalous excess of charged-current quasi-elastic ve interactions with the MicroBooNE experiment using deep-learning-based reconstruction
New theory-driven GENIE tune for MicroBooNE
Search for an anomalous excess of inclusive charged-current ν_e interactions in the MicroBooNE experiment using Wire-Cell reconstruction
Search for an excess of electron neutrino interactions in MicroBooNE using multiple final state topologies
Wire-Cell 3D pattern recognition techniques for neutrino event reconstruction in large LArTPCs
Electromagnetic shower reconstruction and energy validation with Michel electrons and π^0 samples for the deep-learning-based analyses in MicroBooNE
Search for neutrino-induced NC Δ radiative decay in MicroBooNE and a first test of the MiniBooNE low-energy excess under a single-photon hypothesis
First measurement of inclusive electron-neutrino and antineutrino charged current differential cross sections in charged lepton energy on argon in MicroBooNE
Calorimetric classification of track-like signatures in liquid argon TPCs using MicroBooNE data
Search for a Higgs Portal Scalar Decaying to Electron-Positron Pairs in the MicroBooNE Detector
Measurement of the Longitudinal Diffusion of Ionization Electrons in the Detector
Cosmic Ray Background Rejection with Wire-Cell LAr TPC Event Reconstruction in the MicroBooNE Detector
Measurement of the Flux-Averaged Inclusive Charged Current Electron Neutrino and Antineutrino Cross Section on Argon using the NuMI Beam in MicroBooNE
Measurement of the Atmospheric Muon Rate with the MicroBooNE Liquid Argon TPC
Semantic Segmentation with a Sparse Convolutional Neural Network for Event Reconstruction in MicroBooNE
High-performance Generic Neutrino Detection in a LAr TPC near the Earth's Surface with the MicroBooNE Detector
Neutrino Event Selection in the MicroBooNE LAr TPC using Wire-Cell 3D Imaging, Clustering, and Charge-Light Matching
A Convolutional Neural Network for Multiple Particle Identification in the MicroBooNE Liquid Argon Time Projection Chamber
Vertex-Finding and Reconstruction of Contained Two-track Neutrino Events in the MicroBooNE Detector
The Continuous Readout Stream of the MicroBooNE Liquid Argon Time Projection Chamber for Detection of Supernova Burst Neutrinos
Measurement of Differential Cross Sections for Muon Neutrino CC Interactions on Argon with Protons and No Pions in the Final State
Measurement of Space Charge Effects in the MicroBooNE LAr TPC Using Cosmic Muons
First Measurement of Differential Charged Current Quasi-Elastic-Like Muon Neutrino Argon Scattering Cross Sections with the MicroBooNE Detector
Search for heavy neutral leptons decaying into muon-pion pairs in the MicroBooNE detector
Reconstruction and Measurement of O(100) MeV Electromagnetic Activity from Neutral Pion to Gamma Gamma Decays in the MicroBooNE LArTPC
A Method to Determine the Electric Field of Liquid Argon Time Projection Chambers Using a UV Laser System and its Application in MicroBooNE
Calibration of the Charge and Energy Response of the MicroBooNE Liquid Argon Time Projection Chamber Using Muons and Protons
First Measurement of Inclusive Muon Neutrino Charged Current Differential Cross Sections on Argon at Enu ~0.8 GeV with the MicroBooNE Detector
Design and Construction of the MicroBooNE Cosmic Ray Tagger System
Rejecting Cosmic Background for Exclusive Neutrino Interaction Studies with Liquid Argon TPCs: A Case Study with the MicroBooNE Detector
First Measurement of Muon Neutrino Charged Current Neutral Pion Production on Argon with the MicroBooNE detector
A Deep Neural Network for Pixel-Level Electromagnetic Particle Identification in the MicroBooNE Liquid Argon Time Projection Chamber
Comparison of Muon-Neutrino-Argon Multiplicity Distributions Observed by MicroBooNE to GENIE Model Predictions
Ionization Electron Signal Processing in Single Phase LArTPCs II: Data/Simulation Comparison and Performance in MicroBooNE
Ionization Electron Signal Processing in Single Phase LArTPCs I: Algorithm Description and Quantitative Evaluation with MicroBooNE Simulation
The Pandora Multi-Algorithm Approach to Automated Pattern Recognition of Cosmic Ray Muon and Neutrino Events in the MicroBooNE Detector
Measurement of Cosmic Ray Reconstruction Efficiencies in the MicroBooNE LAr TPC Using a Small External Cosmic Ray Counter
Noise Characterization and Filtering in the MicroBooNE Liquid Argon TPC
Michel Electron Reconstruction Using Cosmic Ray Data from the MicroBooNE LAr TPC
Determination of Muon Momentum in the MicroBooNE LAr TPC Using an Improved Model of Multiple Coulomb Scattering
Convolutional Neural Networks Applied to Neutrino Events in a Liquid Argon Time Projection Chamber
Design and Construction of the MicroBooNE Detector

MicroBooNE's first series of LEE search analyses

four independent analyses targeting different final states, hence probing different theoretical models

- single photon analysis
  - targeting NC Δ —> Nγ hypothesis (1γ0p, 1γ1p)

- analyses searching for a ν_e rate excess
  - MiniBooNE-like final states (1eNp, 1e0p)
  - restricting to quasi-elastic kinematics (1e1p)
  - all ν_e final states (1eX)

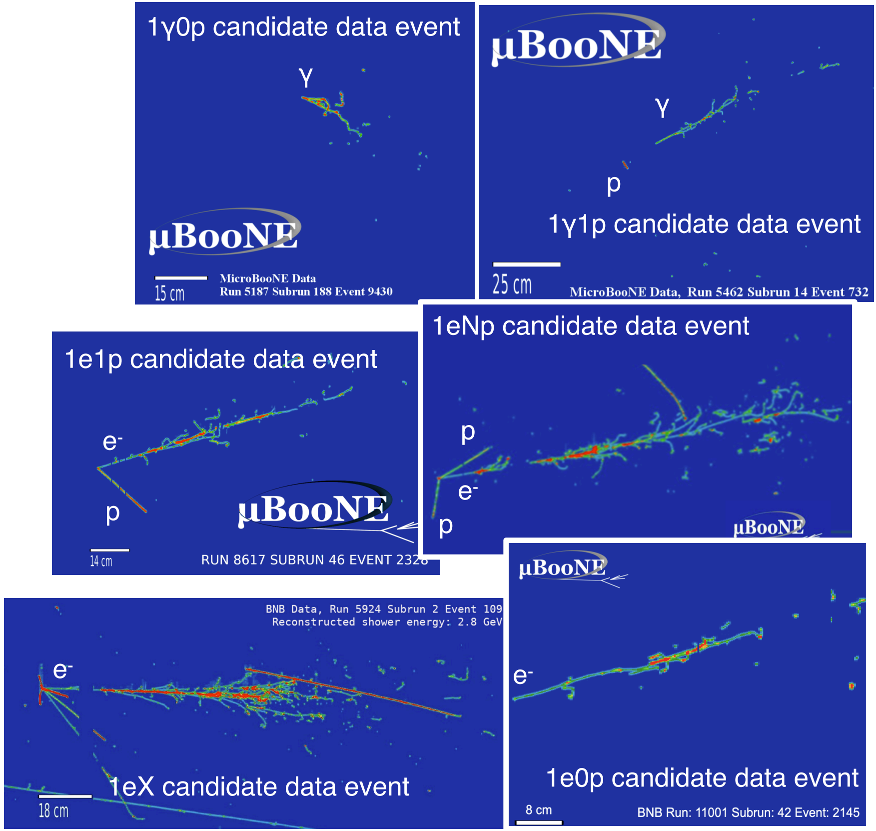

MicroBooNE's first series of LEE search analyses

four independent analyses targeting different final states, hence probing different theoretical models

- single photon analysis
  - targeting NC Δ —> Nγ hypothesis (1γ0p, 1γ1p)

Results presented in [PRL 128.111801]

- analyses searching for a ν_e rate excess
  - MiniBooNE-like final states (1eNp, 1e0p)
  - restricting to quasi-elastic kinematics (1e1p)
  - all ν_e final states (1eX)

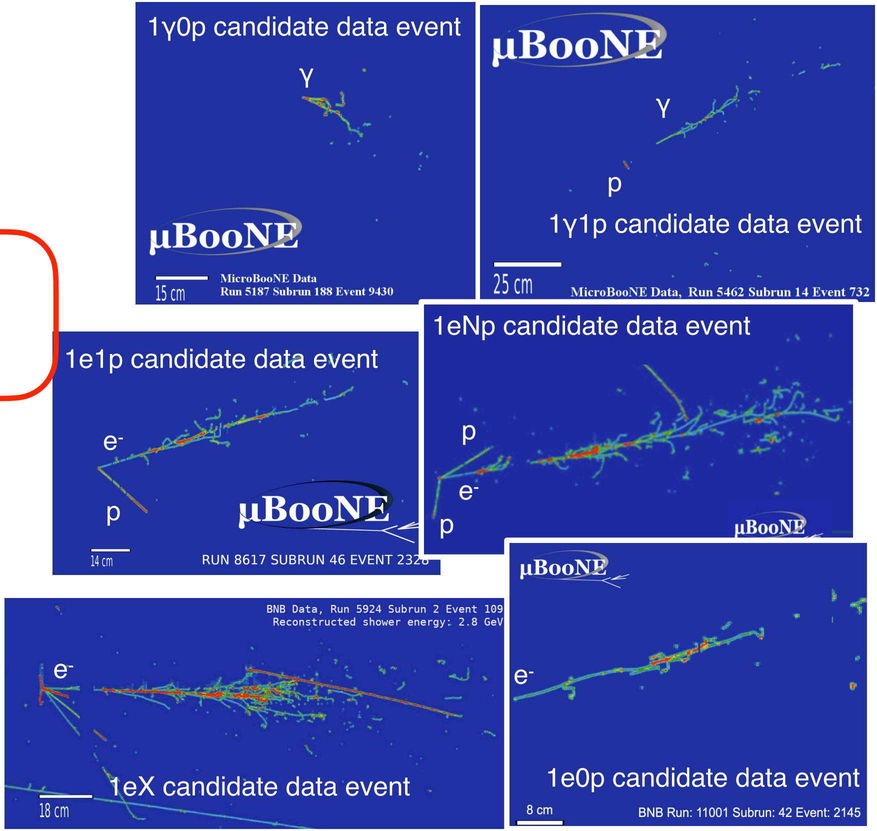

MicroBooNE's first series of LEE search analyses

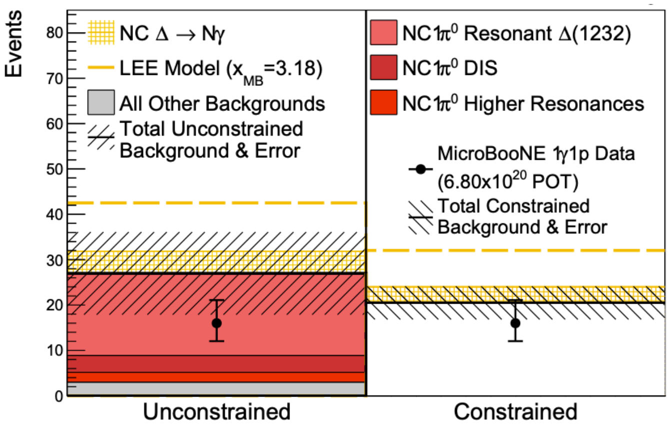

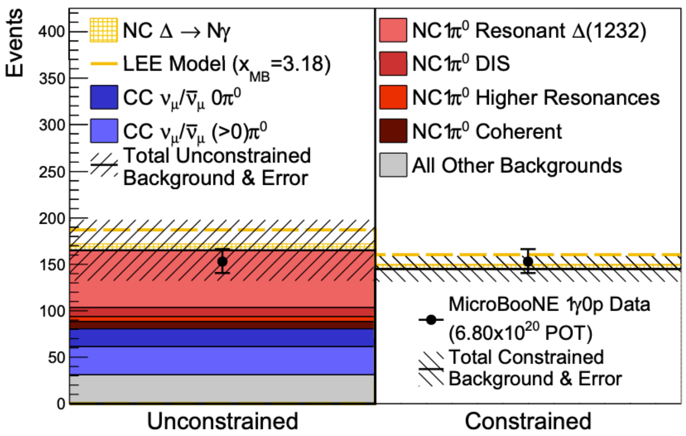

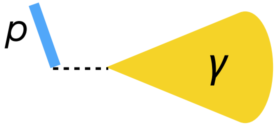

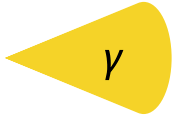

no evidence for enhance rate of single photons from NC $\Delta \rightarrow N\gamma$ decay

disfavor the interpretation of the MiniBooNE anomalous excess as a factor of 3.18 enhancement to the rate NC $\Delta \rightarrow N\gamma$, in favor of the nominal prediction at 94.8% CL

MicroBooNE's first series of LEE search analyses

four independent analyses targeting different final states, hence probing different theoretical models

- single photon analysis
  - targeting NC Δ —> Nγ hypothesis (1γ0p, 1γ1p)

  results in arXiv:2110.14065, arXiv:2110.14080, arXiv:2110.13978, and arXiv:2110.14054

- analyses searching for a ν_e rate excess
  - MiniBooNE-like final states (1eNp, 1e0p)
  - restricting to quasi-elastic kinematics (1e1p)
  - all ν_e final states (1eX)

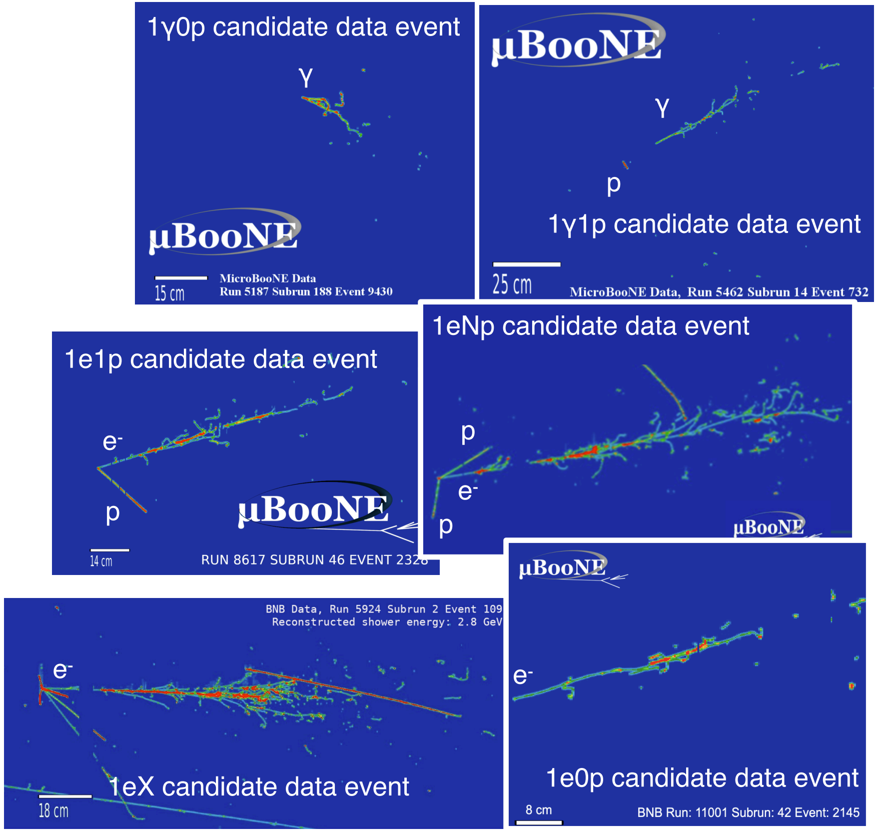

MicroBooNE's search for an excess of electron neutrino interactions

three independent searches across multiple single electron final states

- exclusive two-body charged-current quasi-elastic (CCQE) ν_e scattering [1e1p]

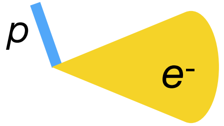

- semi-inclusive ν_e scattering without final state pions [1eNp0π (N≥1) + 1e0p0π]

- inclusive ν_e scattering [1eX]

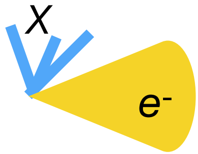

MicroBooNE's search for an excess of electron neutrino interactions

three independent searches across multiple single electron final states

- exclusive two-body charged-current quasi-elastic (CCQE) ν_e scattering [1e1p]
- semi-inclusive ν_e scattering without final state pions [1eN
- inclusive ν_e scattering [1eX] X≥0

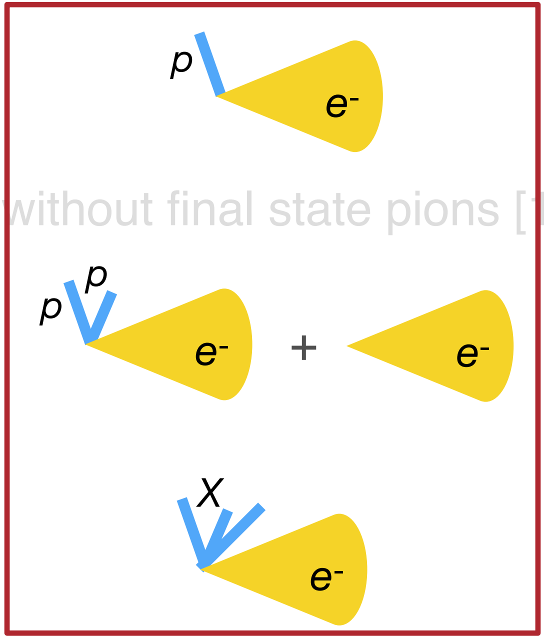

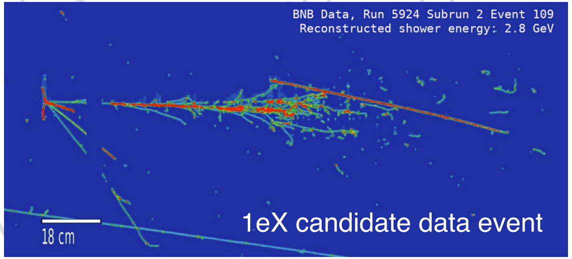

- less cross-section model dependent
- topology-agnostic; high statistics selection
- type of analysis that will be performed in the future wide-band DUNE

simple model of the MiniBooNE low energy excess

- unfold 2018 MiniBooNE excess under ν_e hypothesis
  – considers only E_ν dependence
- derive scaling template to model enhancement of intrinsic ν_e rate in the Booster Neutrino Beam
- apply to MicroBooNE allowing normalization to float
- does the data prefer the constrained ν_e prediction or this simple "eLEE" model?
  – $\Delta\chi^2$ hypothesis testing

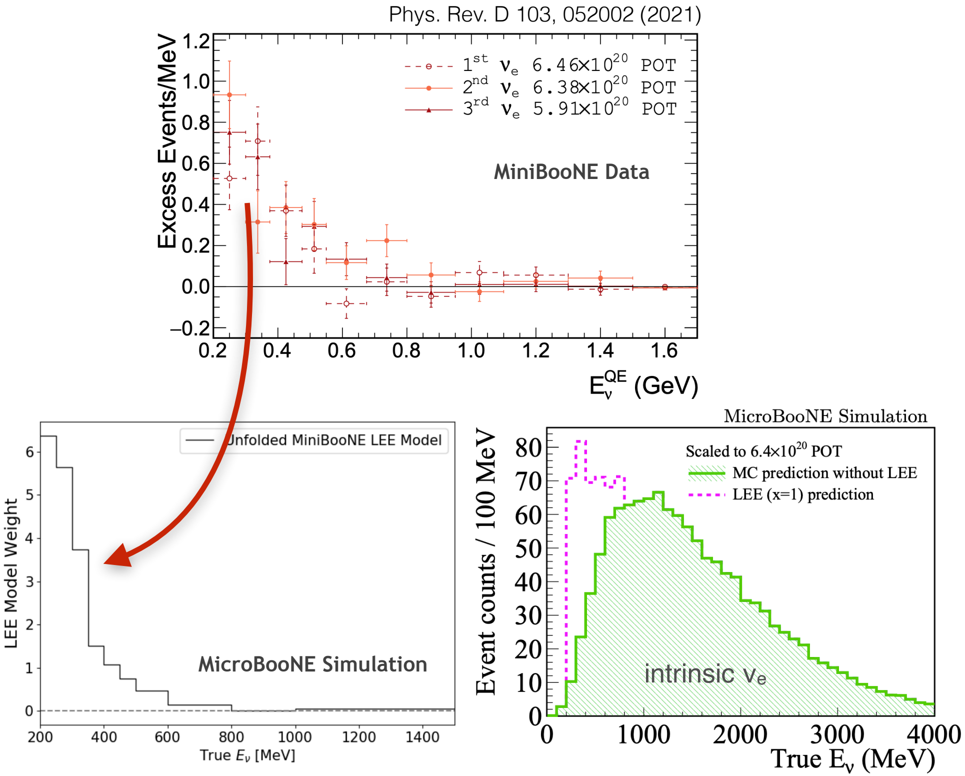

Wire-Cell event reconstruction & pattern recognition: overview

noise filtering

signal processing

3D imaging

clustering

charge-light matching

3D trajectory & dQ/dx fitting

cosmic muon tagger

multi-track fitting

3D vertexing

particle identification

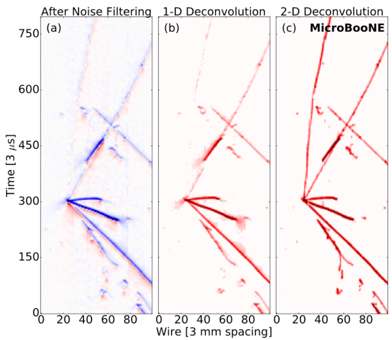

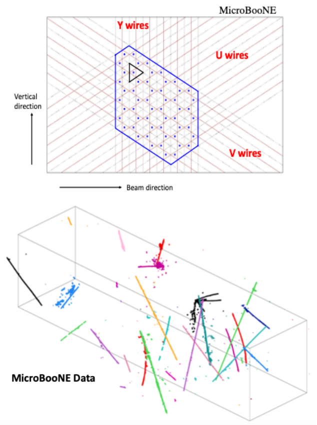

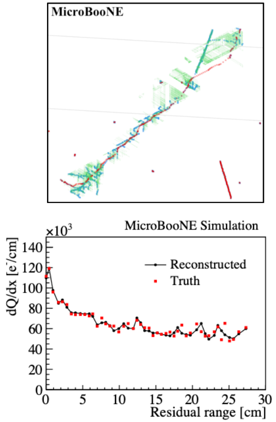

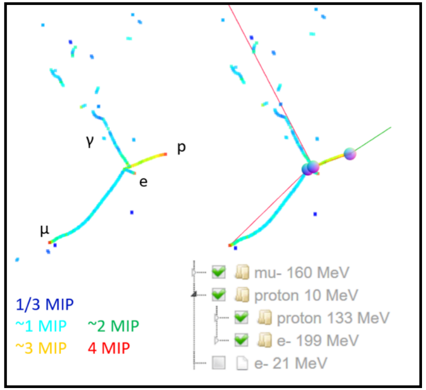

Wire-Cell event reconstruction & pattern recognition

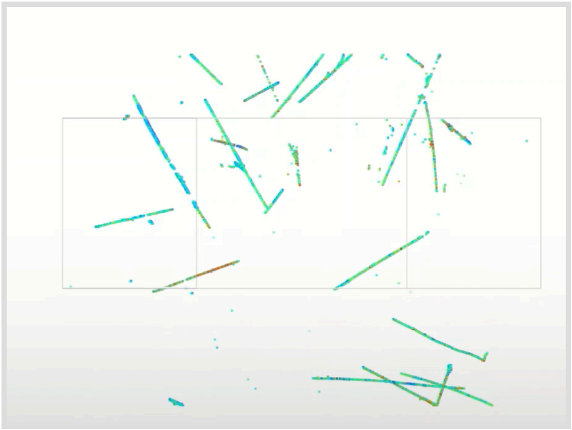

first projection view

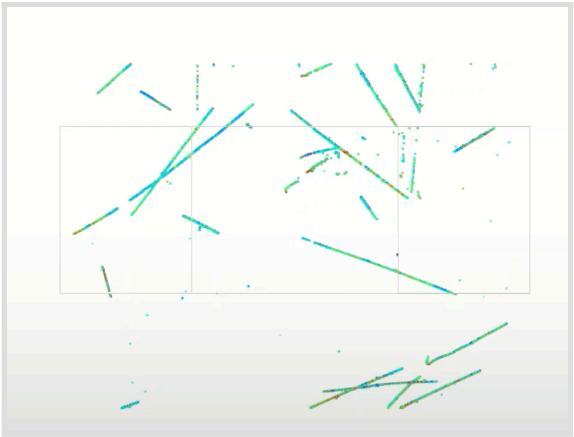

second projection view

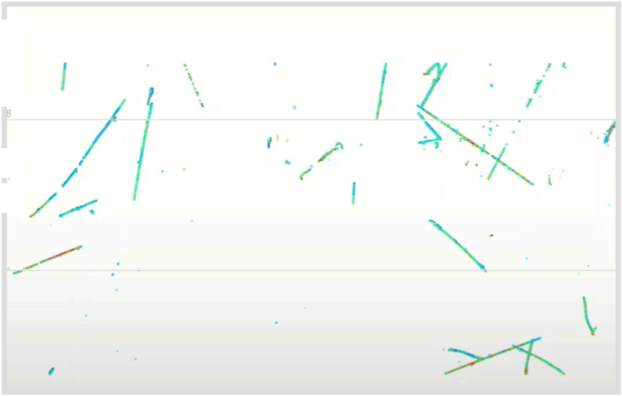

third projection view

- starting with three 2D recorded images, one for each wire plane
- each image is at 60 degrees to others

Wire-Cell event reconstruction & pattern recognition: 3D imaging & clustering

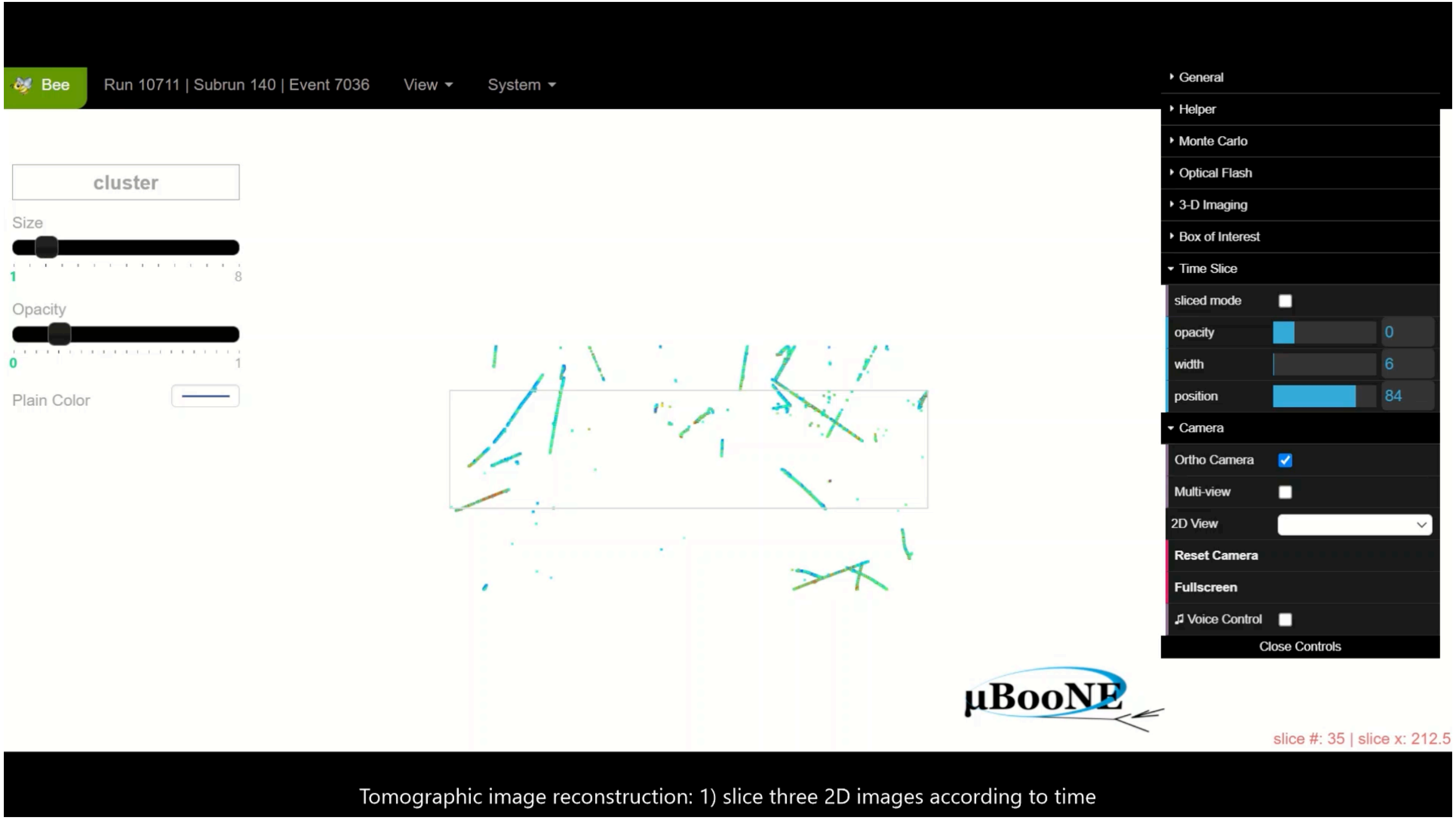

Wire-Cell event reconstruction & pattern recognition: charge-light matching

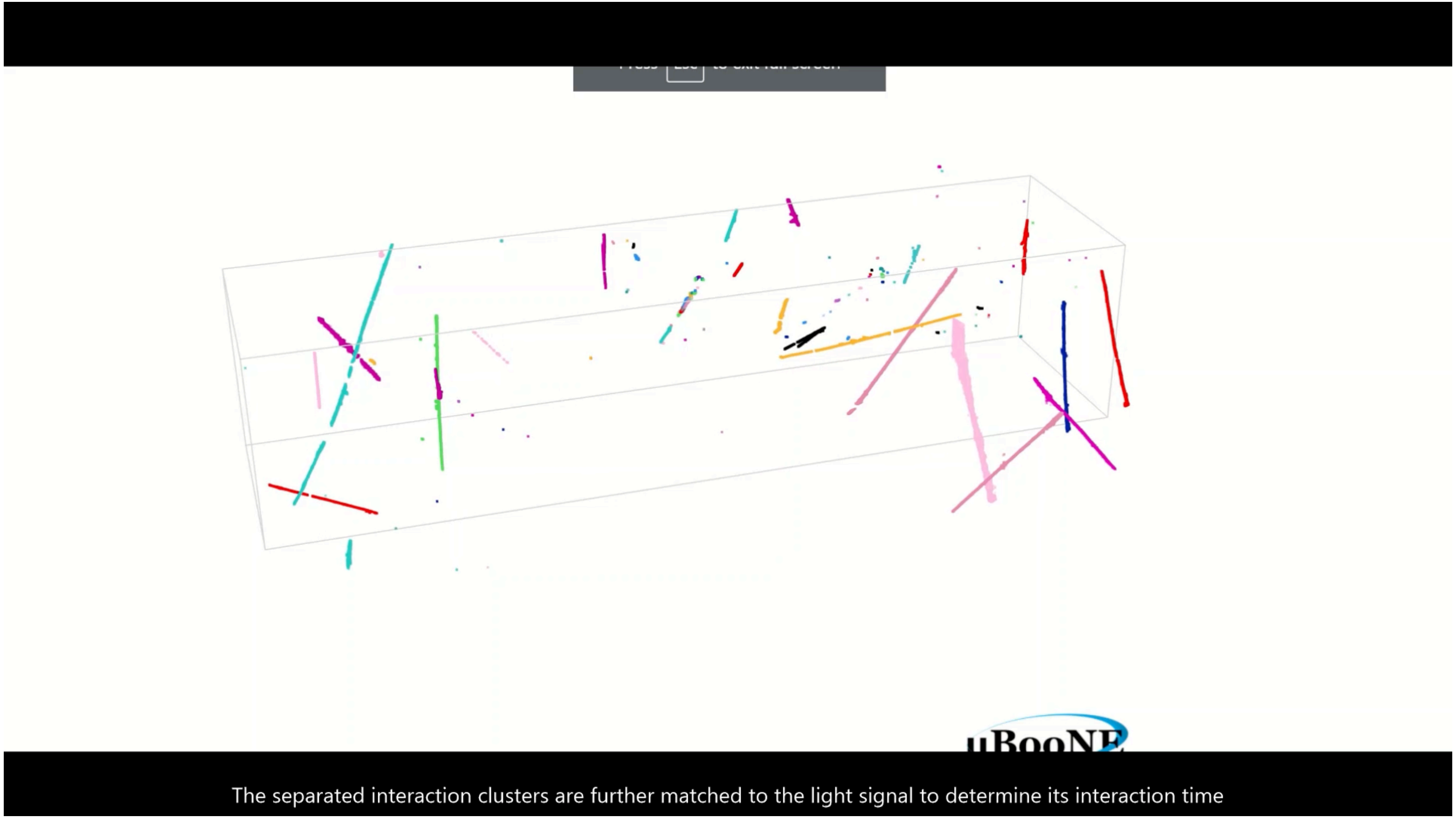

Wire-Cell event reconstruction & pattern recognition

selected neutrino event

track/shower separation

particle-level sub-clustering

3D dQ/dx information with PID capability

particle flow with DL-assisted neutrino vertex

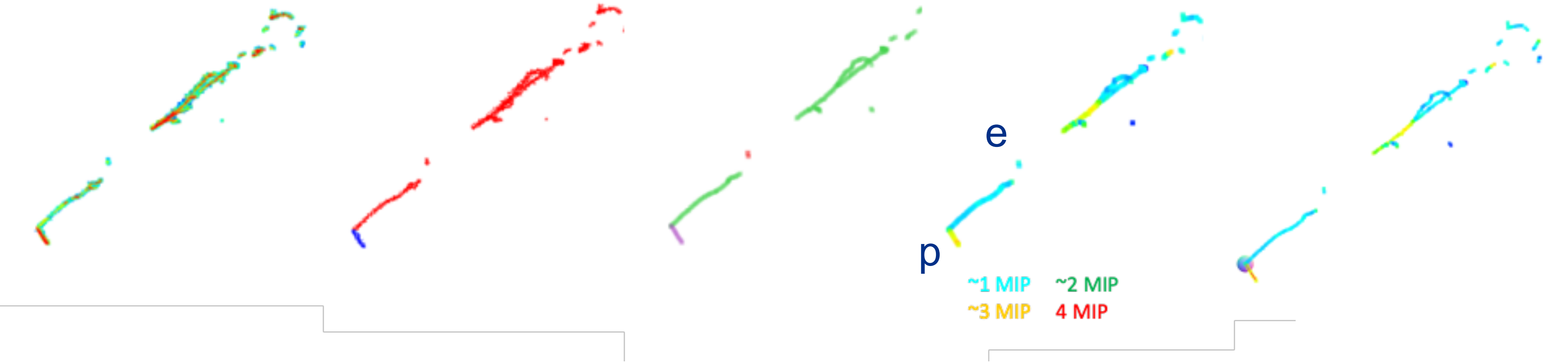

event reconstruction performance

arXiv:2110.13978

- neutrino energy reconstruction is performed based on calorimetry with particle ID information
  - 15-20% resolution for fully contained ν_μ CC
  - 10-15% resolution for fully contained ν_e CC
- track energy is calibrated with muons and protons
- shower energy is calibrated with π^0 invariant mass

FC* ν_μ CC

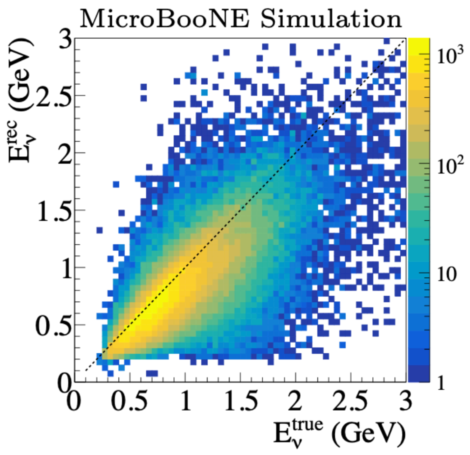

FC* ν_e CC

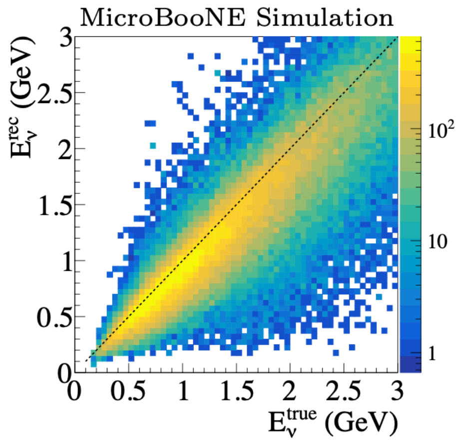

*FC "fully contained": events with reconstructed activity entirely within fiducial volume

event reconstruction performance

arXiv:2110.13978

- neutrino energy reconstruction is performed based on calorimetry with particle ID information
  - 15-20% resolution for fully contained ν_μ CC
  - 10-15% resolution for fully contained ν_e CC
- track energy is calibrated with muons and protons
- shower energy is calibrated with π^0 invariant mass

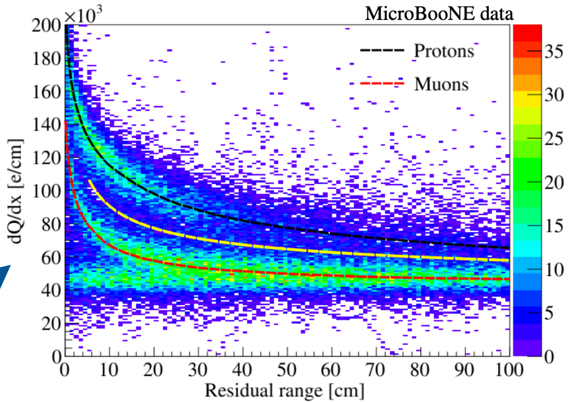

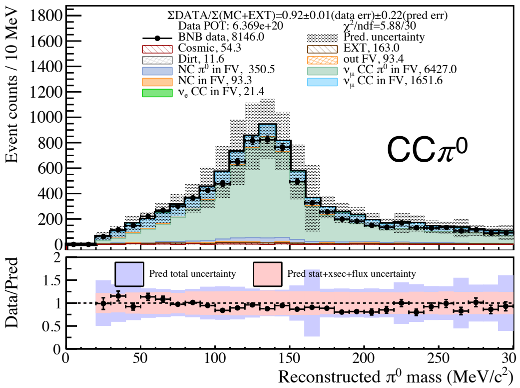

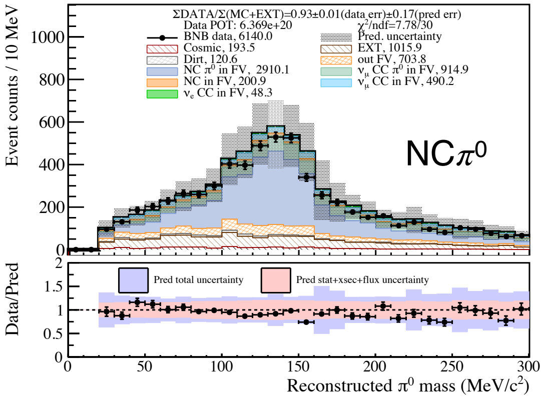

preselection: generic neutrino selection

- using Wire-Cell cosmic rejection, achieved high efficiency/purity neutrino selection
  - 99.999% cosmic background rejection
    - ν:cosmic-ray improved from 1:20k to 5.2:1
  - high ν_μ and ν_e selection efficiency
  - ν_e purity is only 0.4% at this stage
- serves as a preselection for ν_e and ν_μ selection for eLEE analysis

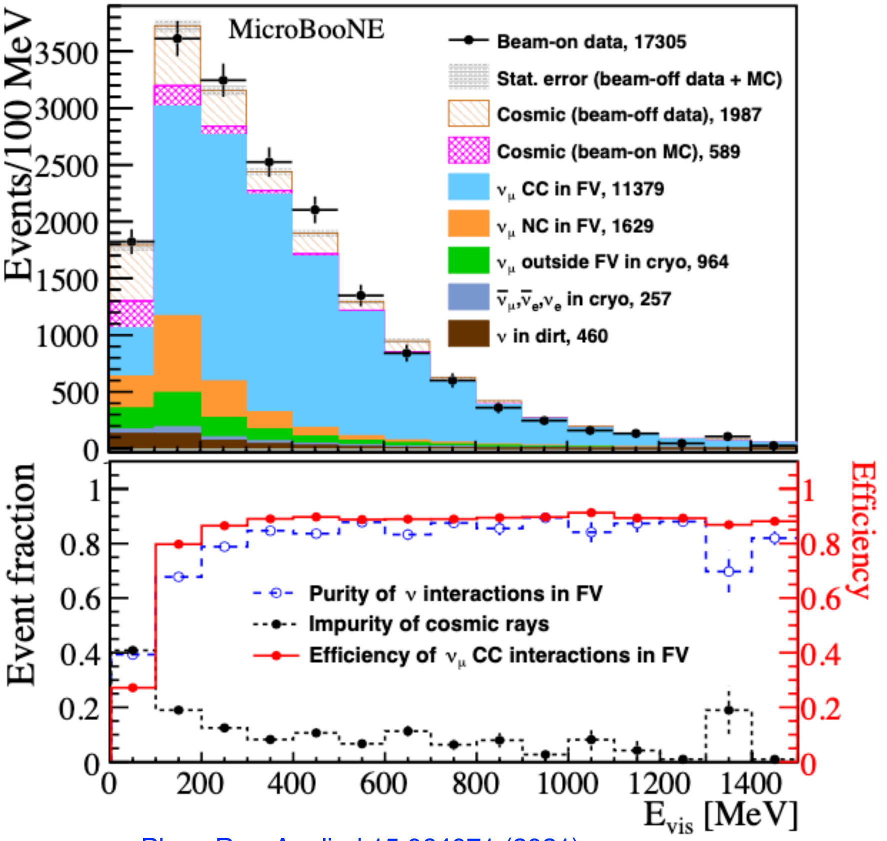

Phys. Rev. Applied 15 064071 (2021)

event selection: ν_μ CC & ν_e CC

arXiv:2110.13978

68% efficiency, 92% purity

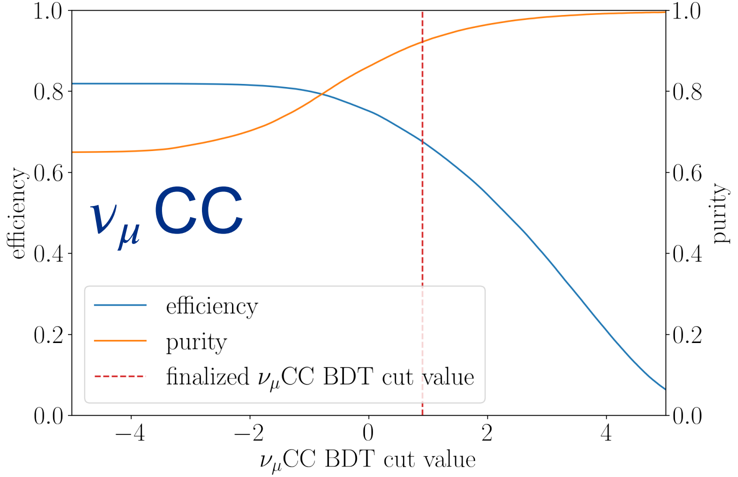

46% efficiency, 82% purity

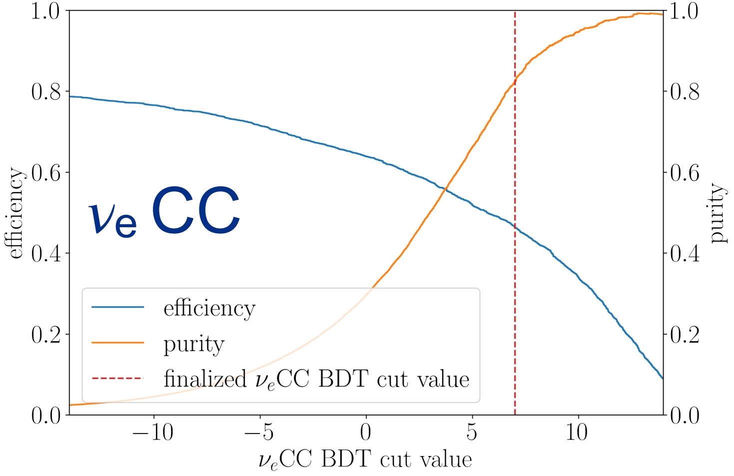

- combination of traditional tagging technique and machine-learning (BDT/XGBoost)
- excellent performance in ν_μ and ν_e selection
  - ν_e purity improved by more than a factor of 800 from the preselection stage
  - absolute efficiency is estimated with respect to total number of ν_μ/ν_e in active volume

event selection: ν_μ CC & ν_e CC

68% efficiency, 92% purity

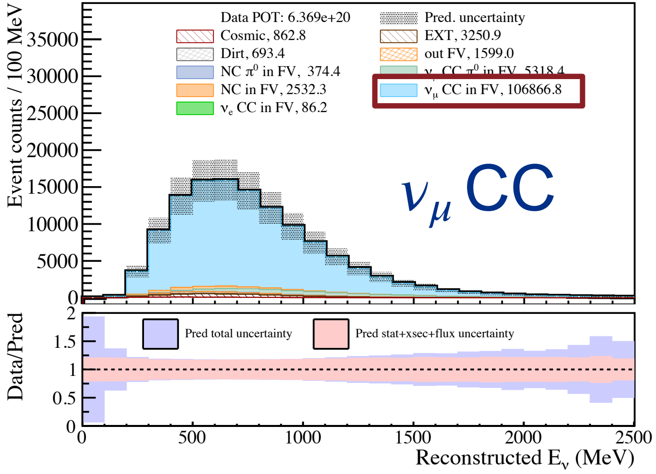

46% efficiency, 82% purity

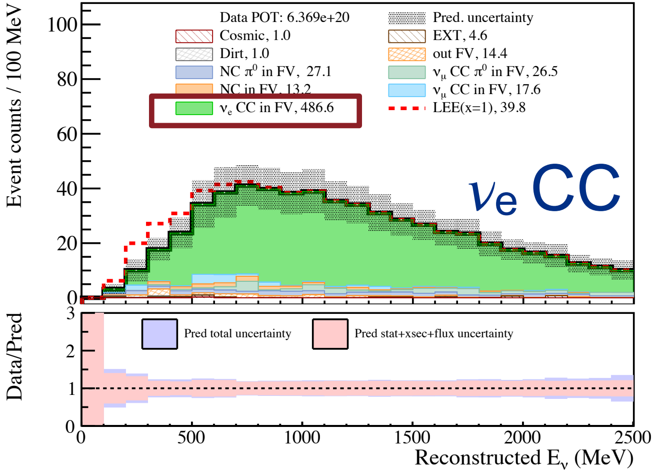

- combination of traditional tagging technique and machine-learning (BDT/XGBoost)
- excellent performance in ν_μ and ν_e selection
  - ν_e purity improved by more than a factor of 800 from the preselection stage
  - absolute efficiency is estimated with respect to total number of ν_μ/ν_e in active volume

7-channel selection & fit

- utilize 7 neutrino interaction channels to cross-check and constrain uncertainties in the ν_e signal channel and enhance eLEE sensitivity
- **signal**: fully contained ν_e CC
    - partially contained ν_e CC **sideband**: less sensitive to eLEE search, mainly serves as control sample
    - FC/PC ν_μ CC **sidebands**: mainly constrains flux & cross section systematics
    - FC/PC CC π^0, NC π^0 **sidebands**: mainly constrains background components in signal channel

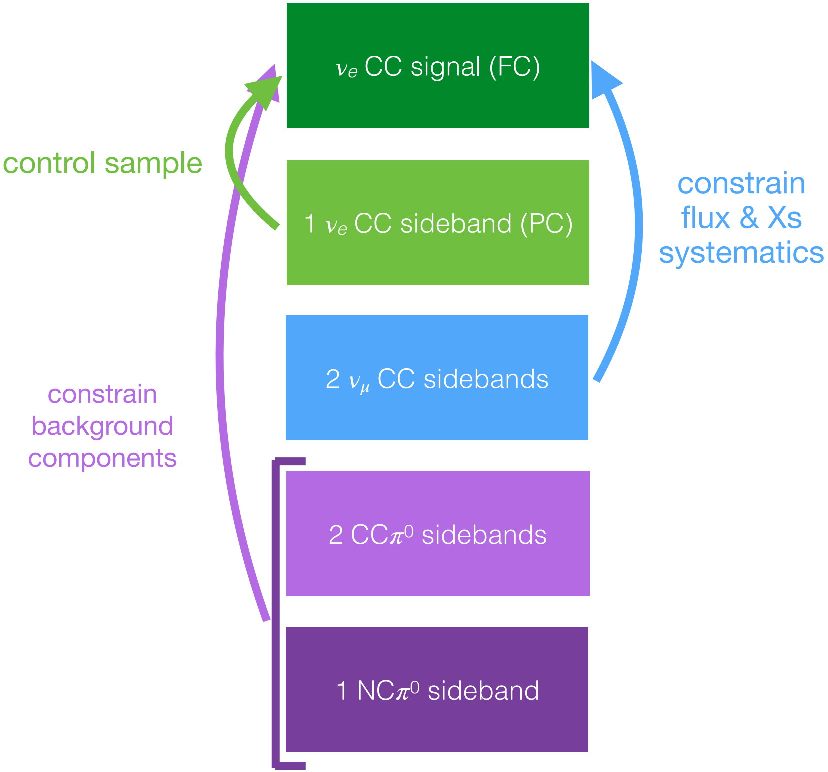

7-channel selection & fit

arXiv:2110.13978

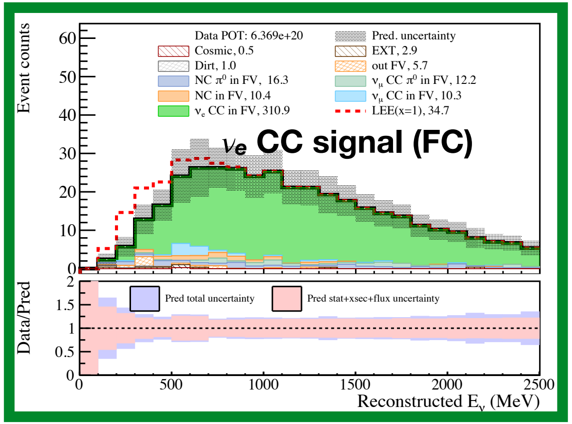

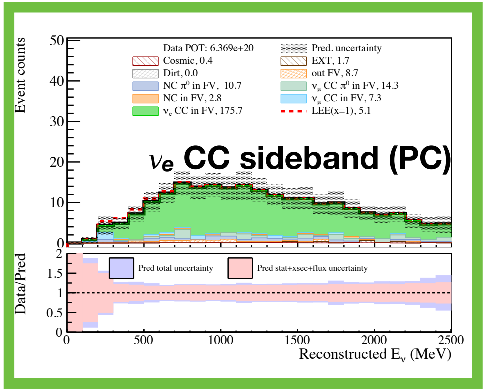

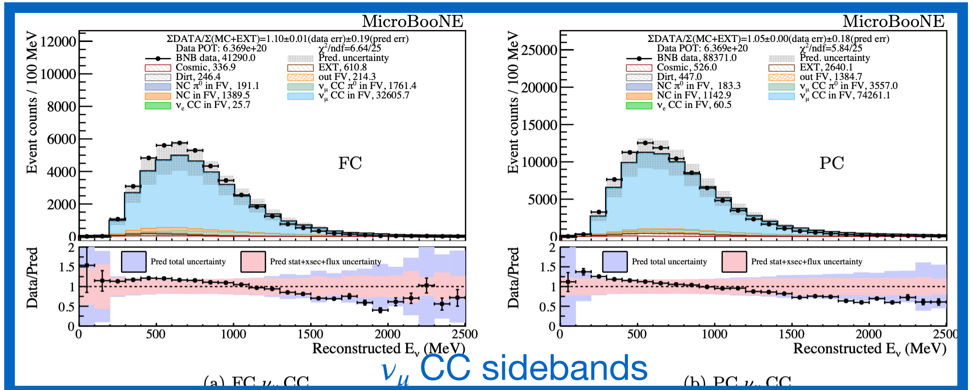

ν_μ CC sidebands

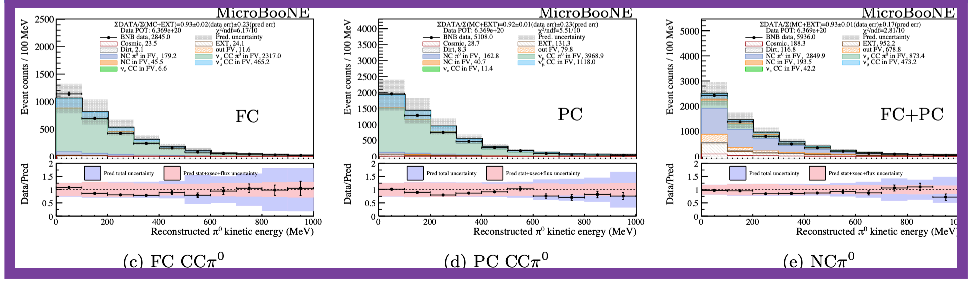

π^0 sidebands

sideband channels with high-statistic,
good data-MC agreement within systematics

systematic uncertainties

arXiv:2110.13978

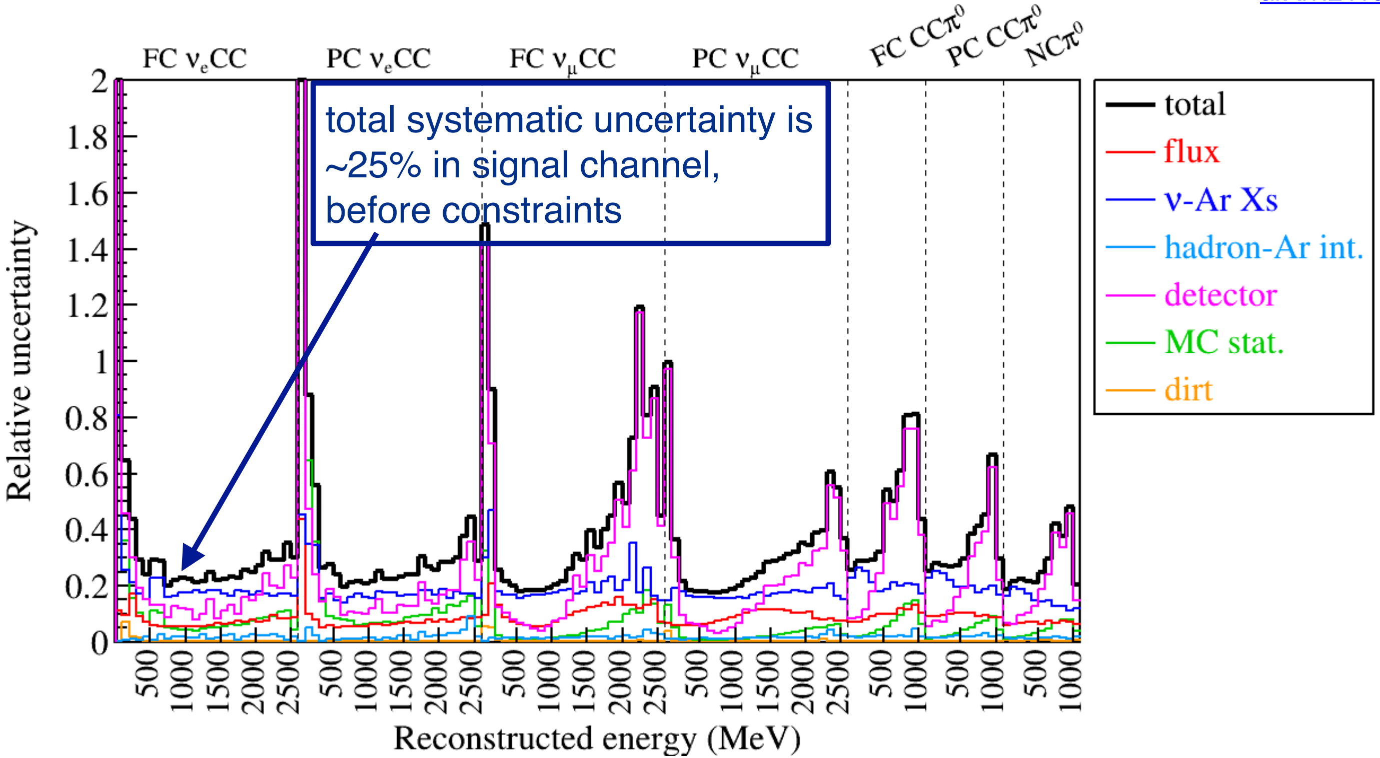

systematic uncertainties

arXiv:2110.13978

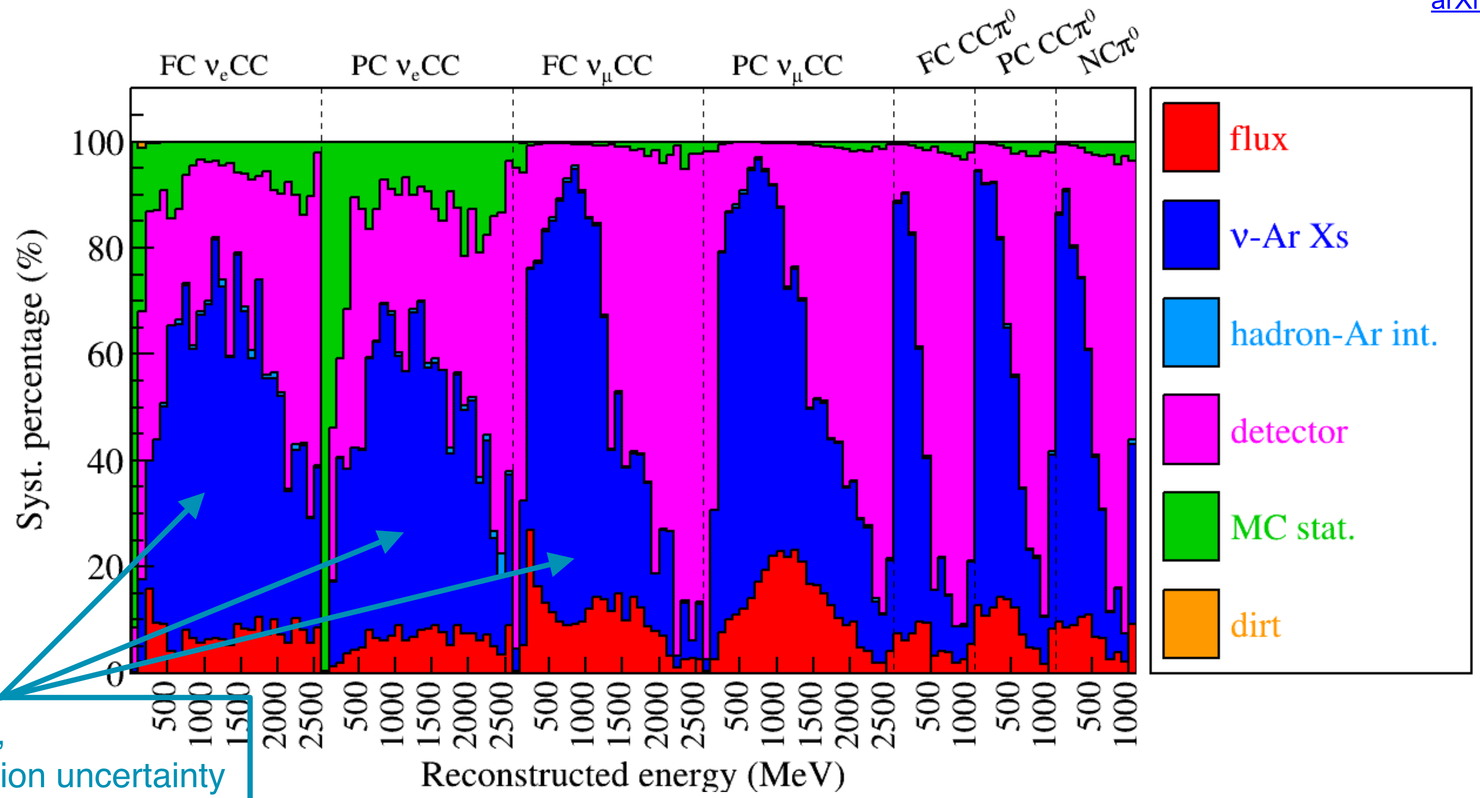

in general,
cross section uncertainty
dominates

µBooNE

systematic uncertainties

arXiv:2110.13978

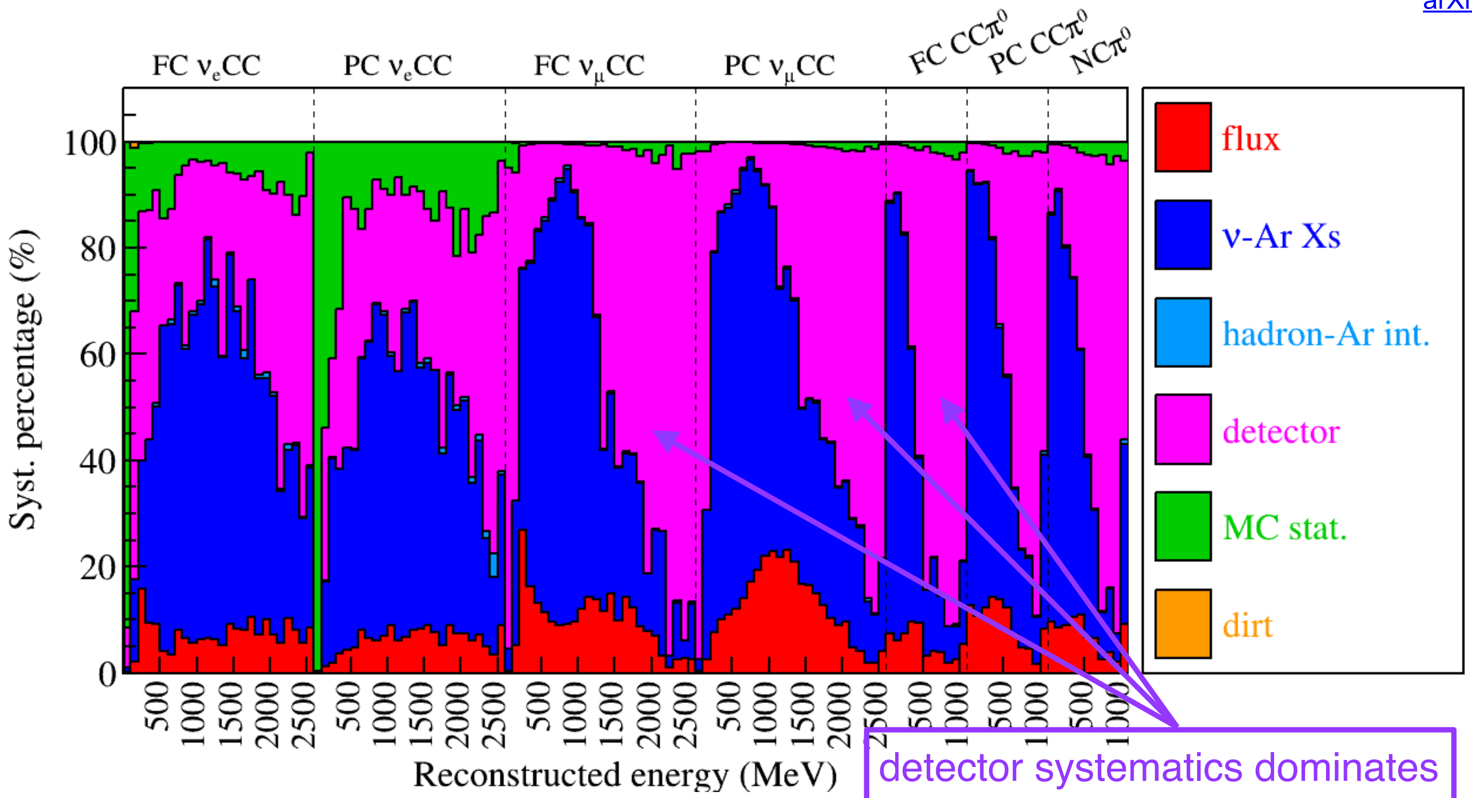

detector systematics dominates where statistics are low

impact of constraints from sidebands

arXiv:2110.13978

- ν_e prediction increases, mainly driven by ν_μ sidebands
- systematic uncertainty decreases by more than a factor of 3

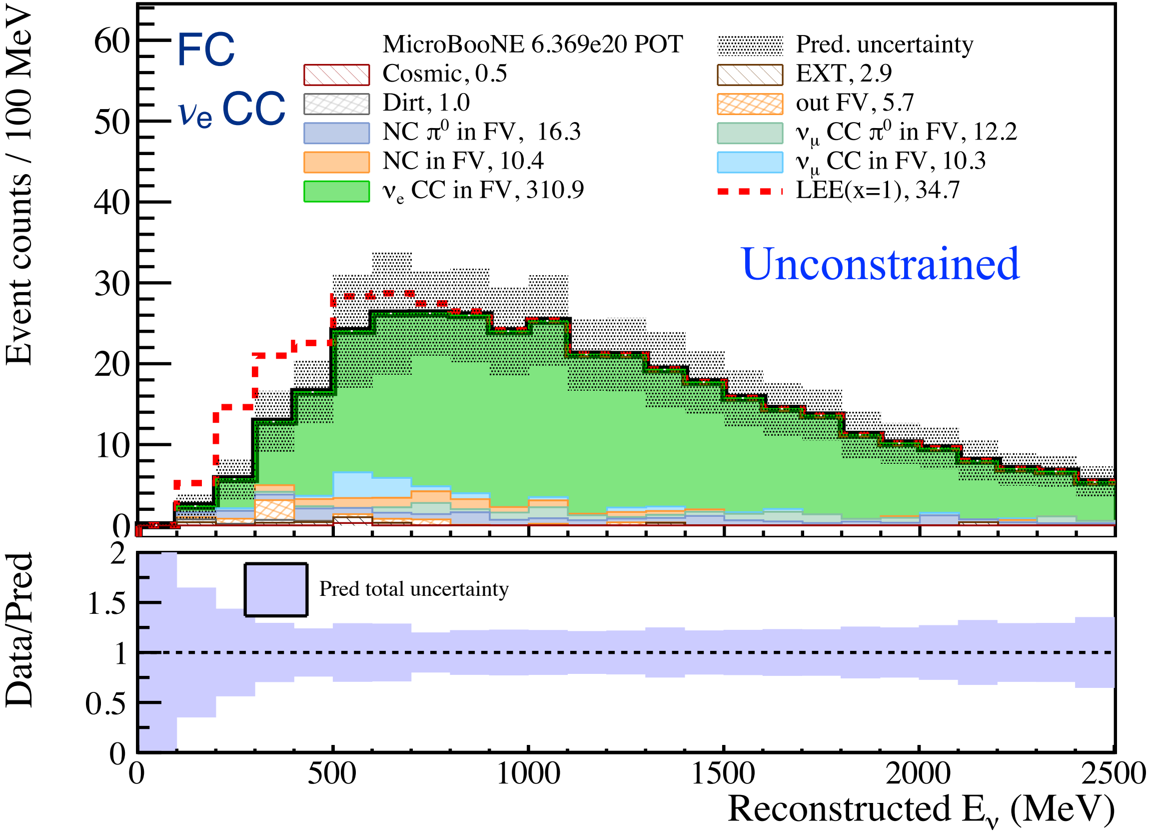

µBooNE

impact of constraints from sidebands

arXiv:2110.13978

- ν_e prediction increases, mainly driven by ν_μ sidebands
- systematic uncertainty decreases by more than a factor of 3

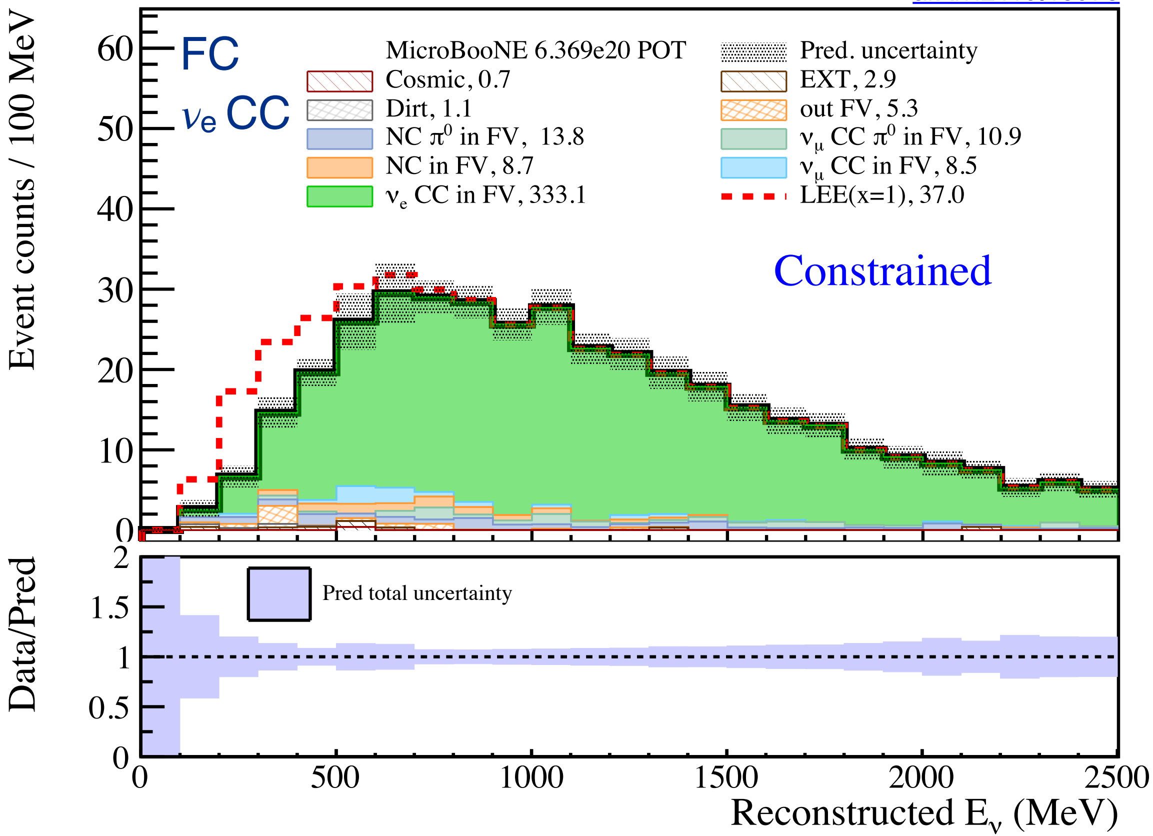

blind analysis

- sequentially unblind sample from higher to lower energy region
  - far sideband: $E_\nu > 800$ MeV
  - near sideband: 800 MeV > E_ν > 600 MeV
  - signal: $E_\nu < 600$ MeV

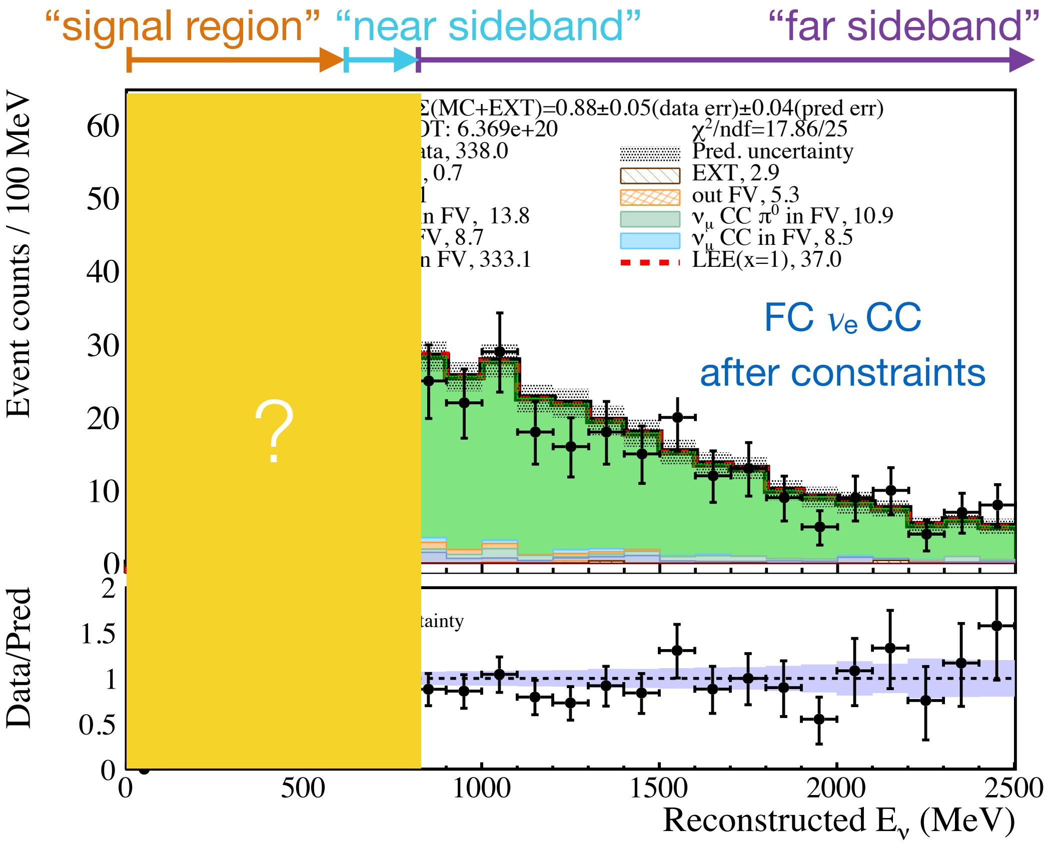

arXiv:2110.13978

blind analysis

- sequentially unblind sample from higher to lower energy region
  - far sideband: $E_\nu > 800$ MeV
  - near sideband: 800 MeV $> E_\nu >$ 600 MeV
  - signal: $E_\nu < 600$ MeV

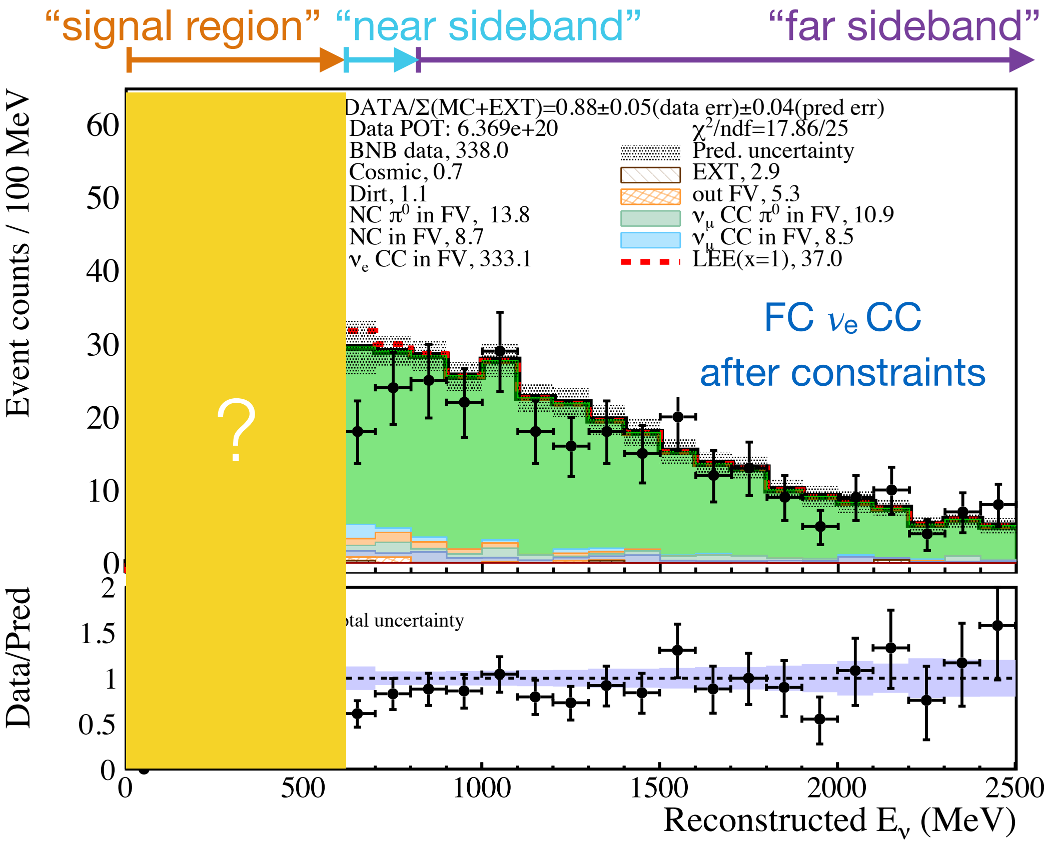

arXiv:2110.13978

blind analysis

- sequentially unblind sample from higher to lower energy region
  - far sideband:
    $E_\nu > 800$ MeV
  - near sideband:
    800 MeV $> E_\nu >$ 600 MeV
  - signal:
    $E_\nu < 600$ MeV

Image credit: seekpng.com

µBooNE

blind analysis

- sequentially unblind sample from higher to lower energy region
  - far sideband: $E_\nu > 800$ MeV
  - near sideband: 800 MeV $> E_\nu >$ 600 MeV
  - signal: $E_\nu < 600$ MeV

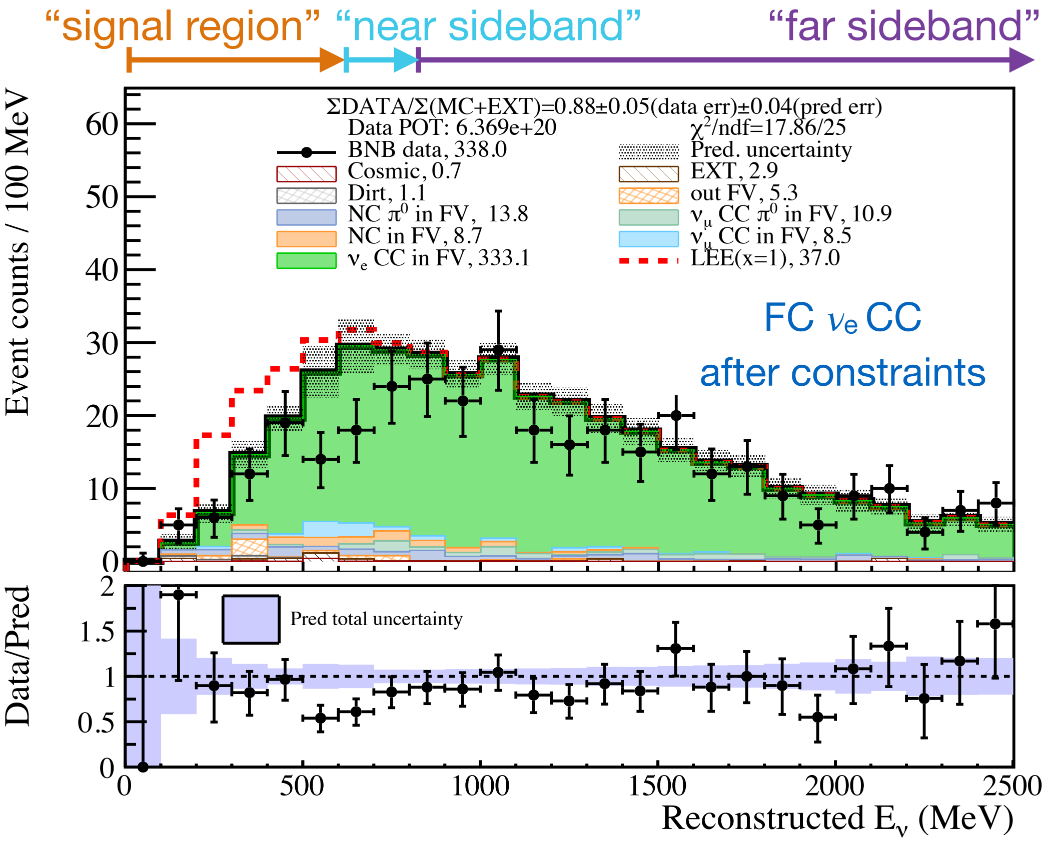

arXiv:2110.13978

results: CC selection

- observed 56 events in reconstructed E_ν 0-600 MeV range
- after constraints, we predict
  - 69.6 ± 5.0 (sys) ± 8.0 (stat) events with no LEE hypothesis ($eLEE_{x=0}$)
  - 103.8 ± 7.4 (sys) ± 9.0 (stat) events with LEE hypothesis ($eLEE_{x=1}$)
- data agrees better with $eLEE_{x=0}$ than $eLEE_{x=1}$

no excess of low energy ν_e candidates is observed!

arXiv:2110.13978

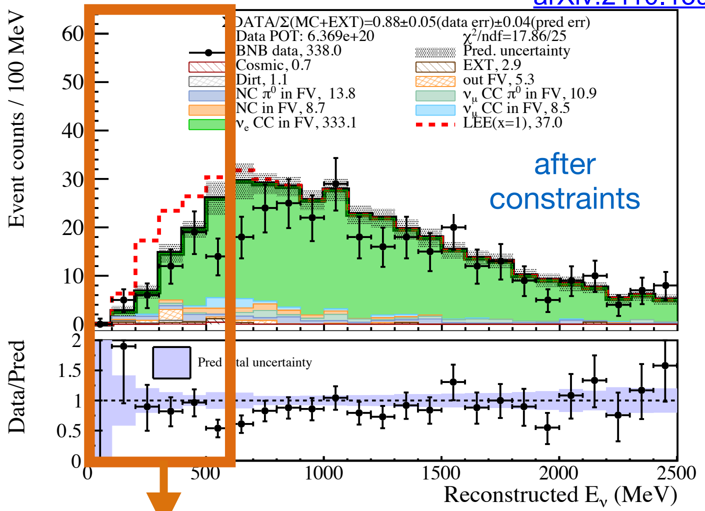

Category	Evts w/o constr.	Evts w/ constr.
Beam ν_eCC	42.6 ± 10.6	51.5 ± 2.6
ν_μCC π^0	0.6 ± 0.8	0.8 ± 0.8
ν_μCC (non-π^0)	3.9 ± 4.2	3.1 ± 3.1
NC π^0	4.5 ± 2.3	4.3 ± 1.6
NC (non-π^0)	3.0 ± 1.4	2.9 ± 1.2
Out of FV	3.8 ± 2.0	3.4 ± 1.6
Dirt	1.0 ± 1.0	1.2 ± 0.9
Cosmic	0.3 ± 0.6	0.5 ± 0.6
EXT (beam-off data)	1.9 ± 1.7	
Pred. total ($eLEE_{x=0}$)	61.5 ± 15.3 ± 7.7	69.6 ± 5.0 ± 8.0
Pred. total ($eLEE_{x=1}$)	91.8 ± 23.4 ± 8.7	103.8 ± 7.4 ± 9.0
BNB data	56	

simple vs. simple likelihood ratio test

arXiv:2110.13978

probability of the data rejecting one hypothesis assuming the other is true

nominal nue model

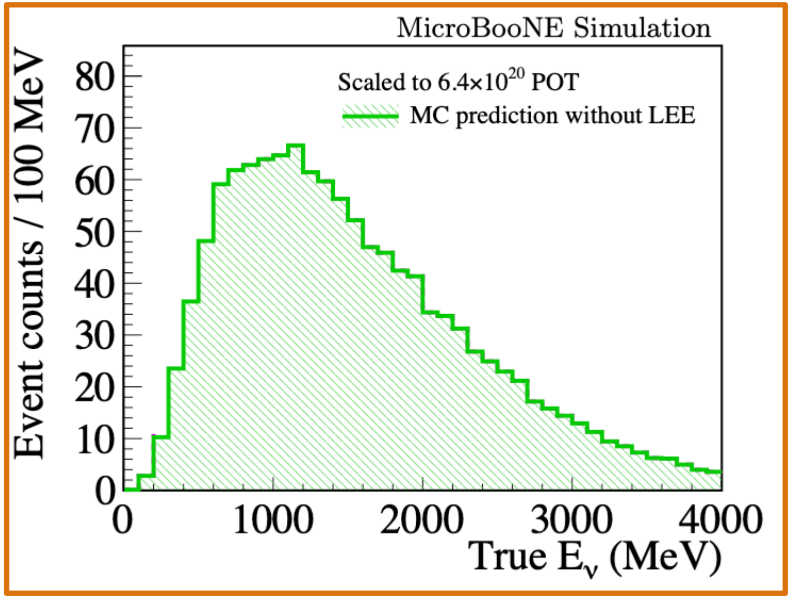

vs.

nominal nue + eLEE model

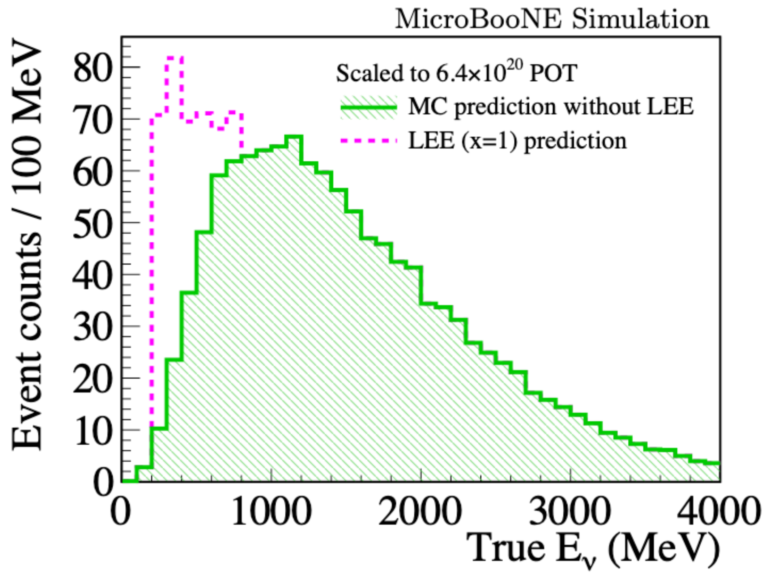

results: simple vs. simple likelihood ratio test

arXiv:2110.13978

assuming $eLEE_{x=0}$ hypothesis is true

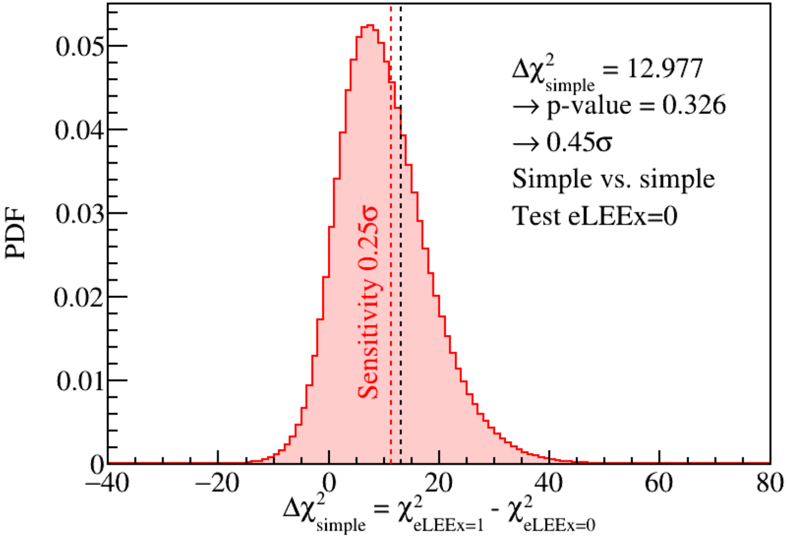

assuming $eLEE_{x=1}$ hypothesis is true

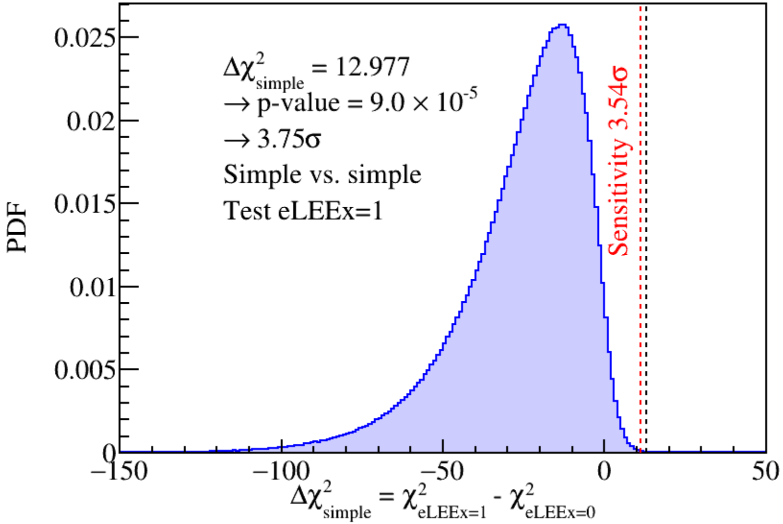

- $\Delta\chi^2_{\text{simple}} = \chi^2|_{\text{eLEEx=1}} - \chi^2|_{\text{eLEEx=0}} = 12.977$
- consistent with $eLEE_{x=0}$ at 0.45σ
- **disfavors the $eLEE_{x=1}$ hypothesis at 3.75σ significance level**

µBooNE

MicroBooNE's search for an excess of electron neutrino interactions

three independent searches across multiple single electron final states

- exclusive two-body charged-current quasi-elastic (CCQE) ν_e scattering [1e1p]

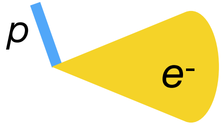

excludes eLEE model at 2.4σ

[arXiv:2110.14080](https://arxiv.org/abs/2110.14080)

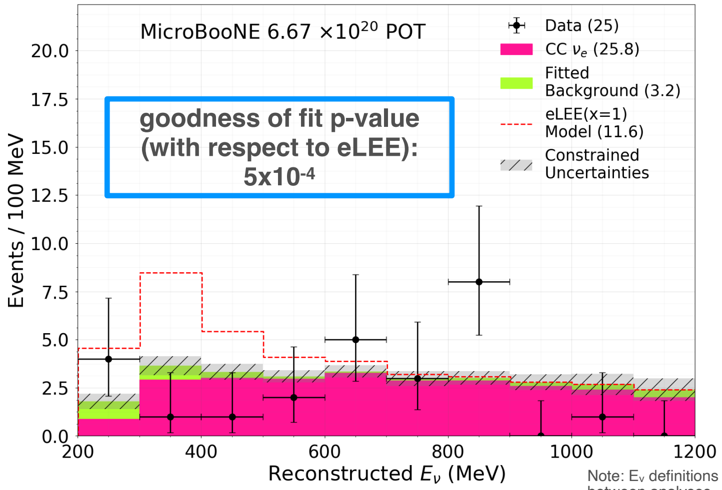

Note: E_ν definitions differ between analyses

MicroBooNE's search for an excess of electron neutrino interactions

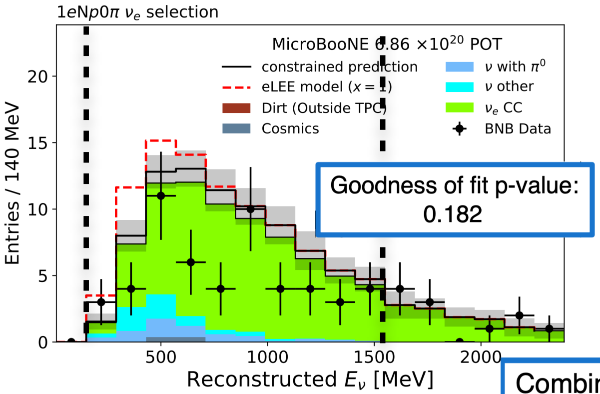

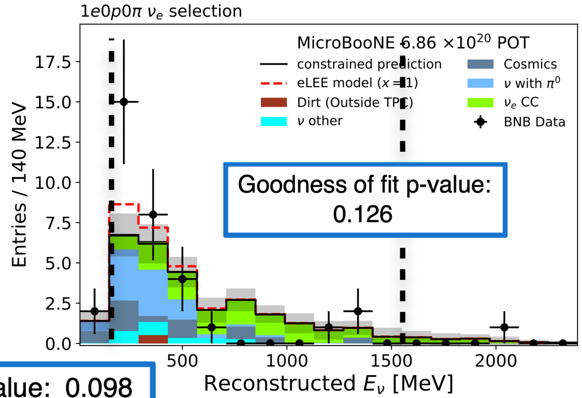

Note: E_ν definitions differ between analyses

Combined p-value: 0.098

arXiv:2110.14065

- semi-inclusive ν_e scattering without final state pions [1eNp0π (N≥1) + 1e0p0π]

Excludes eLEE model at 97.9% level

Low sensitivity, prefers eLEE model over nominal ν_e model

what we've accomplished

- co-developed 3 different fully-automated event reconstructions and 3 distinct LEE search analyses targeting both exclusive and inclusive ν_e final states: CCQE 1e1p, 1eNp0π + 1e0p0π, 1eX
- used the powerful imaging capabilities of the LArTPC to isolate high-purity ν_e CC event samples with excellent rejection backgrounds
- both are transformative for the field and feed directly into DUNE

arXiv:2110.14080

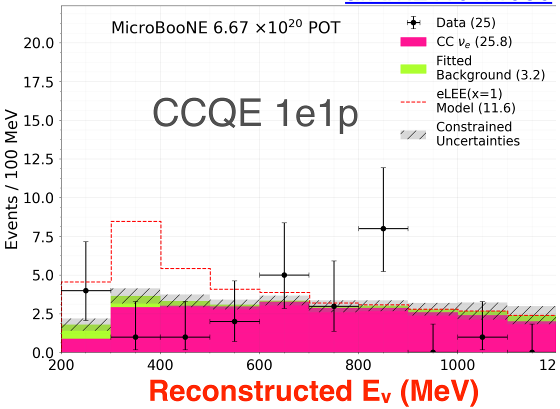

arXiv:2110.14065

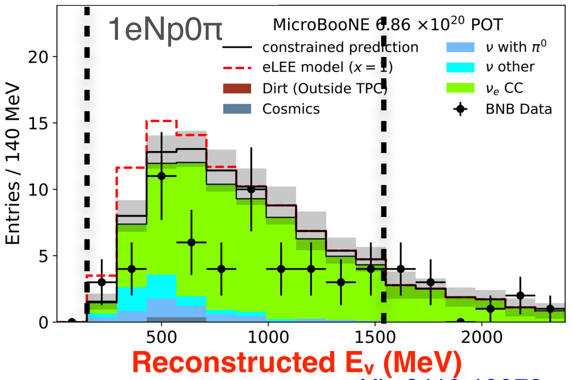

arXiv:2110.14065

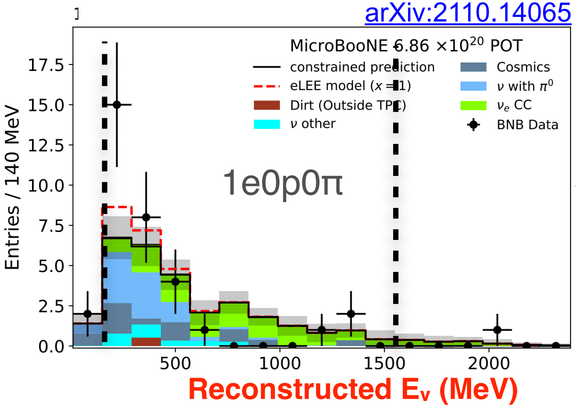

arXiv:2110.13978

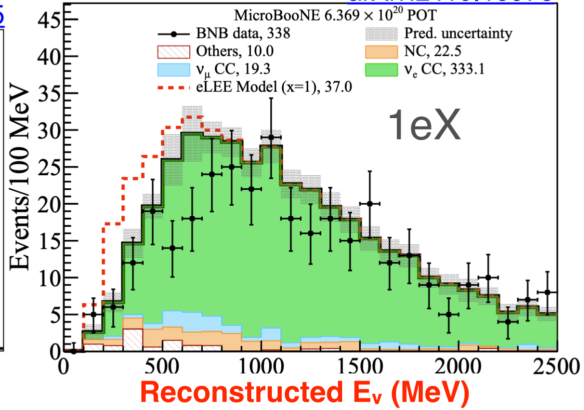

comparisons to ν_e prediction

arXiv:2110.14054

- ν_e prediction adequately describes the data across many different kinematic quantities
- observe ν_e candidate event rates in general agreement with or below the predicted rates
  - same overall picture in the low-energy region

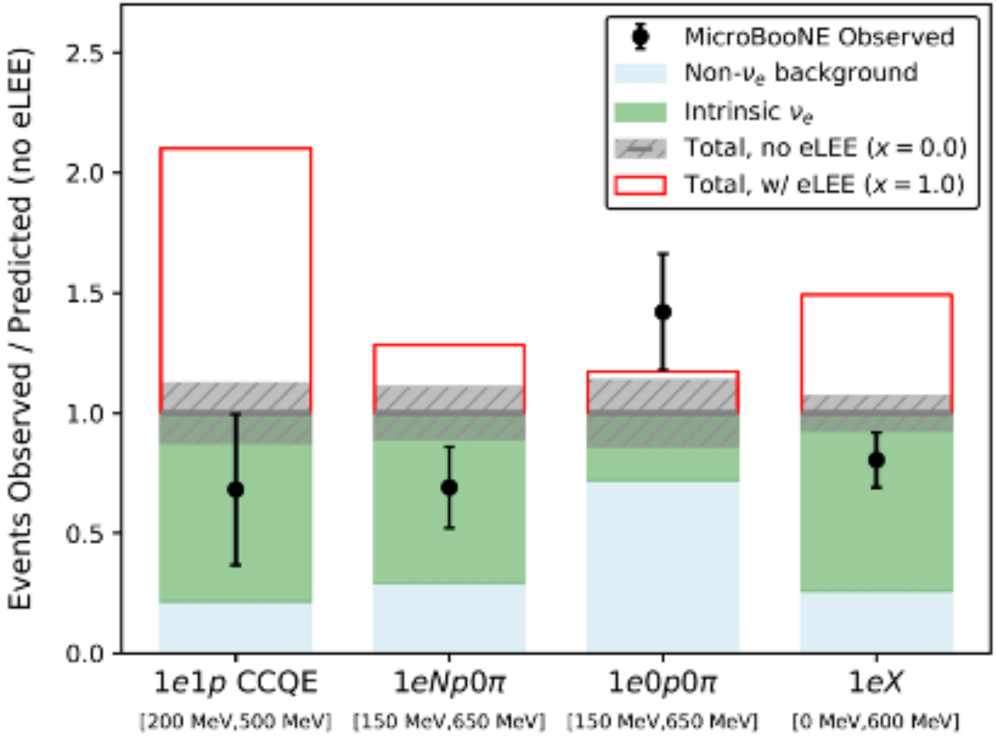

comparisons to ν_e prediction

arXiv:2110.14054

- ν_e prediction adequately describes the data across many different kinematic quantities

- observe ν_e candidate event rates in general agreement with or below the predicted rates
  - same overall picture in the low-energy region

Channels	Reconstruction	Efficiency	Purity	Data Events
CCQE 1e1p	Deep Learning	6.6%	75%	25
1e0p0π	Pandora	9%	43%	34
1eNp0π	Pandora	15%	80%	64
Inclusive 1eX	Wire-Cell	46%	82%	606

MicroBooNE’s exploration of the MiniBooNE excess

First series of results (1/2 the MicroBooNE data set)

Models \ Reco topology	1e0p	1e1p	1eNp	1eX	e^+e^- + nothing	e^+e^-X	$1\gamma 0p$	$1\gamma 1p$	$1\gamma X$
eV Sterile ν Osc	✔	✔	✔	✔					
Mixed Osc + Sterile ν	✔ [7]	✔ [7]	✔ [7]	✔ [7]			✔ [7]		
Sterile ν Decay	✔ [13,14]	✔ [13,14]	✔ [13.14]	✔ [13,14]			✔ [4,11,12,15]	✔ [4]	✔ [4]
Dark Sector & Z’ *	✔ [2,3]				✔ [2,3]	✔ [2,3]	✔ [1,2,3]	✔ [1,2,3]	✔ [1,2,3]
More complex higgs *					✔ [10]	✔ [10]	✔ [6,10]	✔ [6,10]	✔ [6,10]
Axion-like particle *					✔ [8]		✔ [8]		
Res matter effects	✔ [5]	✔ [5]	✔ [5]	✔ [5]					
SM γ production							✔	✔	✔

* Requires heavy sterile/other new particles also

evolving theory landscape

motivated by attempts to explain the new MiniBooNE results as well as other experimental data; eg., ν_e appearance but no ν_μ disappearance *(Caution: not an exhaustive list!)*

- Decay of O(keV) Sterile Neutrinos to active neutrinos
  - *[13] Dentler, Esteban, Kopp, Machado Phys. Rev. D 101, 115013 (2020)*
  - *[14] de Gouvêa, Peres, Prakash, Stenico JHEP 07 (2020) 141*
- New resonance matter effects
  - *[5] Asaadi, Church, Guenette, Jones, Szelc, PRD 97, 075021 (2018)*
- Mixed O(1eV) sterile oscillations and O(100 MeV) sterile decay
  - *[7] Vergani, Kamp, Diaz, Arguelles, Conrad, Shaevitz, Uchida, arXiv:2105.06470*
- Decay of heavy sterile neutrinos produced in beam
  - *[4] Gninenko, Phys.Rev.D83:015015,2011*
  - *[12] Alvarez-Ruso, Saul-Sala, Phys. Rev. D 101, 075045 (2020)*
  - *[15] Magill, Plestid, Pospelov, Tsai Phys. Rev. D 98, 115015 (2018)*
  - *[11] Fischer, Hernandez-Cabezudo, Schwetz, PRD 101, 075045 (2020)*
- Decay of upscattered heavy sterile neutrinos or new scalars mediated by Z' or more complex higgs sectors
  - *[1] Bertuzzo, Jana, Machado, Zukanovich Funchal, PRL 121, 241801 (2018)*
  - *[2] Abdullahi, Hostert, Pascoli, Phys.Lett.B 820 (2021) 136531*
  - *[3] Ballett, Pascoli, Ross-Lonergan, PRD 99, 071701 (2019)*
  - *[10] Dutta, Ghosh, Li, PRD 102, 055017 (2020)*
  - *[6] Abdallah, Gandhi, Roy, Phys. Rev. D 104, 055028 (2021)*
- Decay of axion-like particles
  - *[8] Chang, Chen, Ho, Tseng, Phys. Rev. D 104, 015030 (2021)*
- A model-independent approach to any new particle
  - *[9] Brdar, Fischer, Smirnov, PRD 103, 075008 (2021)*

Produces true electrons

Produces true photons

Produces e^+e^- pairs

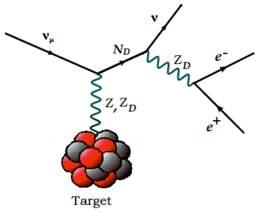

PRL 121, 241801 (2018)

- many of these models predict more complex final states (e^+e^-) and/or differing levels of hadronic activity

→ *the **hadronic state** is becoming increasingly more important as a model discriminator*

- we are fortunate that LArTPCs are sensitive to these possibilities

summary

- our results are found to be consistent with the nominal ν_e rate expectations from the Booster Neutrino Beam
  - no excess of ν_e events is observed
  - disfavor generic ν_e interactions as the primary contributor to the excess
  - reject simple eLEE model of the MiniBooNE low energy excess at >97% for both exclusive and inclusive event classes

- we disfavor the interpretation of MiniBooNE LEE as a x3.18 enhancement of NC $\Delta \rightarrow N\gamma$ rate at 94.8% CL

- together, these are the first detailed study of the MiniBooNE low energy excess that first appeared in 2007

- MicroBooNE laid groundwork for the SBN and DUNE experiments

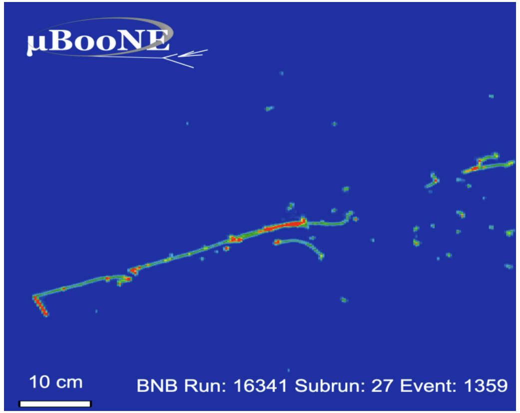

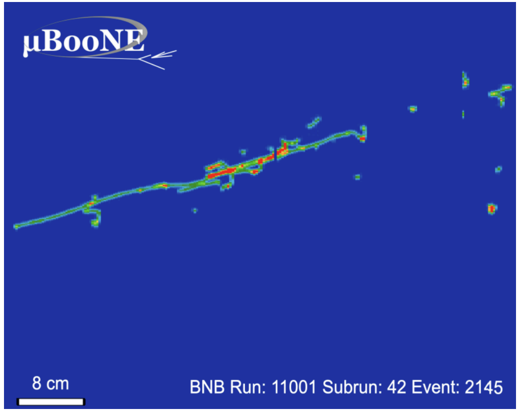

summary

- stay tuned—more to come!
  - tests of additional LEE models
    - analyses targeting additional models and new final states topologies are well underway
  - x2 data statistics
    - all LEE search analyses reported here are still statistics-limited
  - Fermilab Short-Baseline Neutrino Program will soon add further to this picture

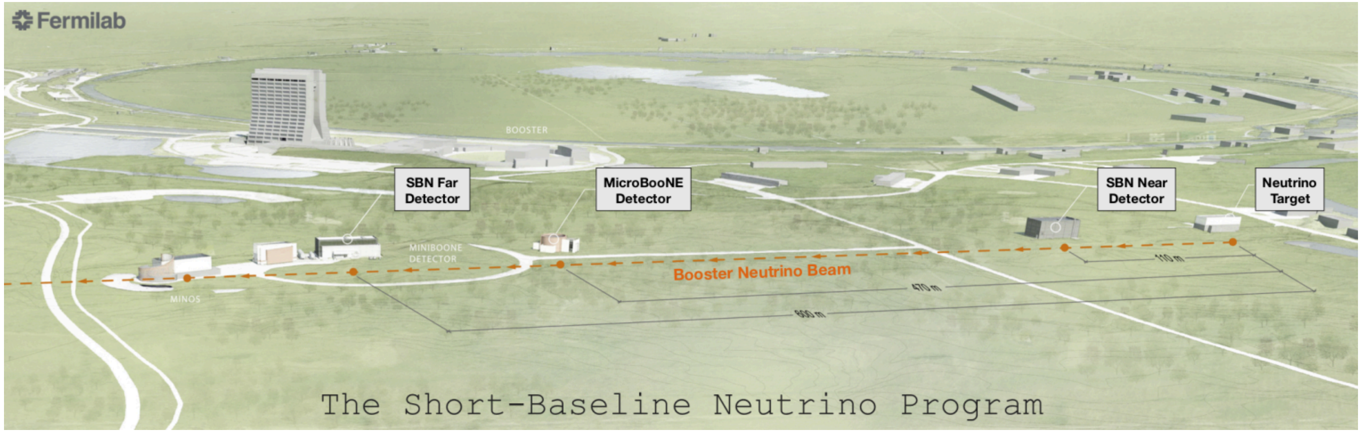

Backup slides

reactor anomaly and gallium anomaly

- measurements of $\overline{\nu}_e$ disappearance from nuclear reactor
- ~6% discrepancy from the standard fit
- current running experiments addressed this fairly well: issues in predicting reactor neutrino flux (e.g. PROSPECT, STEREO)
- could this still be consistent of sterile neutrinos scenario?

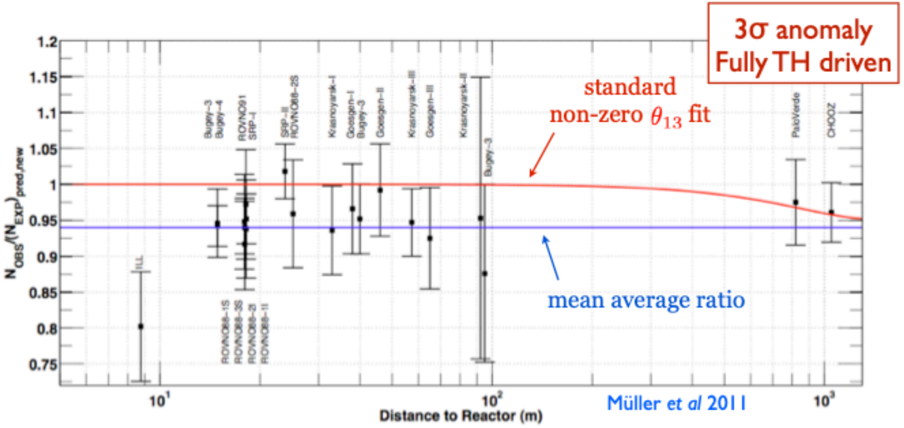

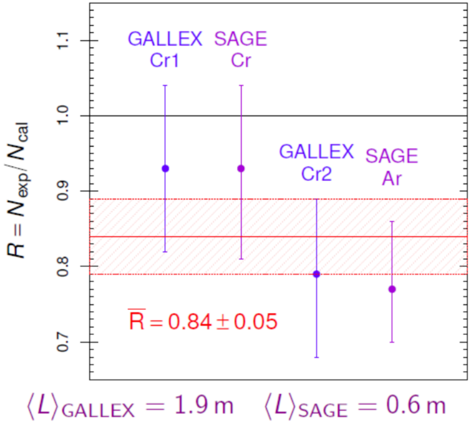

Phys. Rev. C 73, 045805 (2006)

- gallium-based experiments (GALLEX, SAGE) measured a deficit of ν_e in their calibration run
  - recent BEST result confirmed this deficit
- possible hint of ν_e disappearance?

LSND & MiniBooNE anomaly

Phys. Rev. D 64 112007, 2001

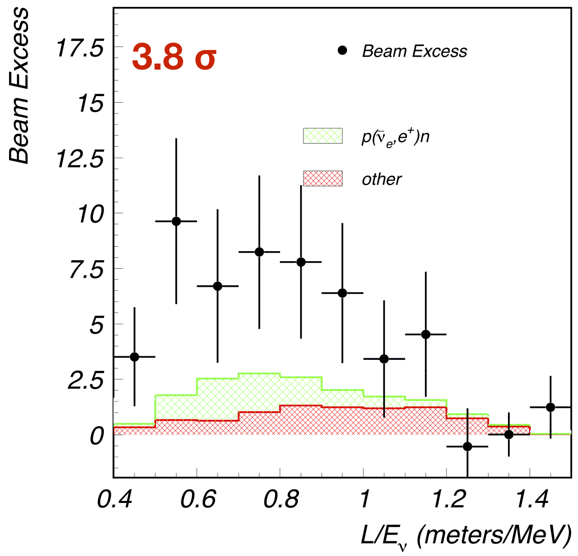

- **LSND** (1990-2001)
- $\overline{\nu}_\mu \rightarrow \overline{\nu}_e$ excess over background suggests evidence for oscillation at $\Delta m^2 \sim 1 eV^2$

Phys. Rev. D 103, 052002 (2021)

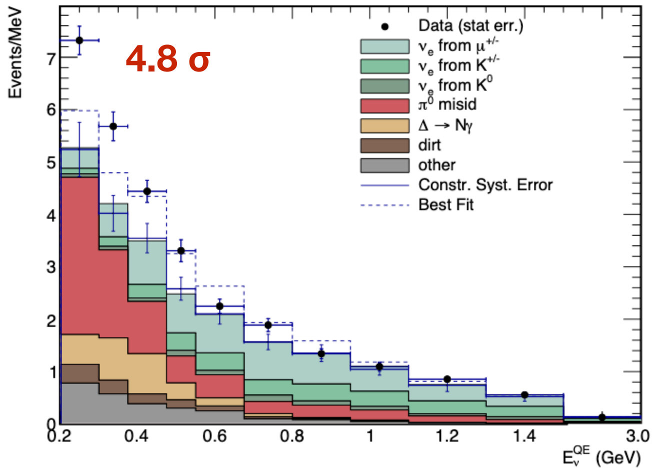

- **MiniBooNE** (1998-2020)
- measured $\nu_\mu \rightarrow \nu_e$ and $\overline{\nu}_\mu \rightarrow \overline{\nu}_e$ appearance
- the excess of events at low energy

tension in global picture

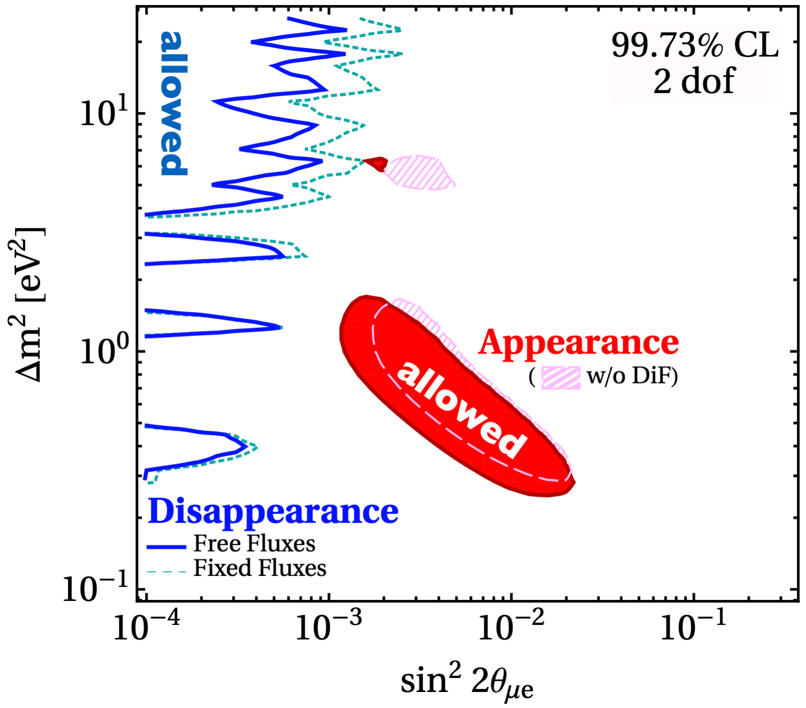

- *unfortunately, it's more complicated than that…*
- significant tension between ν_e appearance and ν_e and ν_μ disappearance
- lots of different independent observations currently unexplained
- *we need to understand the anomalies better!*

From Pedro Machado's Neutrino 2020 talk: Sterile Neutrino Global Picture

Inclusive 1eX Observations

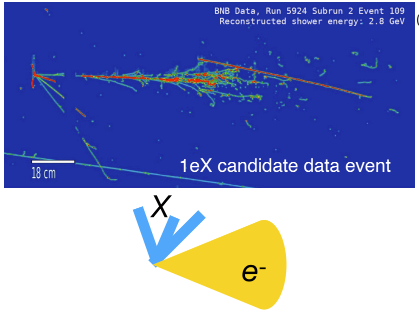

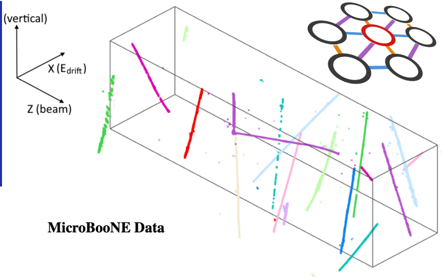

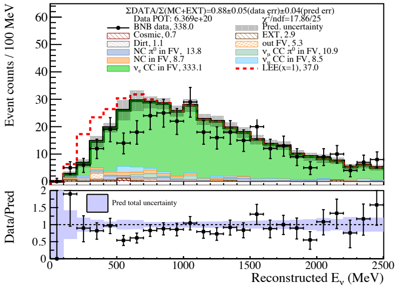

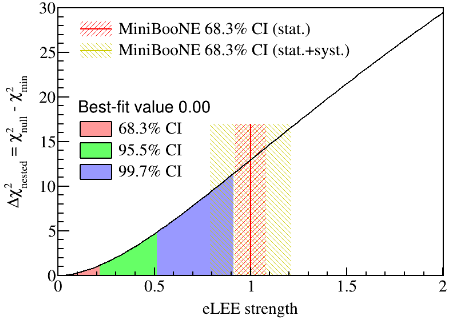

- Wire-Cell eLEE analysis aims to search for anomalous excess of *inclusive* ν_e CC interactions with Wire-Cell 3D tomographic reconstruction and 3D pattern recognition
- leveraging high-statistics sideband samples and using 7-channel fit to enhance eLEE sensitivity
- simple vs. simple hypothesis test **rejects eLEE hypothesis ($eLEE_{x=1}$) at 3.75σ**
- best-fit eLEE strength x is determined to be 0, **disfavoring MiniBooNE 68% confidence interval at over 2.6σ**

eLEE search: why Wire-Cell reconstruction?

- **Wire-Cell**: 3D tomographic imaging reconstruction algorithm
- reconstruct events in **3D**, unlike other 2D-based reconstruction paradigms
  - topology-agnostic reconstruction; good for high efficiency, inclusive selection
  - does not need all 3 wires to be active; resulting in nonfunctional volume decrease from 30% to 3%
  - excellent in recovering “broken” tracks/showers from unresponsive TPC wires; better particle ID performance

JINST 16 P06043 (2021)

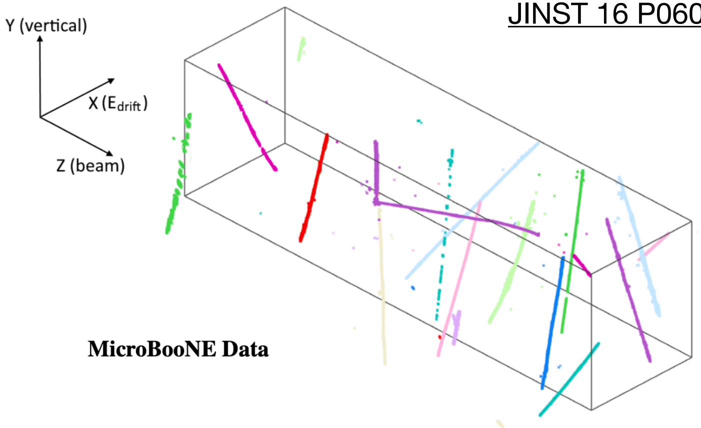

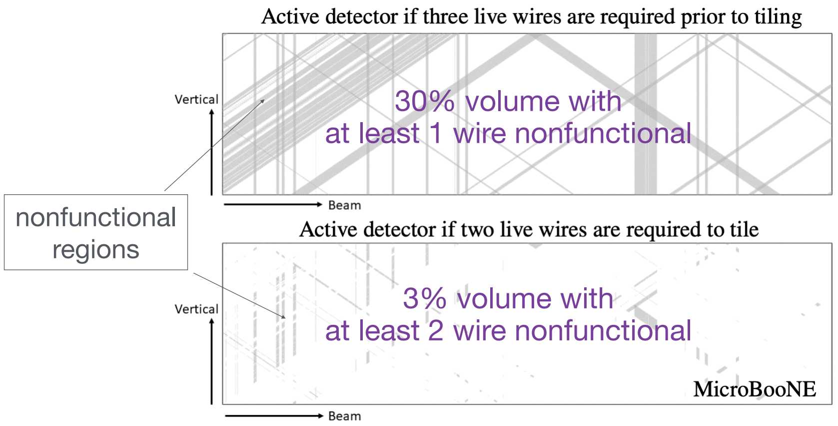

eLEE search: why Wire-Cell reconstruction?

JINST 16 P06043 (2021)

- **Wire-Cell**: 3D tomographic imaging reconstruction algorithm
- reconstruct events in **3D**, unlike other 2D-based reconstruction paradigms
  - topology-agnostic reconstruction; good for high efficiency, inclusive selection
  - does not need all 3 wires to be active; resulting in nonfunctional volume decrease from 30% to 3%
  - excellent in recovering "broken" tracks/showers from unresponsive TPC wires; better particle ID performance

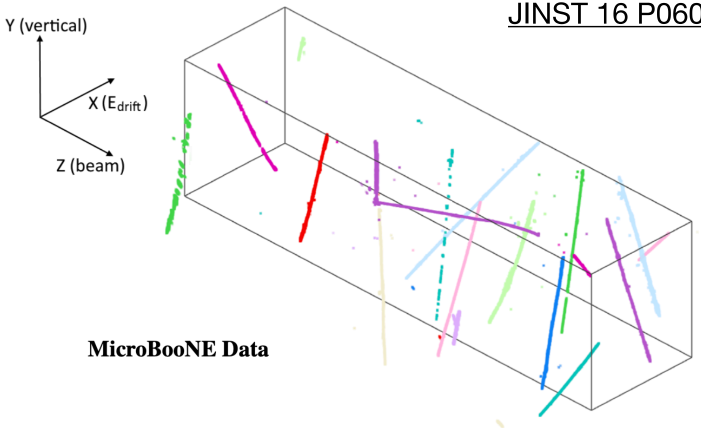

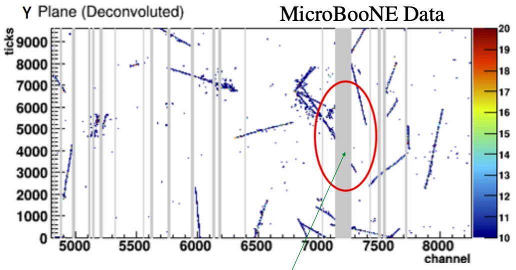

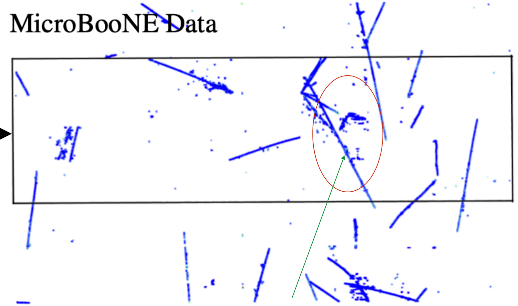

gap in a track from unresponsive wire

gap-recovered track with Wire-Cell reconstruction

Wire-Cell event reconstruction: imaging, clustering, matching

[JINST 16 P06043 (2021)]

- **3D imaging & clustering**
  - 2D wire-to-3D cell: capitalize all information from the TPC 2D wires, reconstruct 3D cell image of ionization electrons

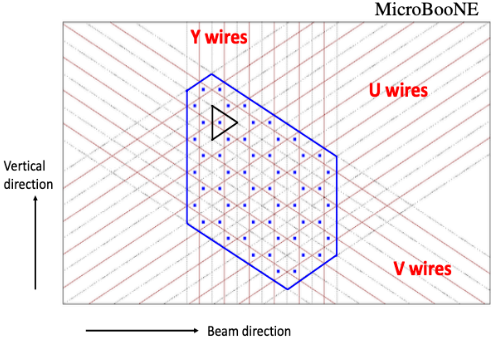

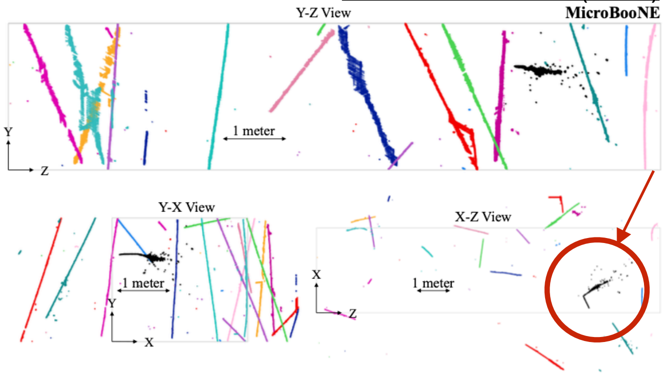

- **(many-to-many) charge-light matching**
  - pairing TPC charge activity to scintillation light signal detected with PMTs
  - among reconstructed 3D images, remove cosmic-ray muon events by a factor or 30-40

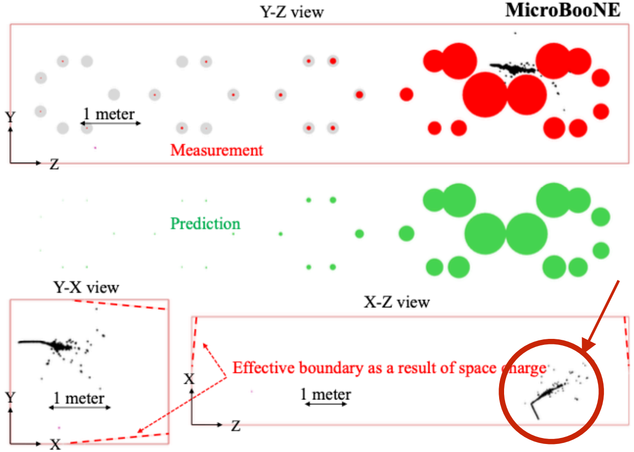

Wire-Cell generic neutrino selection

Phys. Rev. Applied 15 064071 (2021)

- majority of the remaining in-beam candidates still originate from cosmic-ray muons, such as: through-going mons, stopped muons, or light-mismatched events
- advanced tools developed
  - precise estimation of effective TPC boundary
  - trajectory and dQ/dx fitting
  - various tagger for cosmic muons

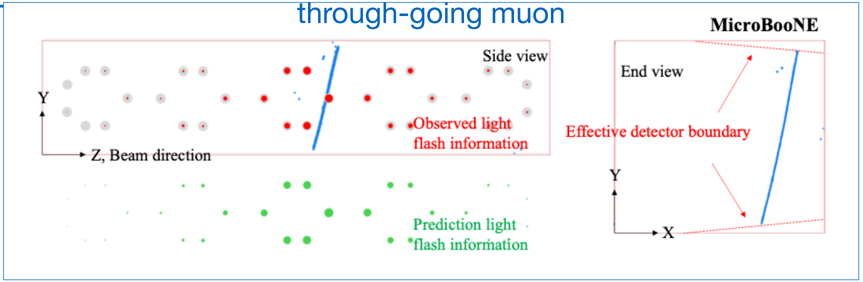

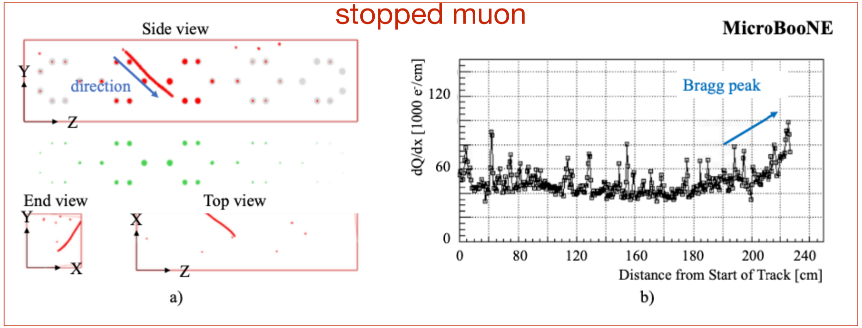

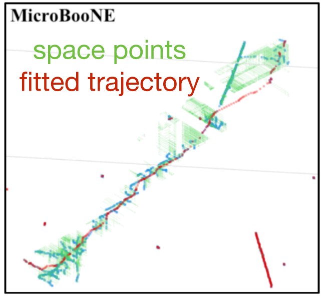

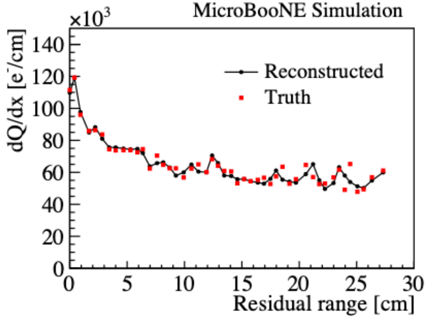

energy resolution & bias

[arXiv:2110.13978](https://arxiv.org/abs/2110.13978)

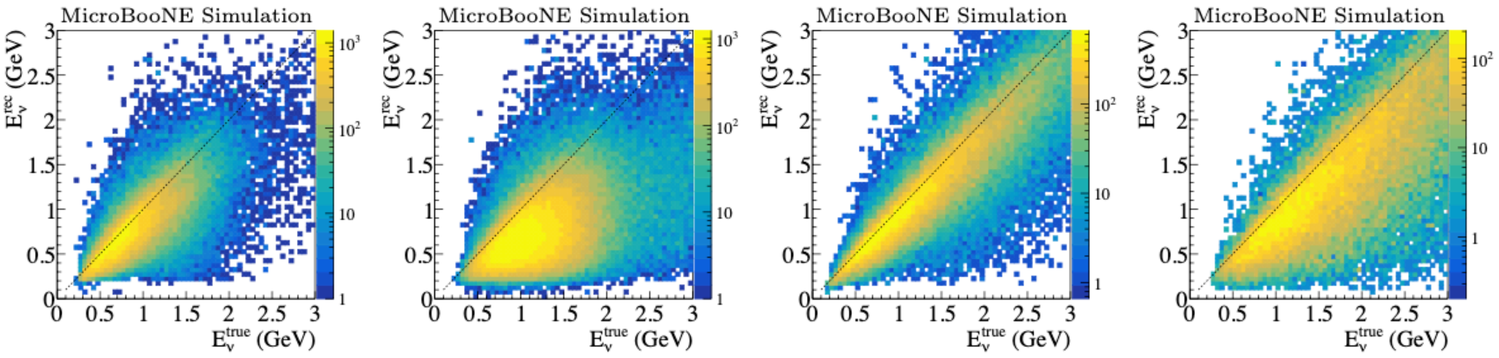

(a) ν_μ CC candidates, FC (b) ν_μ CC candidates, PC (c) ν_e CC candidates, FC (d) ν_e CC candidates, PC

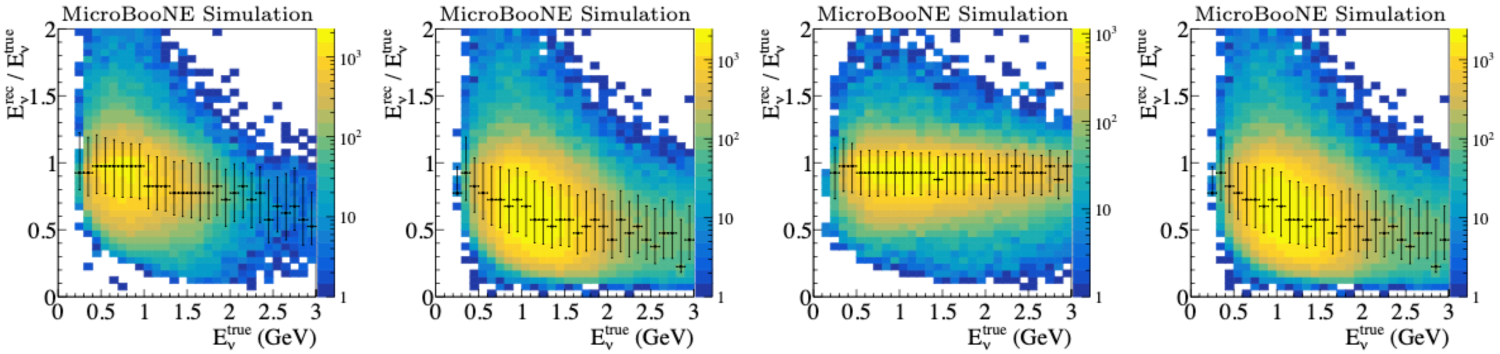

(e) ν_μ CC candidates, FC (f) ν_μ CC candidates, PC (g) ν_e CC candidates, FC (h) ν_e CC candidates, PC

selection efficiency: ν_e CC

arXiv:2110.13978

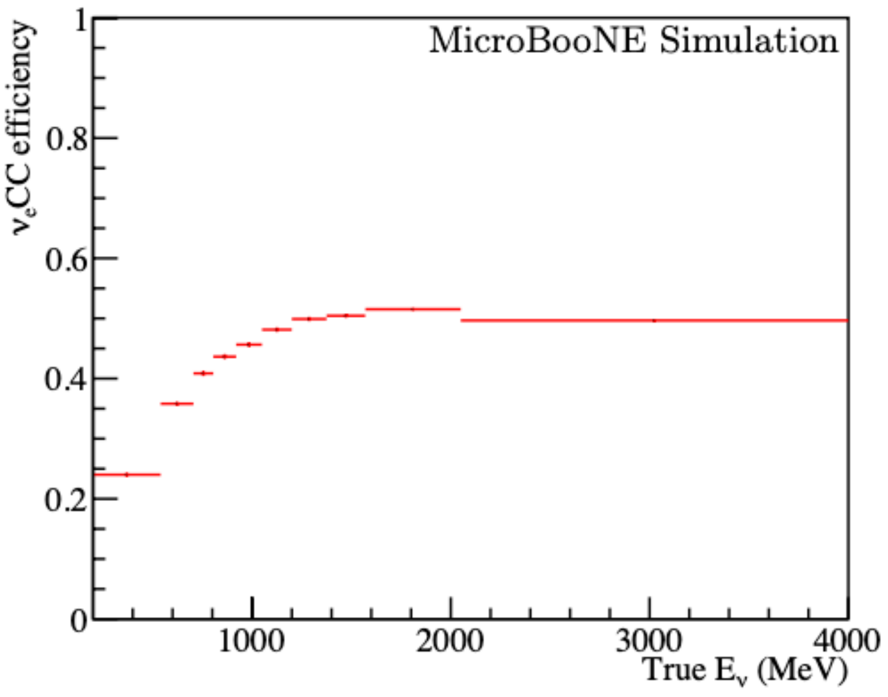

(e) Efficiency as a function of true neutrino energy

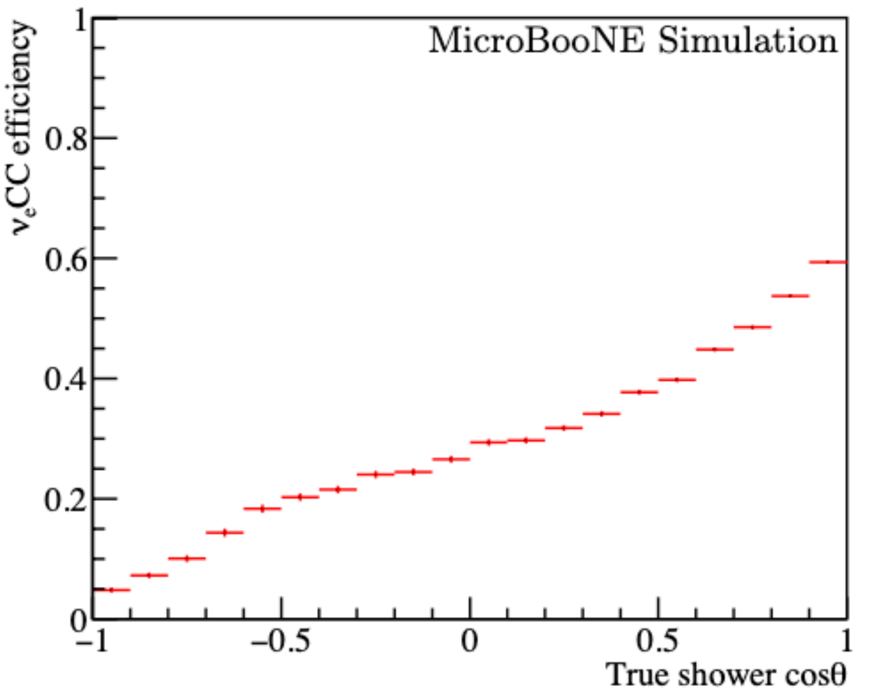

(f) Efficiency as a function of true shower $\cos\theta$

selection efficiency: ν_μ CC

arXiv:2110.13978

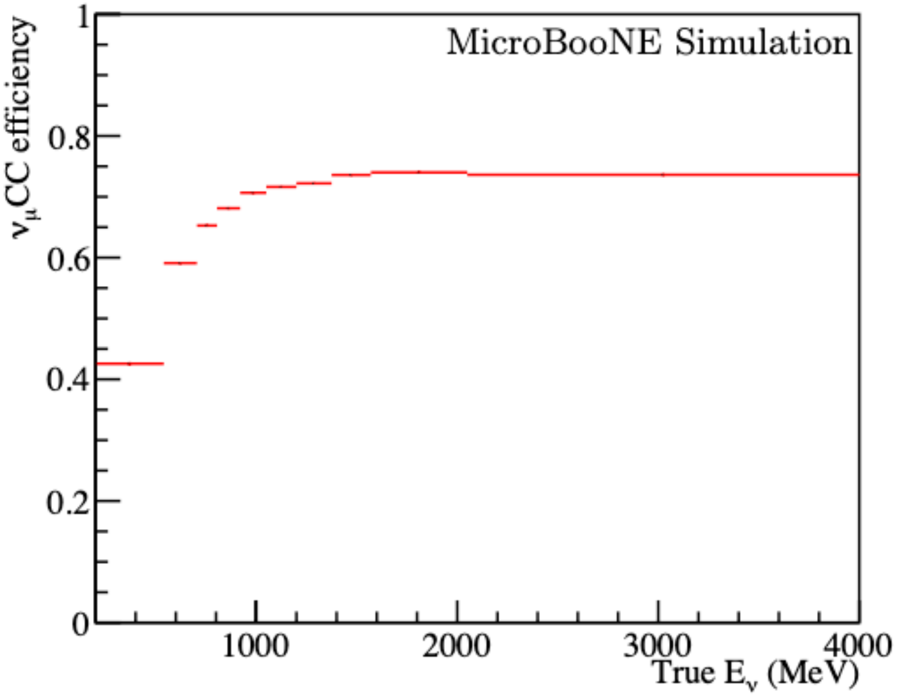

(e) Efficiency as a function of true neutrino energy

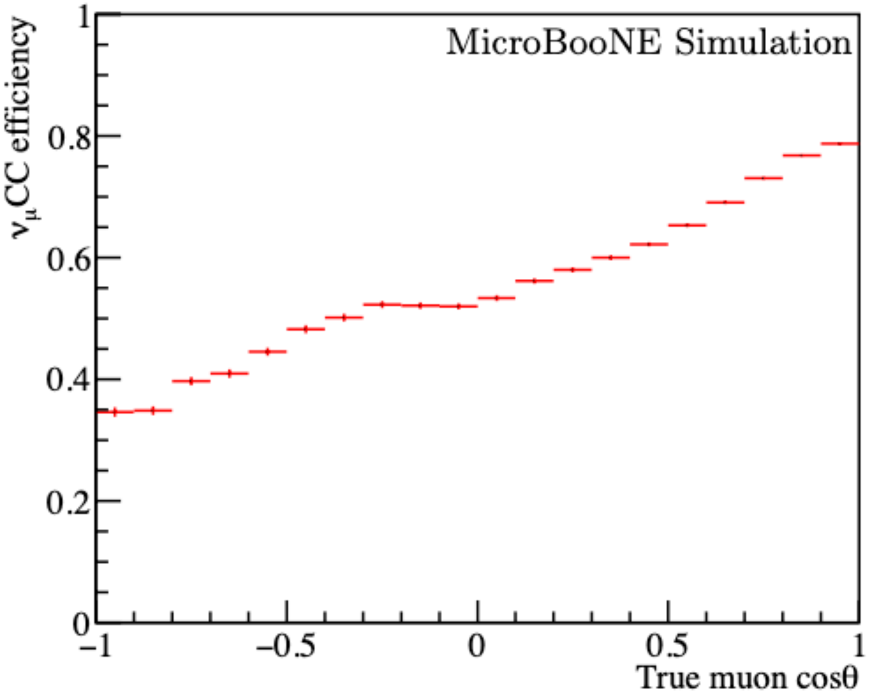

(f) Efficiency as a function of true muon $\cos\theta$

interaction type breakdown: ν_e CC

arXiv:2110.13978

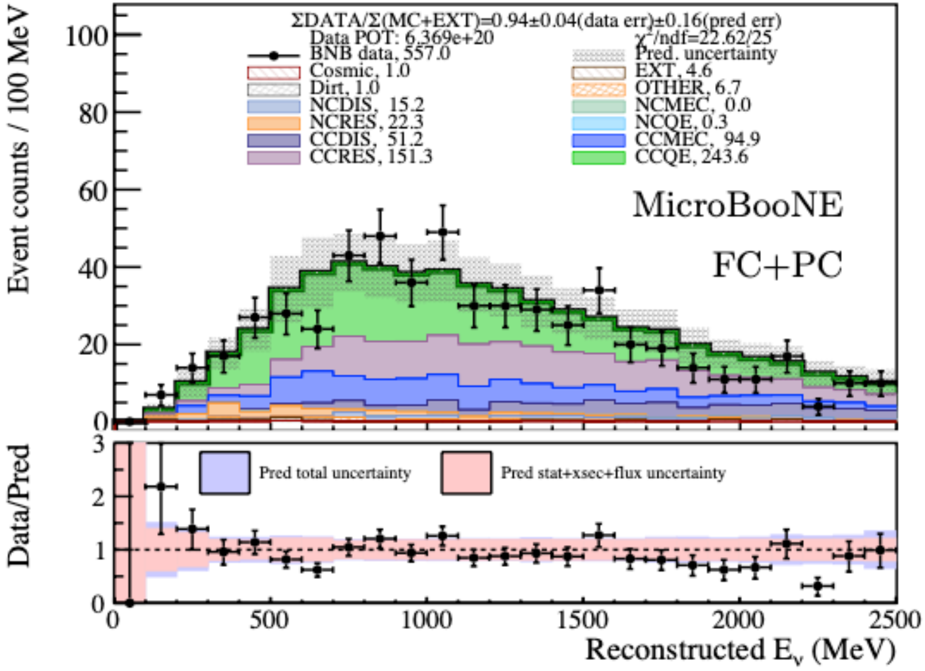

(c) Neutrino energy, broken down with interaction types

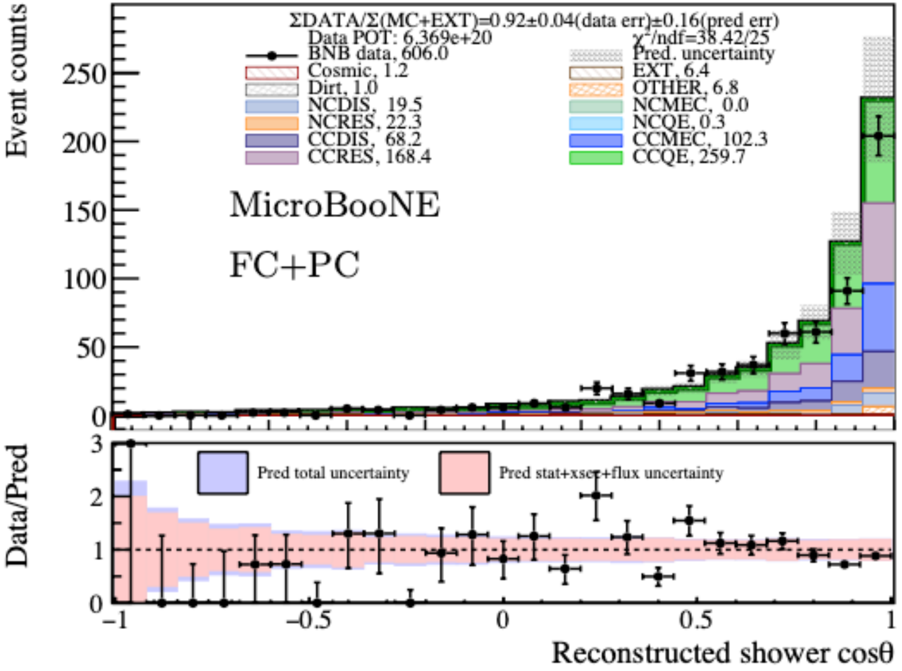

(d) Shower $\cos\theta$, broken down with interaction types

interaction type breakdown: ν_μ CC

[arXiv:2110.13978](https://arxiv.org/abs/2110.13978)

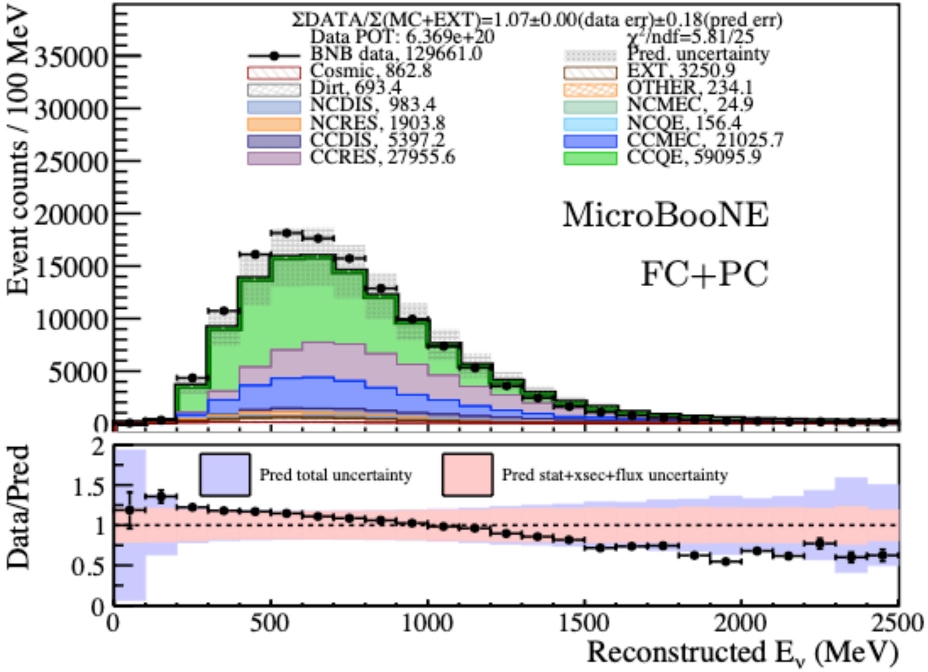

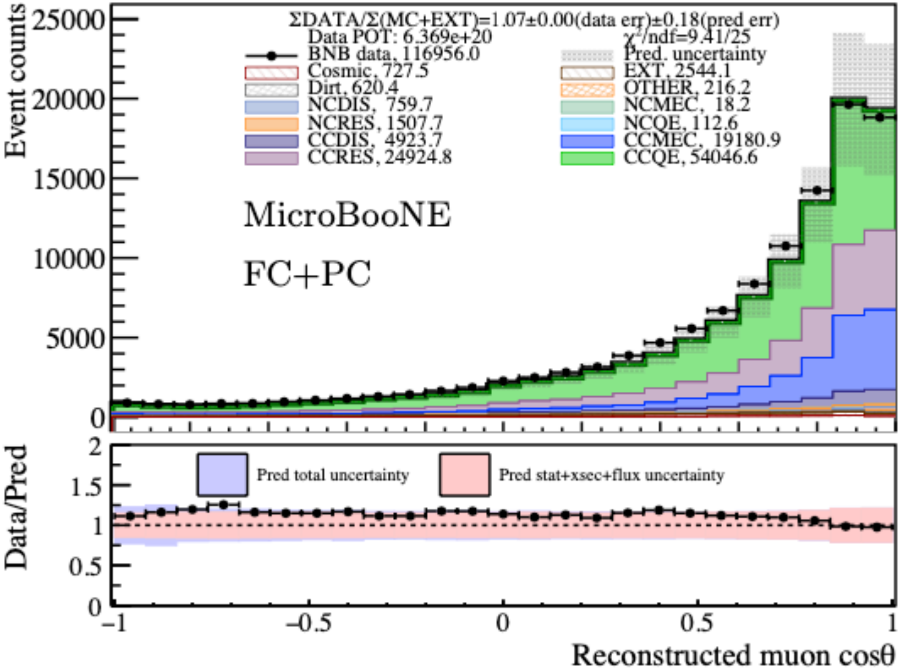

BDT score distribution: ν_e CC

arXiv:2110.13978

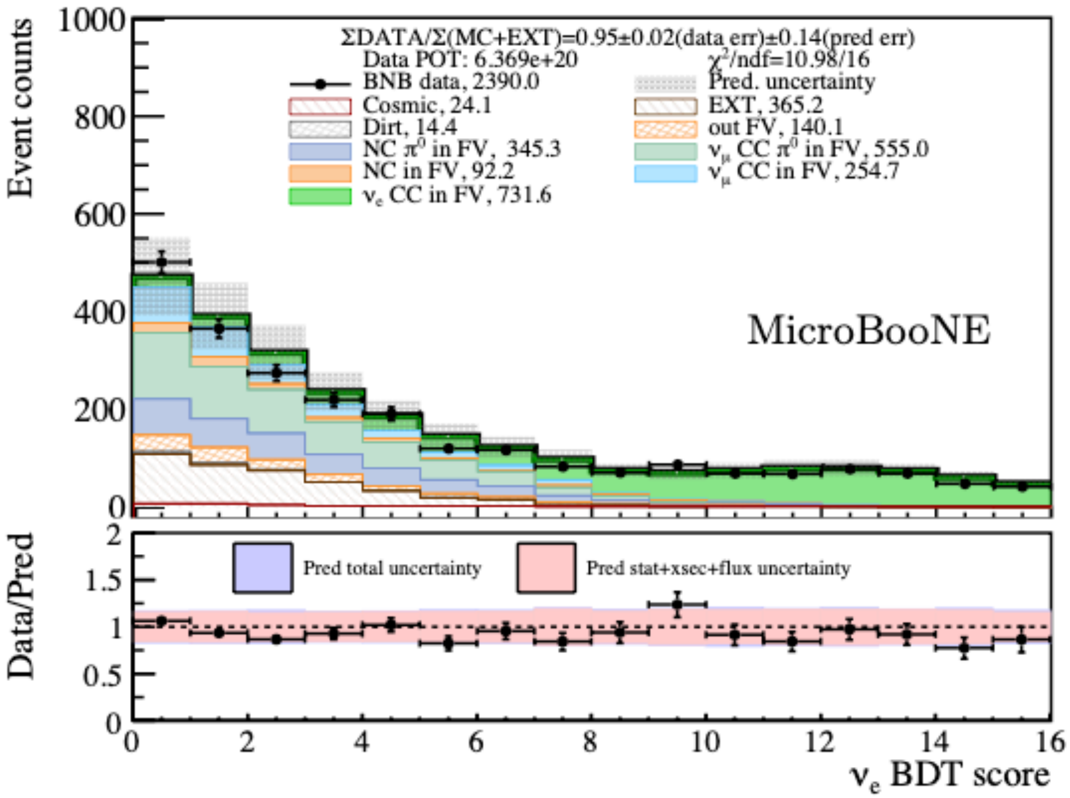

BDT score distribution: ν_μ CC

arXiv:2110.13978

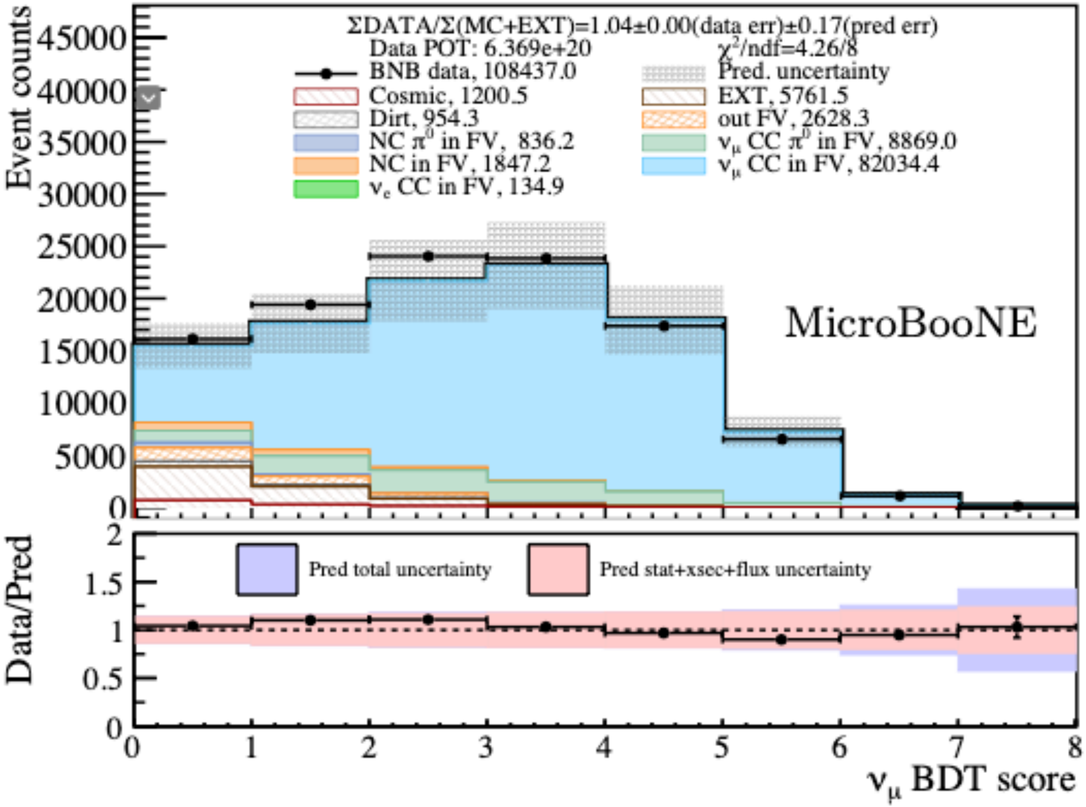

selected ν_e variable: neutrino energy

arXiv:2110.13978

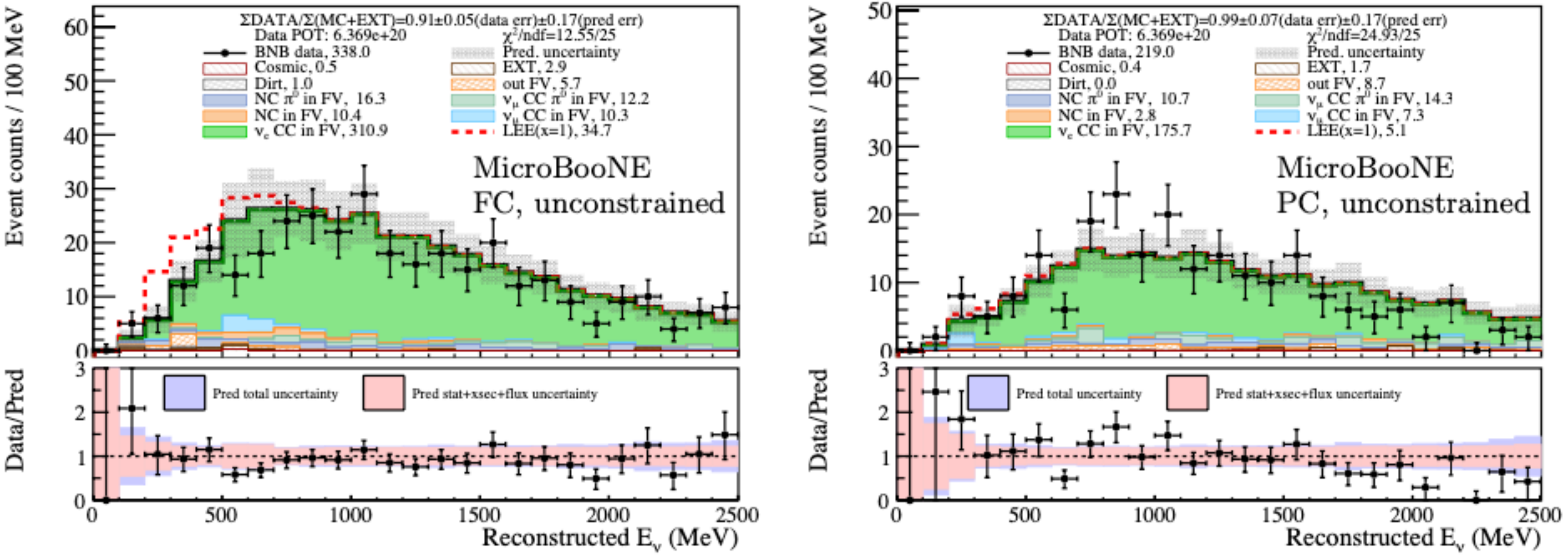

(a) ν_e CC fully contained events.

(b) ν_e CC partially contained events.

selected ν_e variable: shower energy

arXiv:2110.13978

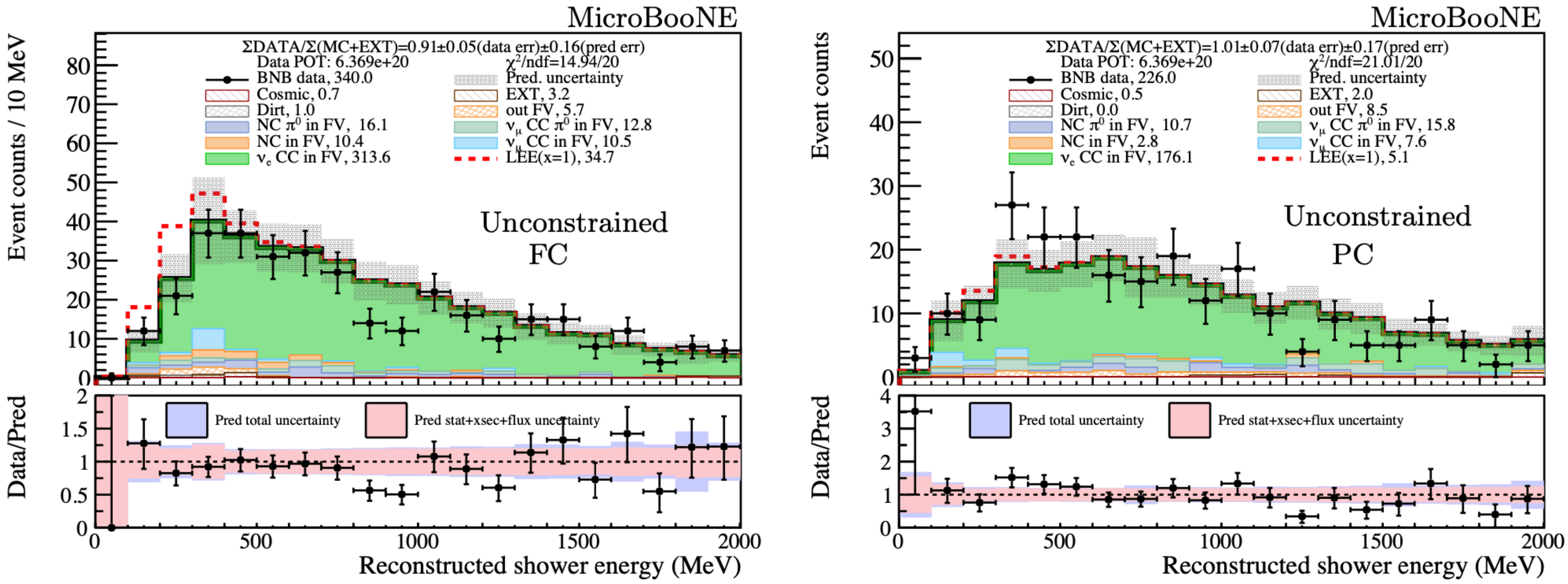

(a) ν_e CC shower energy, fully contained events.

(b) ν_e CC shower energy, partially contained events.

selected ν_e variable: shower cosθ

arXiv:2110.13978

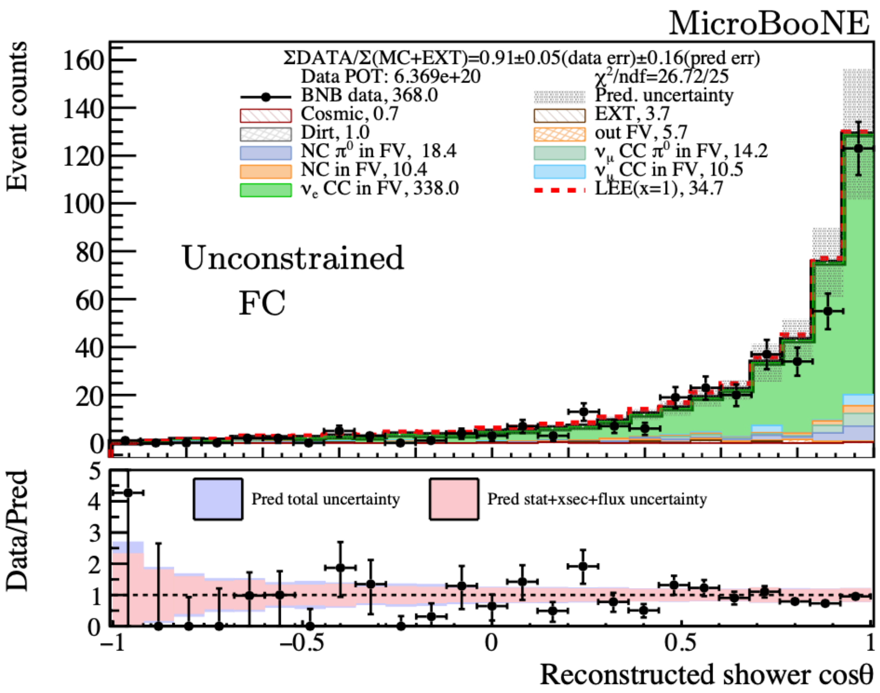

(c) ν_e CC shower cosθ, fully contained events.

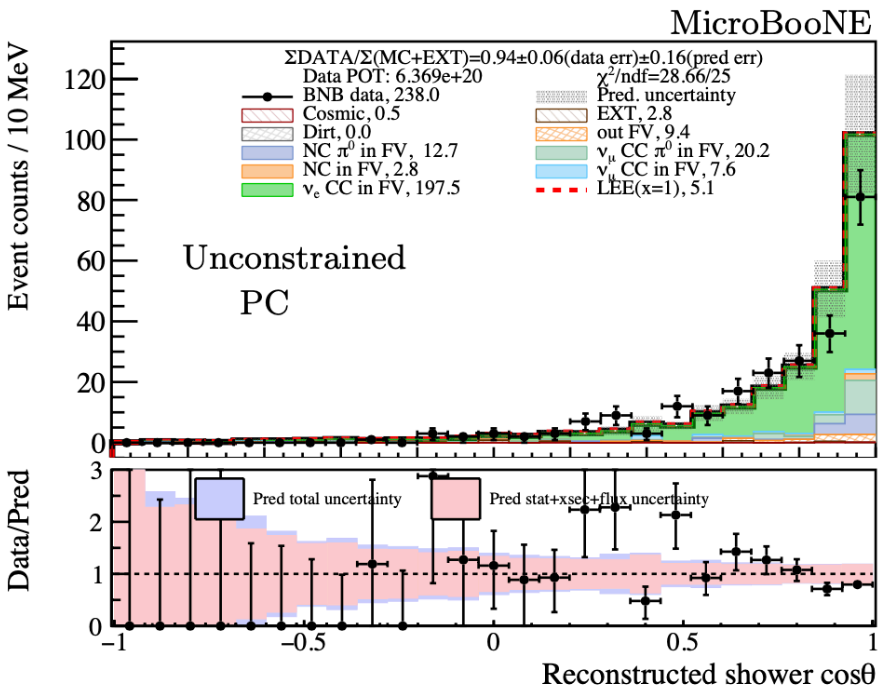

(d) ν_e CC shower cosθ, partially contained events.

selected ν_e variable: hadronic energy

arXiv:2110.13978

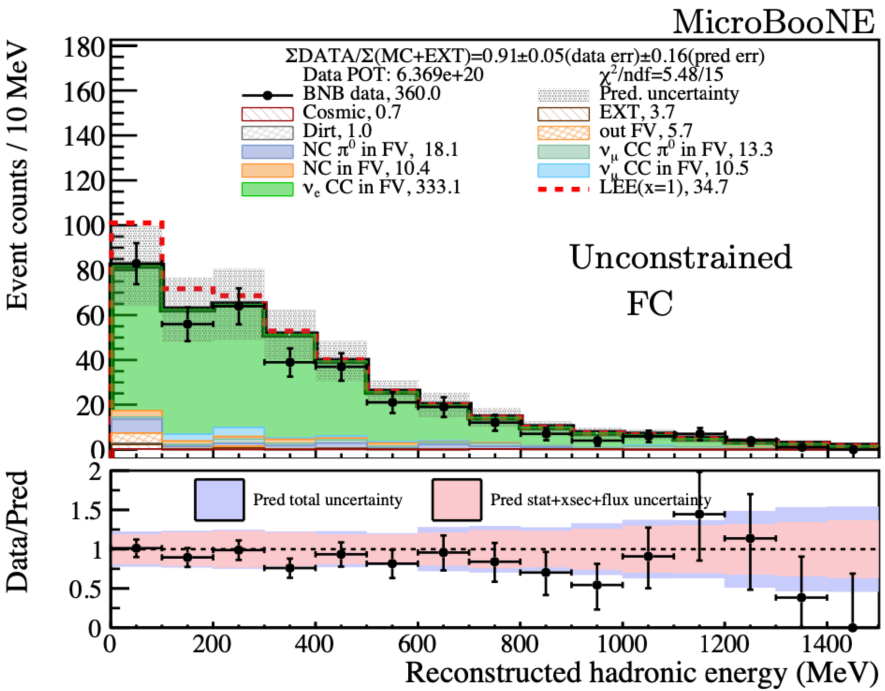

(e) ν_e CC hadronic energy, fully contained events.

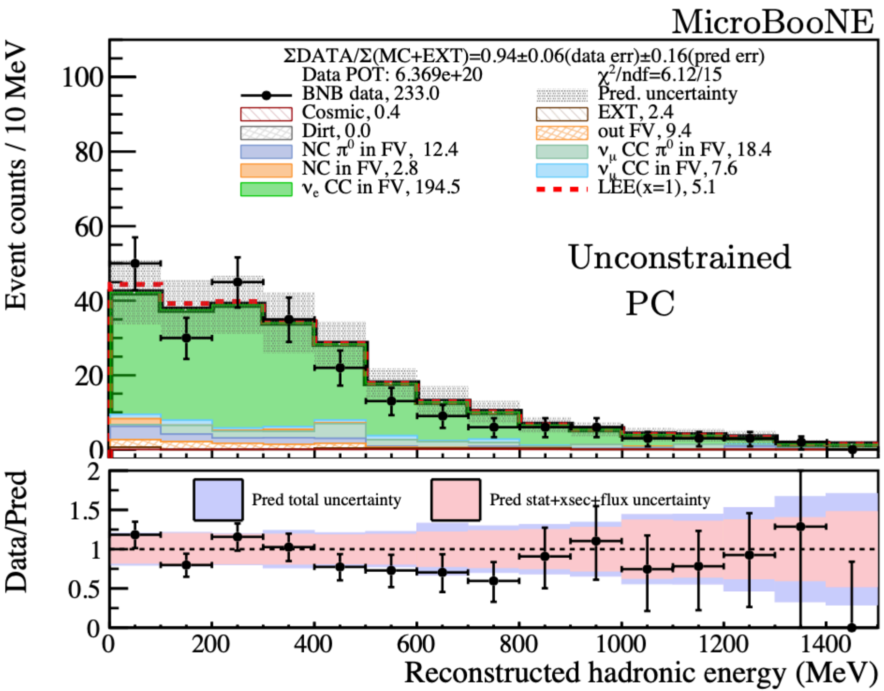

(f) ν_e CC hadronic energy, partially contained events.

7-channel selection & fit

arXiv:2110.13978

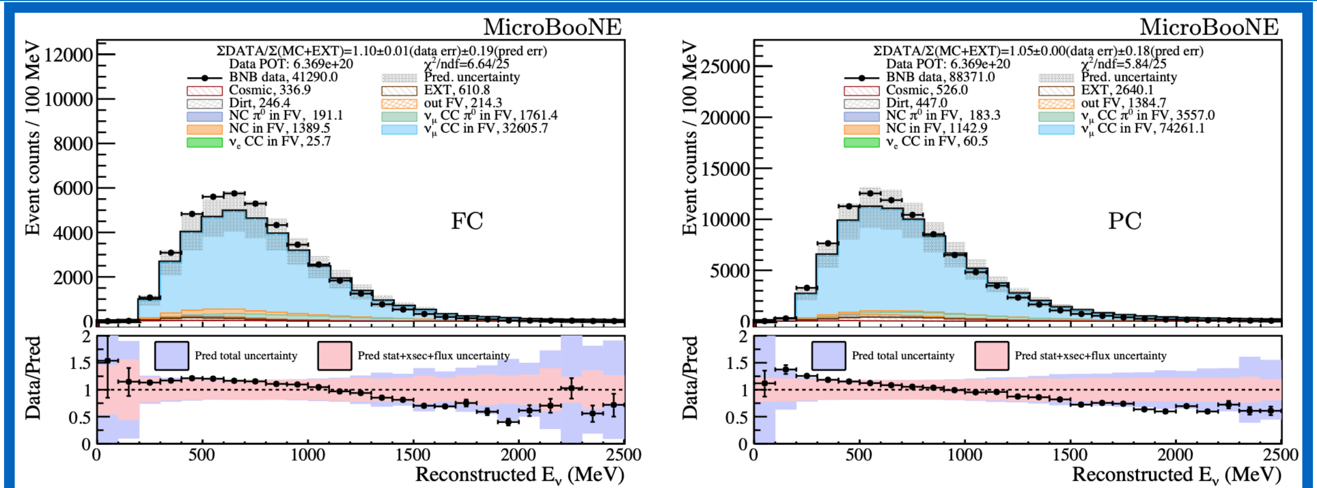

(a) FC ν_μ CC

(b) PC ν_μ CC

ν_μ **CC sidebands**

- high statistics selection
- data excess in lower energy and deficit in higher energy observed
  - lower (higher) energy region is CCQE (CC Resonance) rich
  - hadronic energy studies suggest cross section model is the reason for this behavior
  - data and MC still agrees within systematics

7-channel selection & fit

arXiv:2110.13978

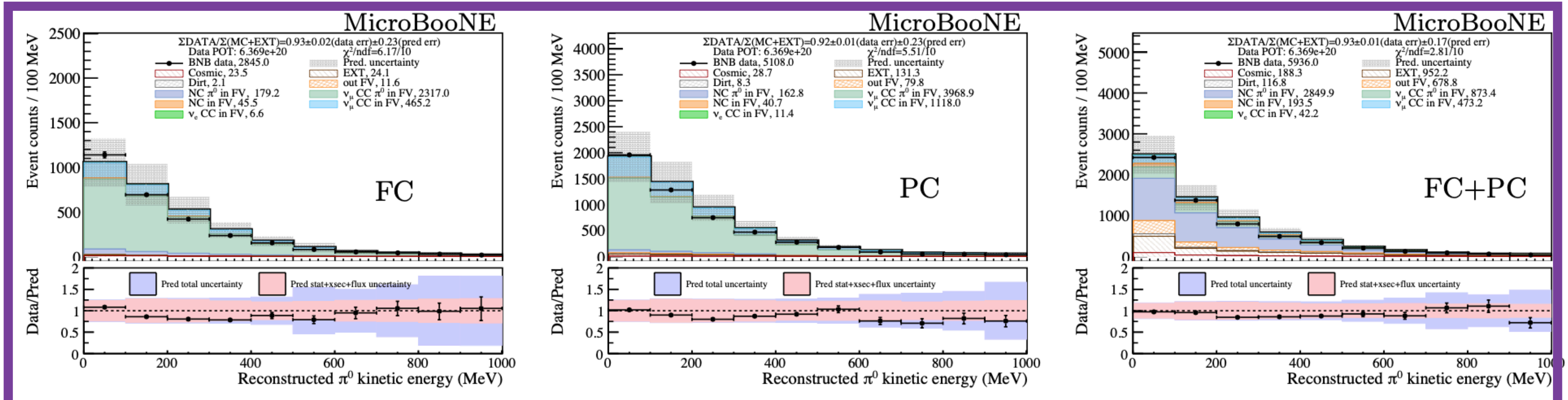

(c) FC CCπ^0 (d) PC CCπ^0 (e) NCπ^0

π^0 sidebands

- high statistics selection
- data deficit is observed in all π^0 channels
  - CC/NC Resonance rich
  - consistent behavior with ν_μ high energy region
  - data and MC agrees within systematics

event breakdown in signal region

arXiv:2110.13978

Category	Evts w/o constr.	Evts w/ constr.
Beam ν_eCC	42.6 ± 10.6	51.5 ± 2.6
ν_μCC π^0	0.6 ± 0.8	0.8 ± 0.8
ν_μCC (non-π^0)	3.9 ± 4.2	3.1 ± 3.1
NC π^0	4.5 ± 2.3	4.3 ± 1.6
NC (non-π^0)	3.0 ± 1.4	2.9 ± 1.2
Out of FV	3.8 ± 2.0	3.4 ± 1.6
Dirt	1.0 ± 1.0	1.2 ± 0.9
Cosmic	0.3 ± 0.6	0.5 ± 0.6
EXT (beam-off data)	1.9 ± 1.7	
Pred. total (eLEE$_{x=0}$)	$61.5 \pm 15.3 \pm 7.7$	$69.6 \pm 5.0 \pm 8.0$
Pred. total (eLEE$_{x=1}$)	$91.8 \pm 23.4 \pm 8.7$	$103.8 \pm 7.4 \pm 9.0$
BNB data	56	

p-values for signal sample

arXiv:2110.13978

χ^2/ndf, $\mathrm{eLEE}_{x=0}$		
Energy region	w/o constr.	w/ constr.
(0, 2500) MeV	12.55/25 $p_{\mathrm{val}} = 0.982$	17.86/25 $p_{\mathrm{val}} = 0.848$
(0, 600) MeV	4.25/6 $p_{\mathrm{val}} = 0.643$	5.78/6 $p_{\mathrm{val}} = 0.448$
χ^2/ndf, $\mathrm{eLEE}_{x=1}$		
Energy region	w/o constr.	w/ constr.
(0, 2500) MeV	13.02/25 $p_{\mathrm{val}} = 0.976$	28.24/25 $p_{\mathrm{val}} = 0.297$
(0, 600) MeV	4.23/6 $p_{\mathrm{val}} = 0.646$	15.73/6 $p_{\mathrm{val}} = 0.015$

0p-Np separation

arXiv:2110.13978

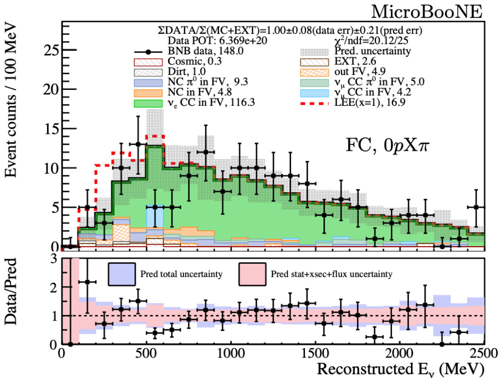

(a) FC ν_e CC, 0pXπ

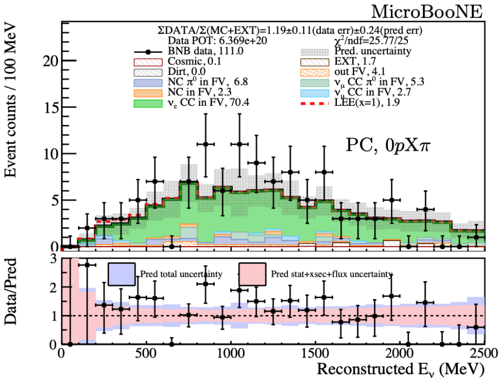

(b) PC ν_e CC, 0pXπ

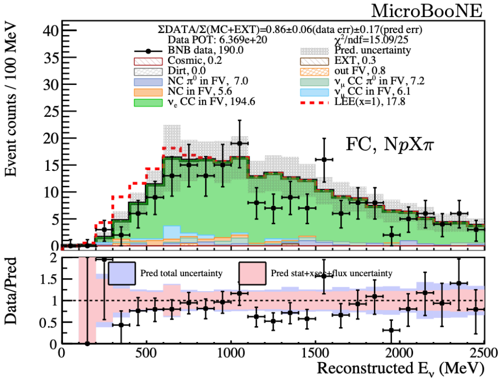

(c) FC ν_e CC, NpXπ

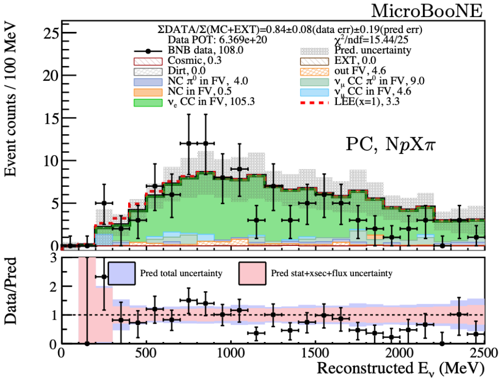

(d) PC ν_e CC, NpXπ

0p-Np separation

arXiv:2110.13978

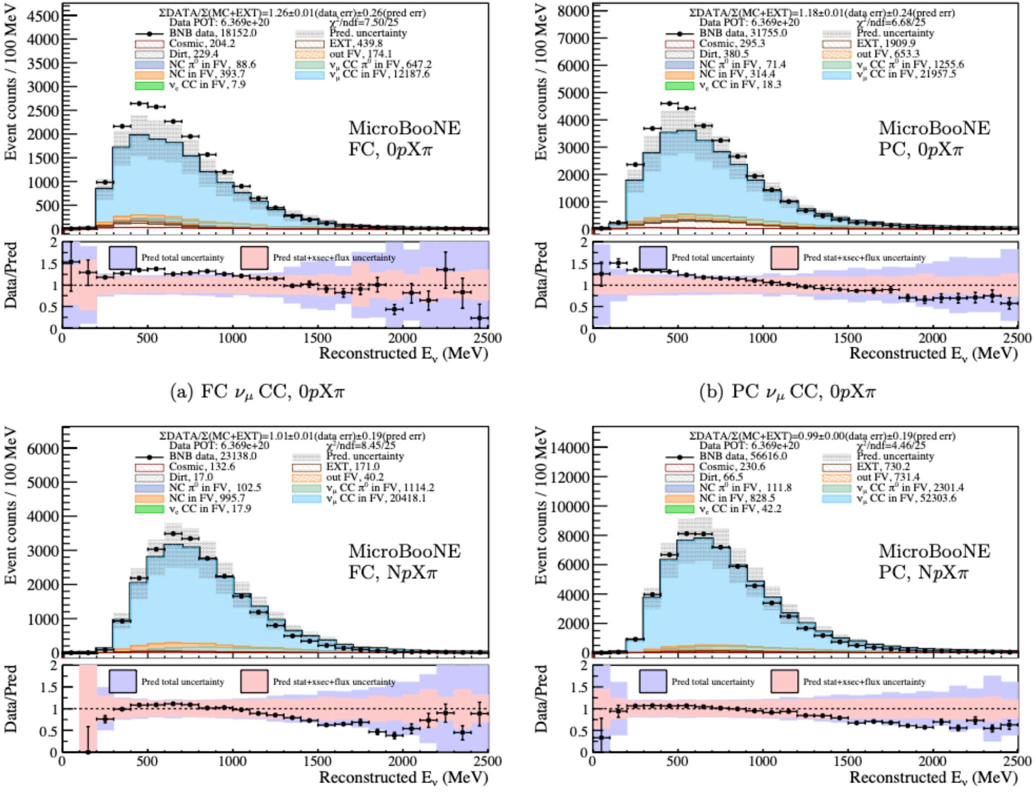

(a) FC ν_μ CC, 0pXπ

(b) PC ν_μ CC, 0pXπ

(c) FC ν_μ CC, NpXπ

(d) PC ν_μ CC, NpXπ

flux uncertainty

arXiv:2110.13978

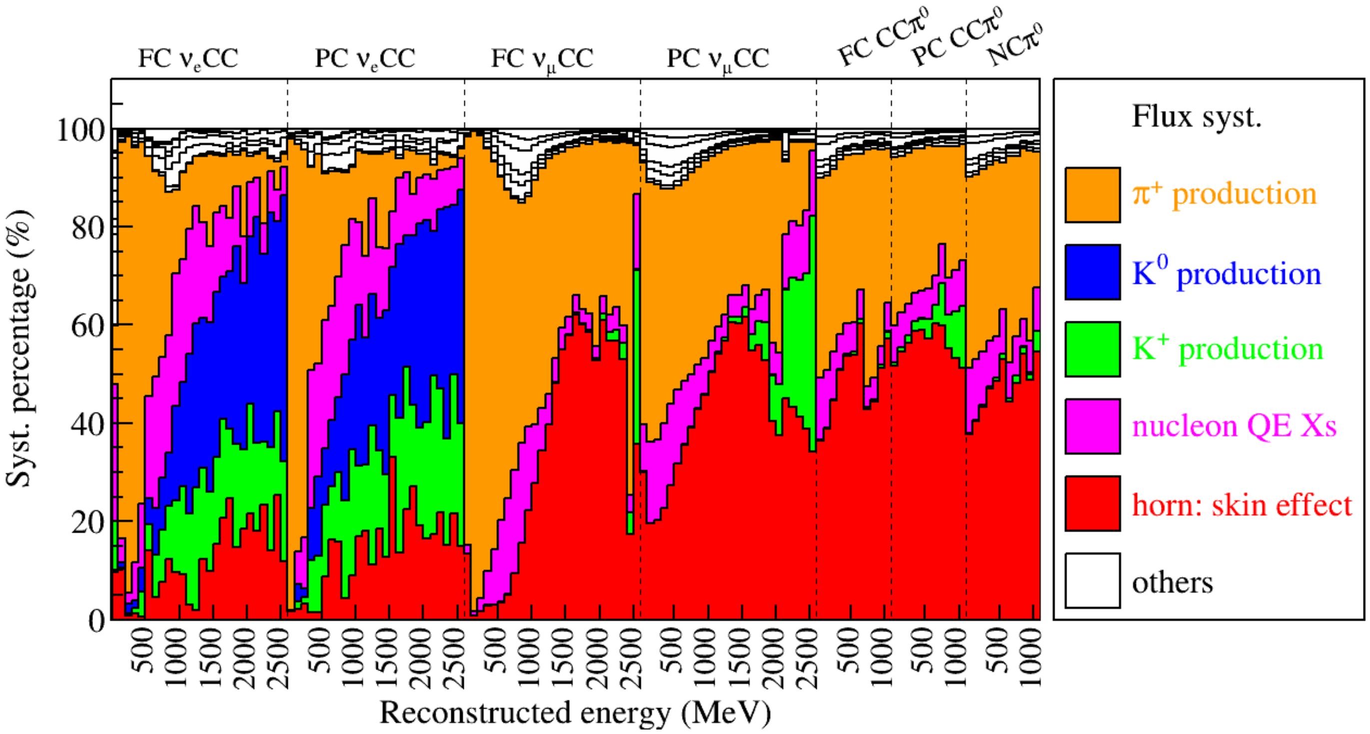

cross section uncertainty

arXiv:2110.13978

- strong correlation of cross section systematics observed between ν_e and ν_μ
- 46 tuning parameters within uB-tuned GENIE v3.0.6 are simultaneously varied

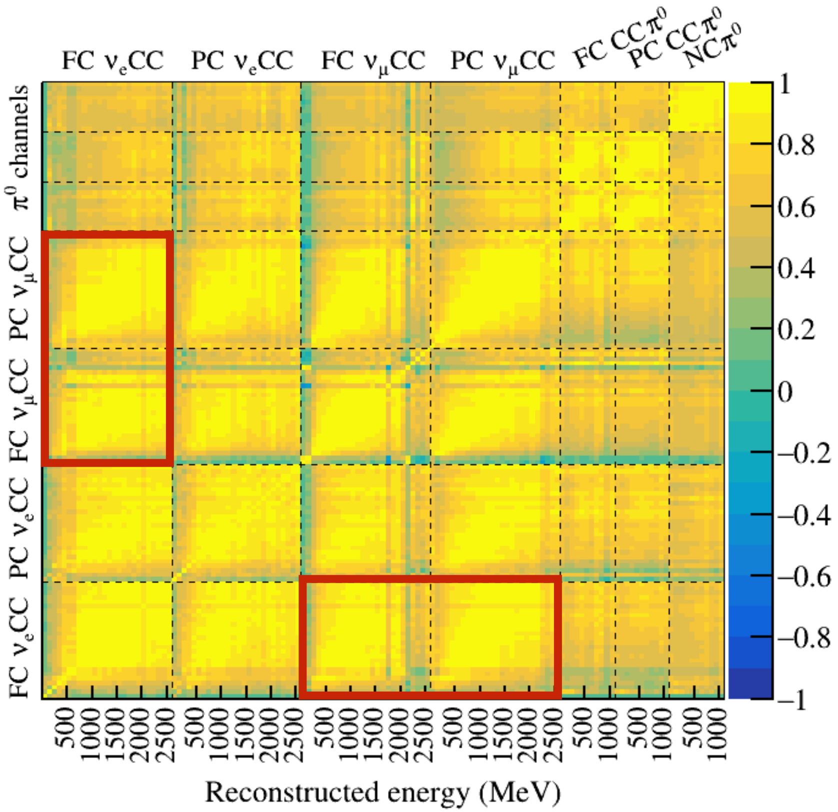

detector systematics

arXiv:2110.13978

- detector systematics are estimated by varying
  - light yield simulation
  - space charge effect
  - recombination model
  - deconvolved ionization charge waveforms
- bootstraping (re-sampling) method is used to improve statistical uncertainty of the used MC samples

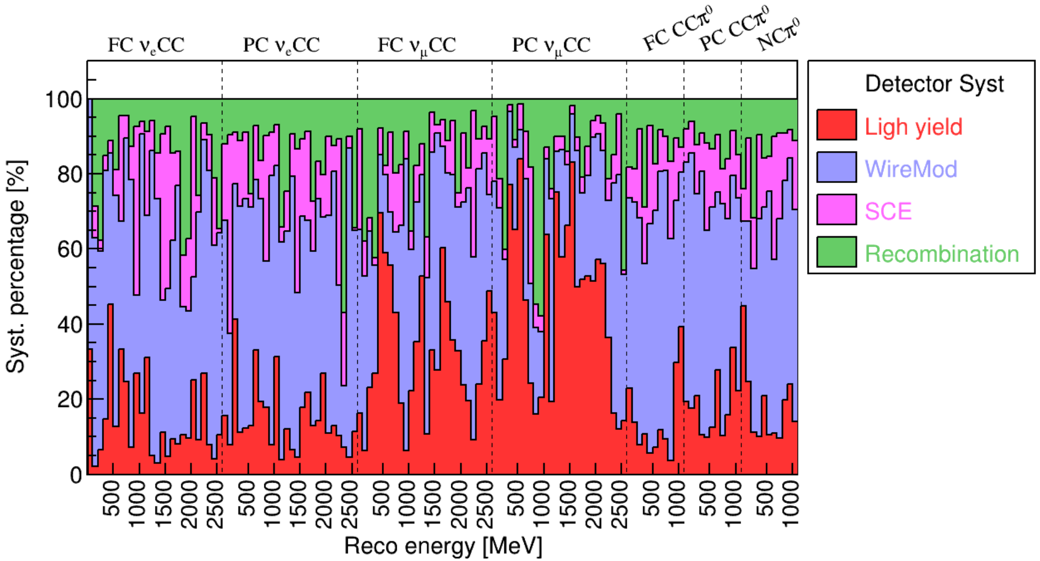

Correlation matrix: Total systematics

arXiv:2110.13978

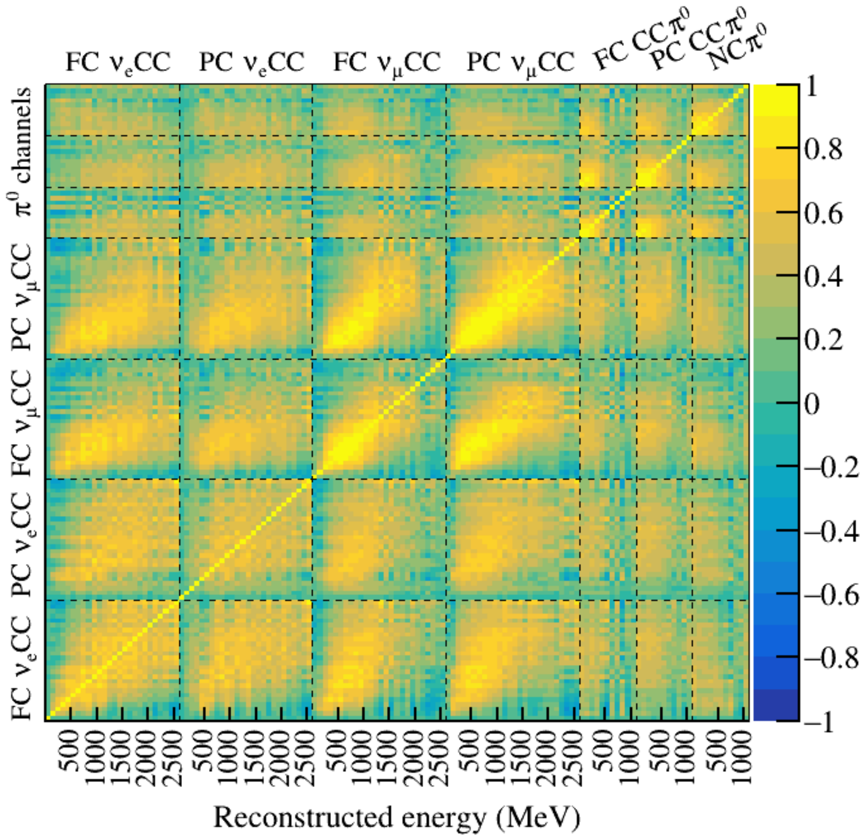

validation process

NuMI data

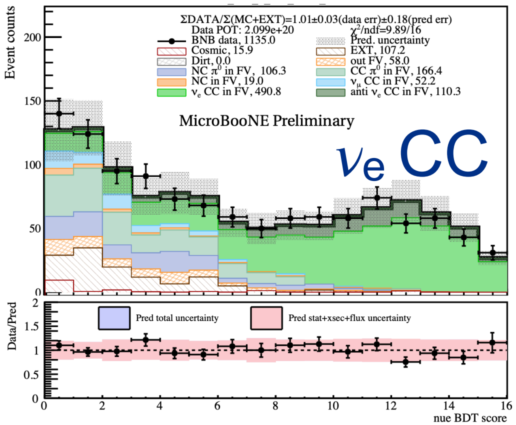

simulated data #5

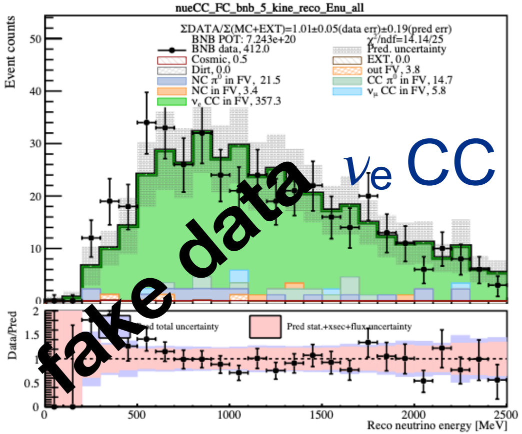

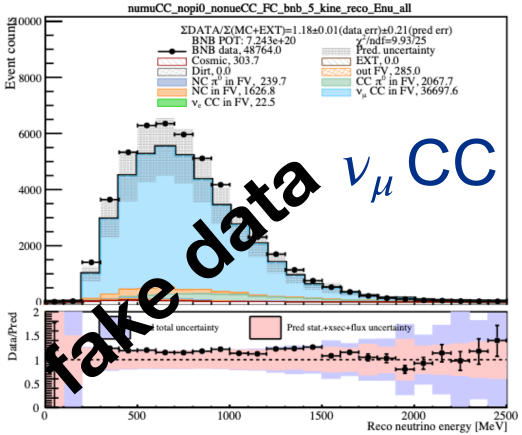

- various checks were performed to validate event selection, analysis chain, and model
  - apply the selection to NuMI & artificially generated “simulated data”
  - goodness of fit of all the sidebands before & after constraints
  - sequentially unblind sample from higher to lower energy region

validation process

NuMI data

simulated data #7

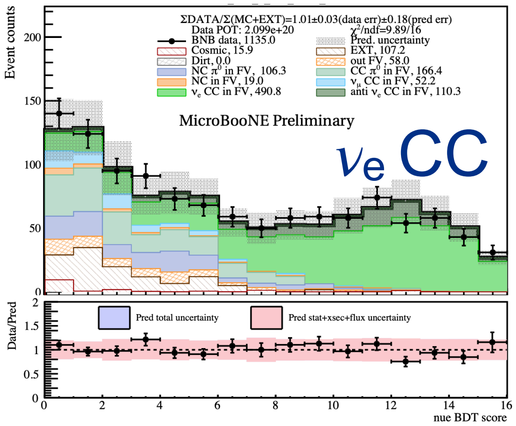

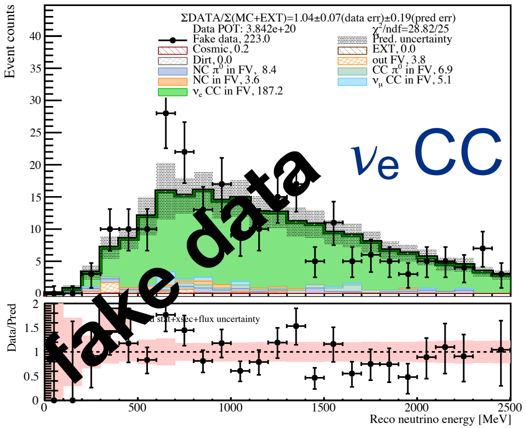

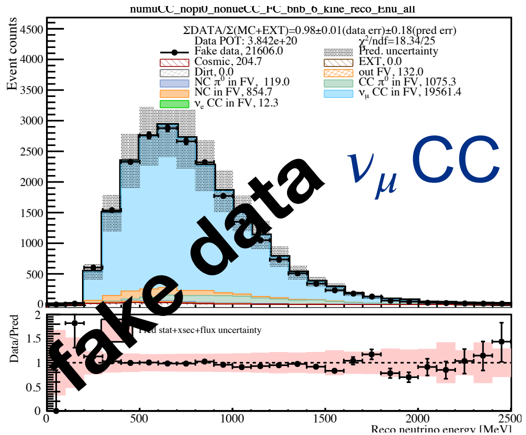

- various checks were performed to validate event selection, analysis chain, and model
  - apply the selection to NuMI & artificially generated “simulated data”
  - goodness of fit of all the sidebands before & after constraints
  - sequentially unblind sample from higher to lower energy region

validation process

Channel	χ^2/ndf w/o constr.	χ^2/ndf w/ constr.	Notes
FC ν_μCC	6.64/25	N/A	No constraint, see other checks
PC ν_μCC	5.84/25	6.94/25	Constrained by FC ν_μCC
FC CCπ^0	6.17/10	7.39/10	Constrained by both FC and PC ν_μCC
PC CCπ^0	5.51/10	6.80/10	
NCπ^0	2.81/10	5.33/10	
PC ν_eCC	24.93/25	24.19/25	See Sec. VII A; constrained by the above five channels; eLEE$_{x=0}$ hypothesis

- various checks were performed to validate event selection, analysis chain, and model
  - apply the selection to NuMI & artificially generated "simulated data"
  - goodness of fit of all the sidebands before & after constraints
  - sequentially unblind sample from higher to lower energy region

model validation

arXiv:2110.13978

- hadronic energy constrained with muon kinematics
- data show good agreement (chi2/ndf) with constrained MC prediction even with significantly reduced systematics
- this is an evidence that the origin of data-MC disagreement is from the common systematics (most likely XS), shared by both leptonic and hadronic final states

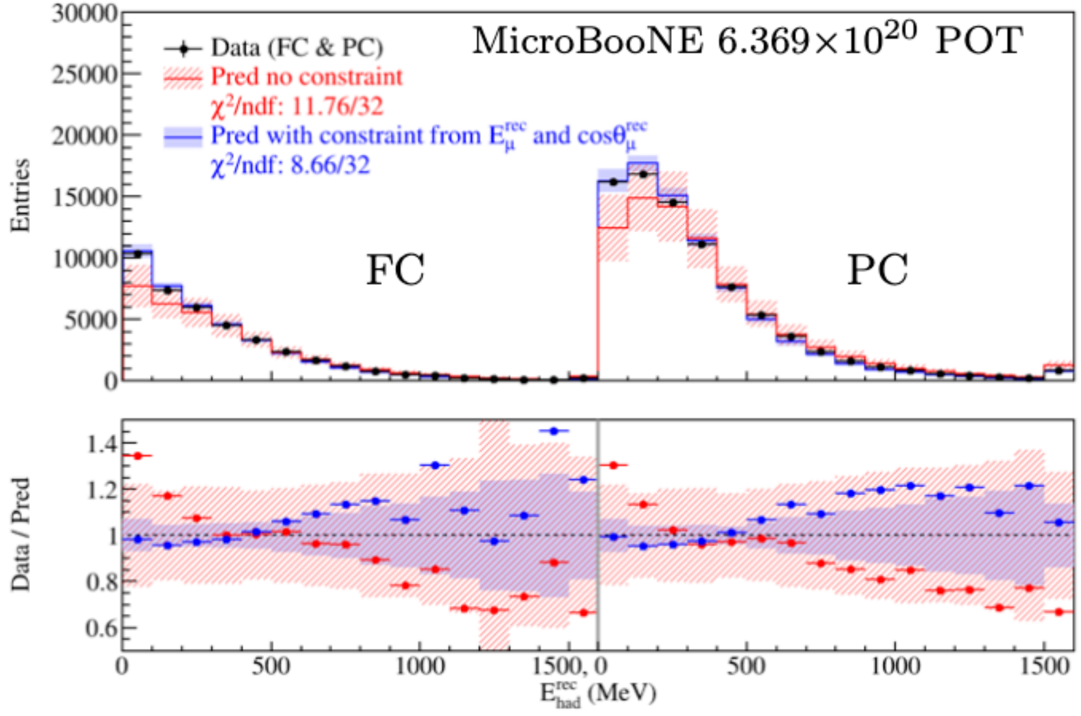

(c) ν_μ CC hadronic energy ($E_{\rm had} = E_\nu$-E_μ).

before & after constraints

arXiv:2110.13978

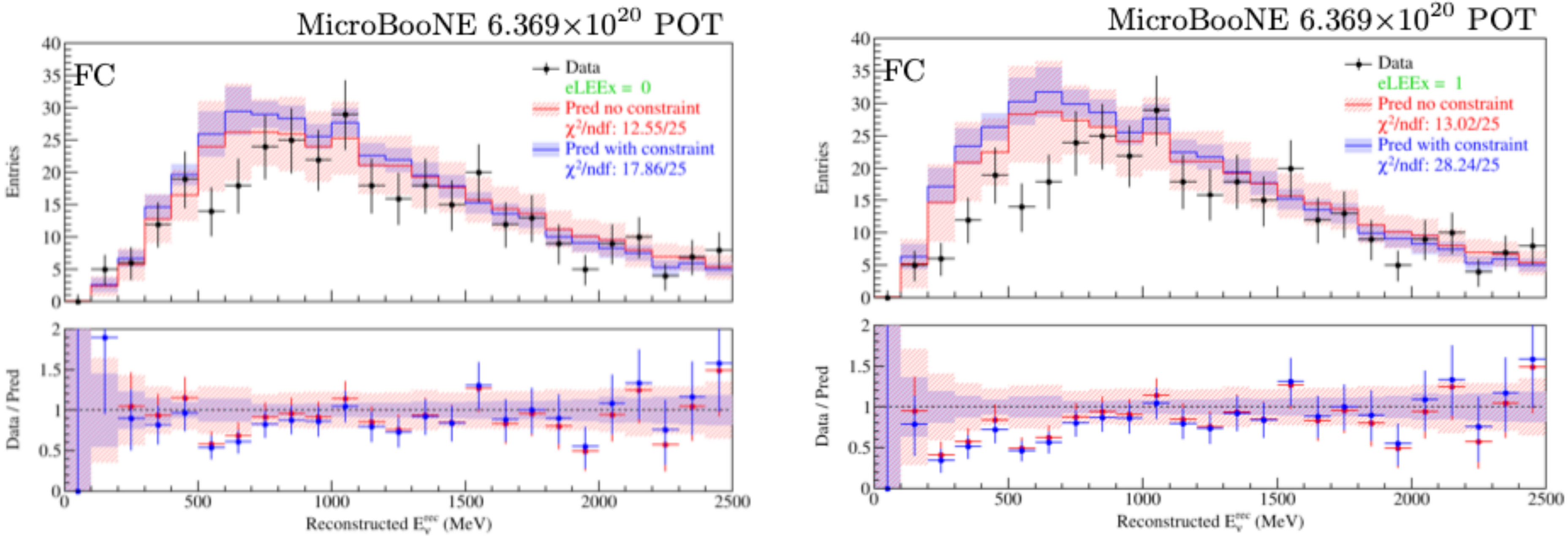

(a) $\mathrm{eLEE}_{x=0}$ hypothesis. (b) $\mathrm{eLEE}_{x=1}$ hypothesis

comparisons to eLEE model

- estimate uncertainty on eLEE model from a simple re-interpretation of MiniBooNE excess significance
  - does not take correlations between MiniBooNE and MicroBooNE into account

- fitting for the eLEE model signal strength, we disfavor generic ν_e interactions as the primary contributor to the excess, with a 1σ (2σ) upper limit on the inclusive ν_e CC contribution to the excess of 22% (51%)

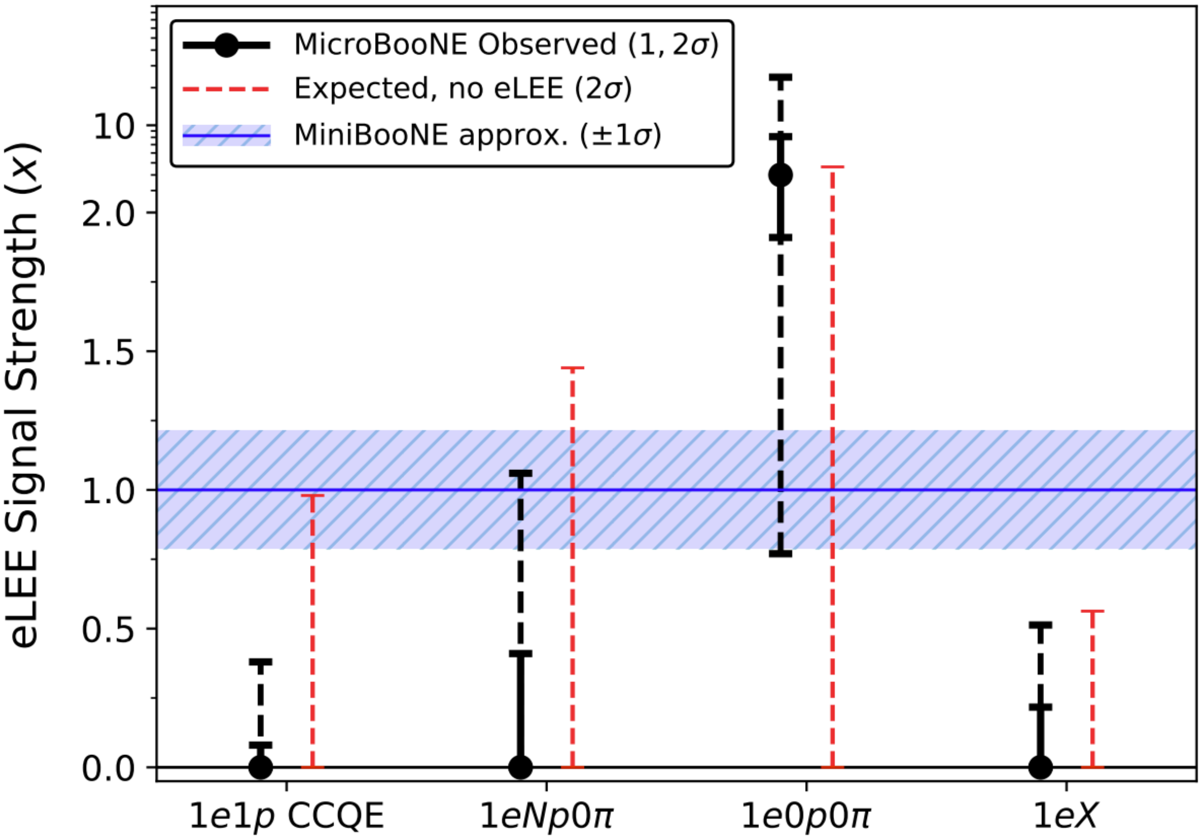

µBooNE

results: nested likelihood ratio test & best-fit of eLEE strength x

arXiv:2110.13978

- $\Delta\chi^2_{\text{nested}} = \chi^2|_{\text{eLEEx}=x_0} - \chi^2_{\text{min}}|_{\text{eLEEx}=x_{\text{min}}}$ (x_0 represents null hypothesis, x_{min} is best-fit value of x)
    - best-fit x is determined to be 0
    - **lower limit of MiniBooNE 68% full (stat-only) confidence interval is disfavored at over 2.6σ (3.0σ)**

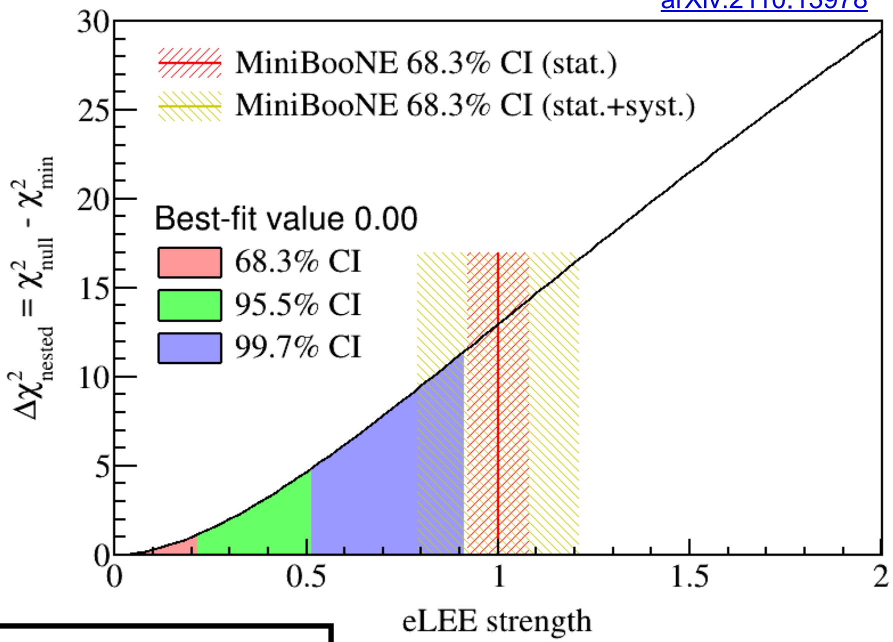

low-energy ν_e cannot solely explain MiniBooNE low energy excess

Wire-Cell "exclusive" selections

arXiv:2110.13978

- to further validate consistency of the model used, separate 1eX selection into 1e0pXπ and 1eNpXπ
  - 35 MeV proton reconstruction threshold
- **eLEE strength fits consistently return 0 for all these exclusive channels**

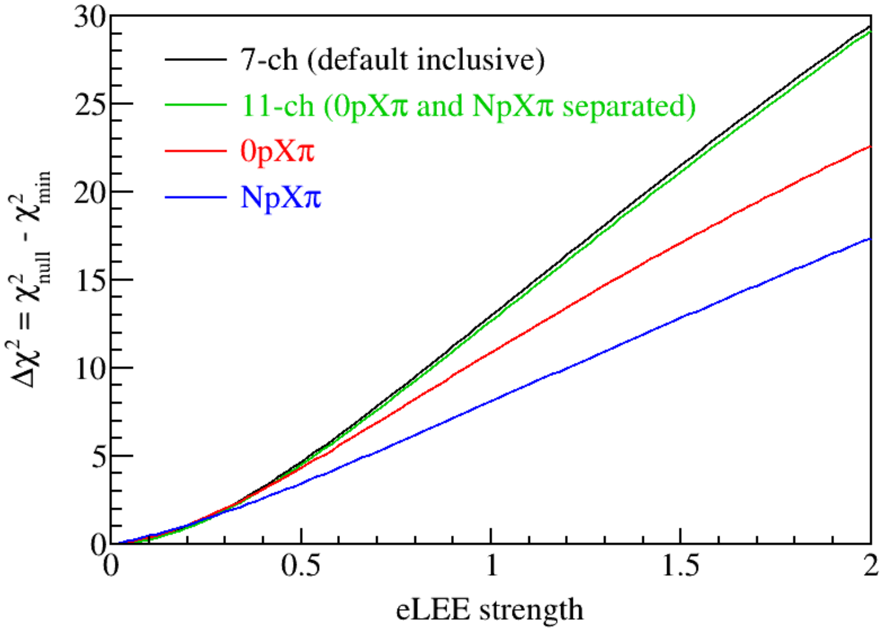

landscape of possible MiniBooNE LEE final state topologies

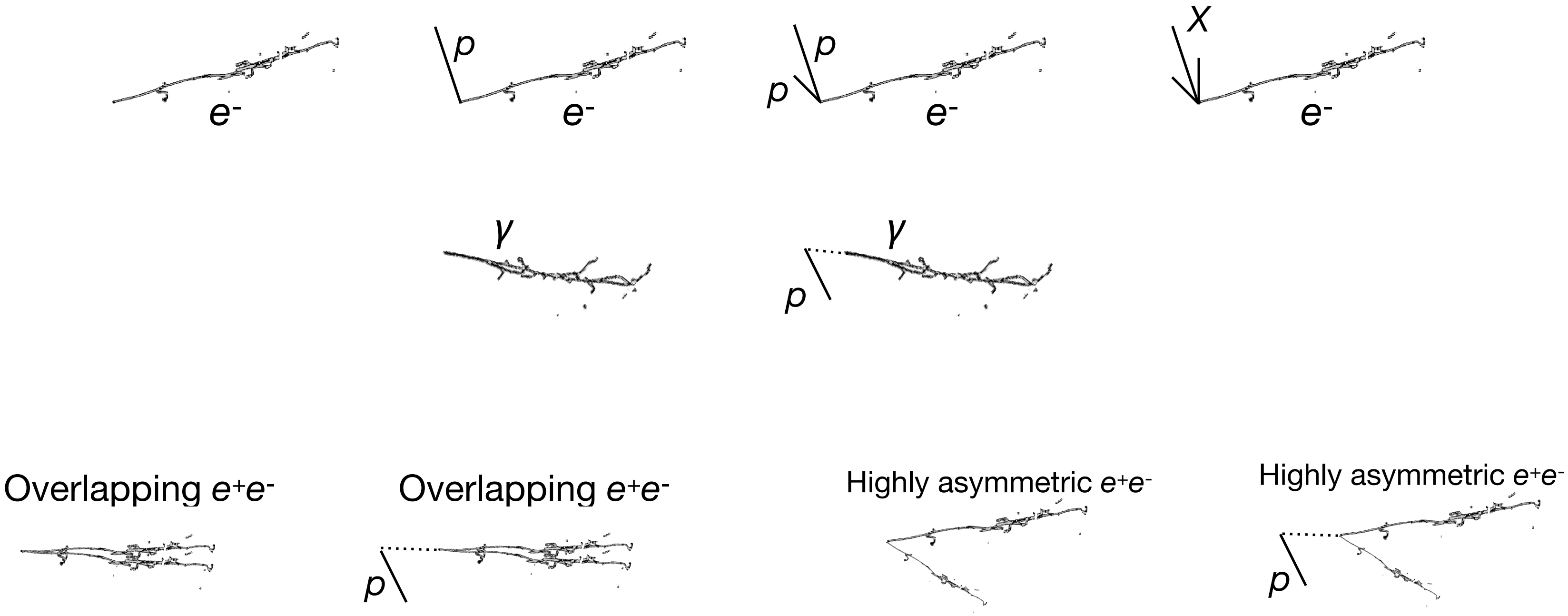

landscape of possible MiniBooNE LEE final state topologies

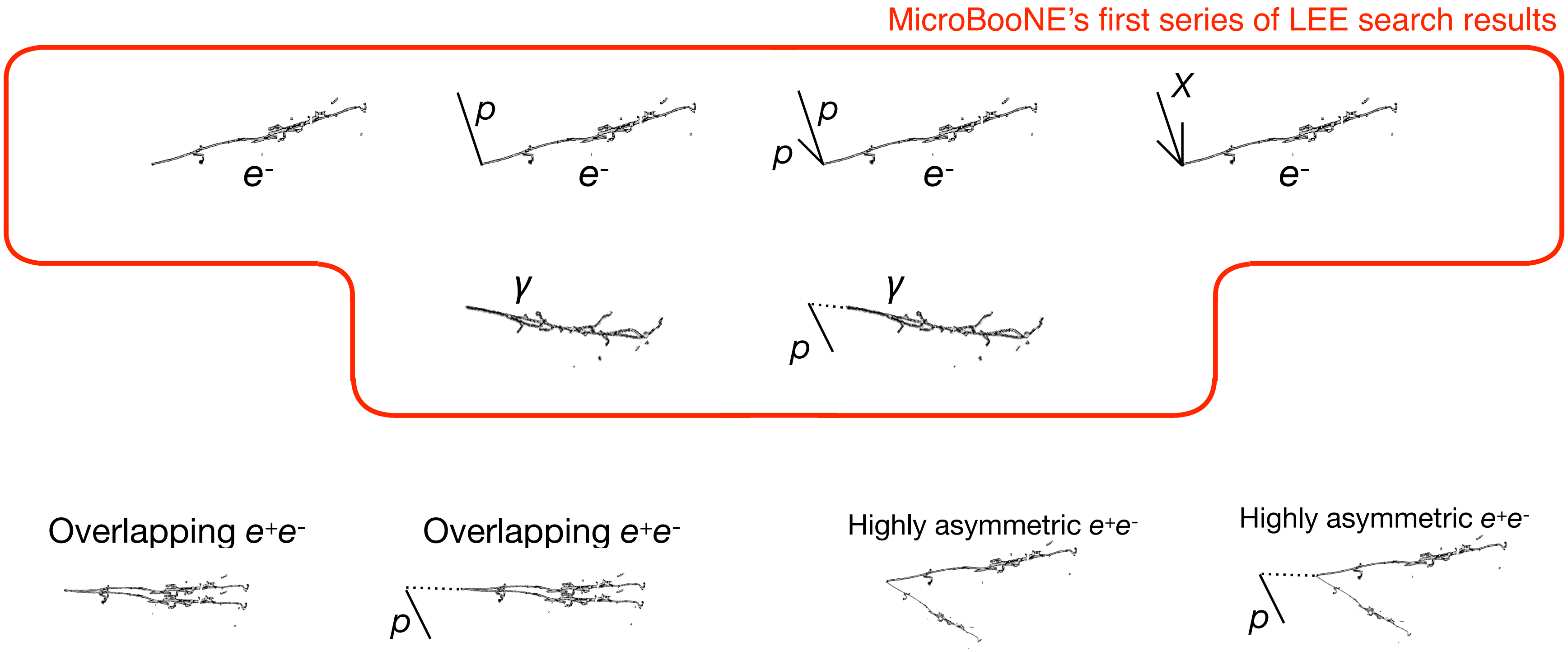

landscape of possible MiniBooNE LEE final state topologies